Children's Health Project: Linking Asthma to PM$_{10}$ in Central Phoenix – a report to the Arizona Department of Environmental Quality

H.J.S. Fernando[1], R. Dimitrova[1], G. Runger[2], N. Lurponglukana[2], P. Hyde[1], B. Hedquist[1], J. Anderson[1]

Arizona State University's [1]Center for Environmental Fluid Dynamics and [2]Center for Health Information and Research

February 16, 2009

TABLE OF CONTENTS

LIST OF FIGURES

LIST OF TABLES

Executive summary

The effects of elevated PM_{10} concentrations on childhood asthma incidents (emergency room visits & hospital admissions) in central Phoenix, AZ were determined. A major portion of this work involved the application of a deterministic, numerical air quality model to produce gridded concentration fields, the development of a neural-network based prediction system for PM_{10}, and the interpolation of PM_{10} concentrations from five monitoring sites to produce census-tract specific concentrations for the statistical health effects analyses. Through the case-crossover method, PM_{10} concentrations were shown to have statistically significant associations with asthma incidents in central Phoenix at the 95% confidence level. For children ages 5-17 an effect *much stronger* than in previous studies was determined, while children ages 0-4 exhibited virtually no effects. Previous studies have reported the risk of adverse health effects as a function of the change of daily mean PM_{10} from the 25th to 75th percentile; in this study that change was 36 $\mu g/m^3$. This change in PM_{10} is associated with a 13% increase in the probability of asthma incidents among children ages 5-17. Within this group, neither age nor gender was significant. The lack of an effect on preschool children was assumed to be due to the difficulty of making accurate asthma diagnoses in the younger ages and/or more time spent indoors.

Chapter 1 Introduction

Voluminous studies on the health effects of particulate matter (PM) have been carried out. Atmospheric scientists deal with the conditions conducive to high PM episodes; the exposure community delves into the duration and severity of ambient PM concentrations to which various populations are subject; toxicologists and biochemists study the effects of the hazardous constituents of PM on human and surrogate organisms and in *in vitro* systems; physiologists and physicians conduct exposure-effect studies on humans in chambers, epidemiologists relate health outcomes to ambient concentrations and exposures, and modelers (including risk assessors) utilize various data to estimate exposure-response relationships for determining safe levels of exposure. Integration of such disparate disciplines is difficult, given the complexity inherent in each of the approaches, though the U.S. Environmental Protection Agency (EPA) and the World Health Organization (WHO) Air Quality Criteria Documents, the EPA Staff Papers, and the EPA Office of Air do make such an attempt. For issuing health warning system is sufficient to establish, if there be any, a reliable association between PM concentrations and health effects such as admittances due to respiratory (or cardiovascular) ailments to allow prediction of such events. The principal goal of the "Children's Health Project" was to clarify the association of children's health with PM_{10} levels to develop a better health warning system in Phoenix. We brought together a partnership among Arizona Department of Environmental Quality (ADEQ), Arizona Department of Health Services (ADHS), Ross & Associates, and two groups of researchers at Arizona State University: the Center for Health Information and Research (CHIR), and the Center for Environmental Fluid Dynamics (EFD). We discussed our findings with University of Arizona medical personnel and the Asthma Coalition.

Work elements of the project

- With the central portion of Phoenix as the study area, PM_{10} concentrations and asthma records were analyzed for each day in 2005 – 2006.

- PM_{10} concentrations were estimated with both deterministic and statistical models.

- The **deterministic models** were the EPA's Community Multi-scale Air Quality Modeling System (CMAQ) and a meteorological model called "MM5." This grid-based weather and pollution simulation system relied on the most recent Western Regional Air Partnership PM inventories. Design days included periods of low, intermediate, and high pollution. The hourly and daily simulated concentrations were compared with data from five permanent monitoring sites with continuous PM_{10} instruments.

- The first type of statistical model employed was **interpolation**. With the interpolation technique called "inverse distance weighting" (IDW), spatial concentration fields were built that provided a PM_{10} concentration for each of the 168 census tracts from measurements at the five central-city monitoring sites. The efficacy of this scheme was verified by deploying four temporary monitors for four months and by using hourly PM_{10} concentrations from two Maricopa County permanent sites whose continuous PM_{10} monitors began operating after 2005. These six additional sites enabled the use of a more sophisticated interpolation technique called "ordinary kriging", which produced results similar to those of the IDW.

- The second type of statistical model was the **neural network**, developed by Italian scientists and applied to a single permanent monitoring site -- Maricopa County's "Central Phoenix" site. This model is a statistical system to predict the next day's PM_{10} concentrations without the labor and emissions-inventory intensive alternative of CMAQ. In the present work, however, its use was limited to estimating PM_{10} concentrations already recorded in 2006.

- About 6,000 **ADHS asthma events** in children ages 0-18 – in a unified area within five miles of the five monitoring sites – comprised 75% of the Maricopa County total. These ADHS records of emergency room treatment and hospital admissions were cross-checked against an independent data set at CHIR and were found to be consistent once duplicate records had been eliminated.

- The census-tract-based health data were linked with the PM_{10} concentrations derived from the IDW interpolations by a statistical method called "**case-crossover**". Asthma has a strong seasonal component and the case-crossover analysis associates a reference time period as a control for each case. Consequently, each patient was treated as a matched case-referent pair with control exposures obtained from the same patient at different times. With an appropriate referent period, the case-crossover analysis controlled for long-term trends, seasonal effects, epidemic, and other covariates that change slowly with time such as behavior and diet. In addition to PM_{10} on the "event" day, 24-hour averages from one to seven days before the event were also examined (this delay is referred to as "lag time"). The patients were also stratified by age group, gender, and race/ethnicity, and interactions between air quality and these variables were explored.

Chapter 2 PM monitoring networks

Permanent PM_{10} network in the central city

Considering "metropolitan Phoenix" to include the city and all of the adjoining suburbs (but excluding Casa Grande and environs), five governmental agencies conduct air quality monitoring:

- Maricopa County Department of Air Quality (MCDAQ)

- Arizona Department of Environmental Quality – Air Quality Division (ADEQ)

- Pinal County Air Quality Control District

- Salt River Pima Maricopa Indian Community, and

- Gila River Indian Community.

Together, these agencies operate about 50 different sites with a variety of instruments and several different objectives. What the U.S EPA terms "criteria pollutants", such as particulate matter, ozone, carbon monoxide, and others, may be the prime focus; but many other aspects of pollution in the planetary boundary layer are also monitored. For example, this monitoring includes meteorological parameters such as wind speed and wind direction, visibility characteristics such as light extinction and photographic views, and the chemical composition of particulates and gaseous pollutant mixtures (MCDAQ, 2007; ADEQ, 2007).

The present work, based on the PM_{10} network and the asthma cases in central Phoenix, relies on the "continuous" meteorological and air pollutant data from the first two agencies in the list above. "Continuous" means that the instruments run round the clock with their meteorological parameters and air pollutant concentrations, including PM_{10}, reported as hourly averages. As described later in this chapter, Arizona State University (ASU) and ADEQ staff set up and operated temporary PM_{10} continuous monitors to supplement the permanent network (Table 2.1 and Figure 2-1).

Table 2.1 Central Phoenix continuous PM_{10} monitoring sites

Symbol	Name	Major streets/city[1]	Duration	Agency
WF	West 43rd Avenue	43rd Avenue & Broadway Rd.	Permanent	MCDAQ or ADEQ
DC	Durango Complex	27th Avenue & Durango Street		
WP	West Phoenix	39th Avenue & Thomas Road		
CP	Central Phoenix	16th Street & Roosevelt Street		
SS[2]	Supersite	15th Avenue & Camelback Rd.		
SP[3]	South Phoenix	Central Ave & Broadway Rd.		
GR[3]	Greenwood	27th Avenue & I-10		
MRV	Maryvale	59th Ave & Indian School Rd.	Temporary: Nov. 2007 – March 2008	ASU/ADEQ
VGC	Valley Garden Center	15th Avenue & McDowell Rd.		
WVR	Weaver's Auto Service	29th Street & Thomas Road		
CSA	Community Service of AZ	59th Ave. & Glendale Avenue, Glendale, AZ		

1. All except CSA are in Phoenix, Arizona.
2. SS, Supersite, is ADEQ; other permanent sites are MCDAQ.
3. Used only in the ordinary kriging interpolation, along with the other permanent and all temporary sites; not used in the inverse distance weighting interpolation for 2005 – 2006, because continuous PM_{10} monitoring did not begin until January 2006.

Each of these sites has its unique combination of local emission sources and its own susceptibility to urban transport that together, along with the desert background, result in the measured concentrations. Each has its own degree of representativeness: i.e. how far away from the monitor do the measured concentrations actually prevail? The permanent county sites, fully described in Maricopa 2007, and the ADEQ Supersite, are also characterized in Appendix A. What follows is a discussion of how their average PM_{10} concentrations fit into the spatial distribution of PM_{10} concentrations throughout metropolitan Phoenix.
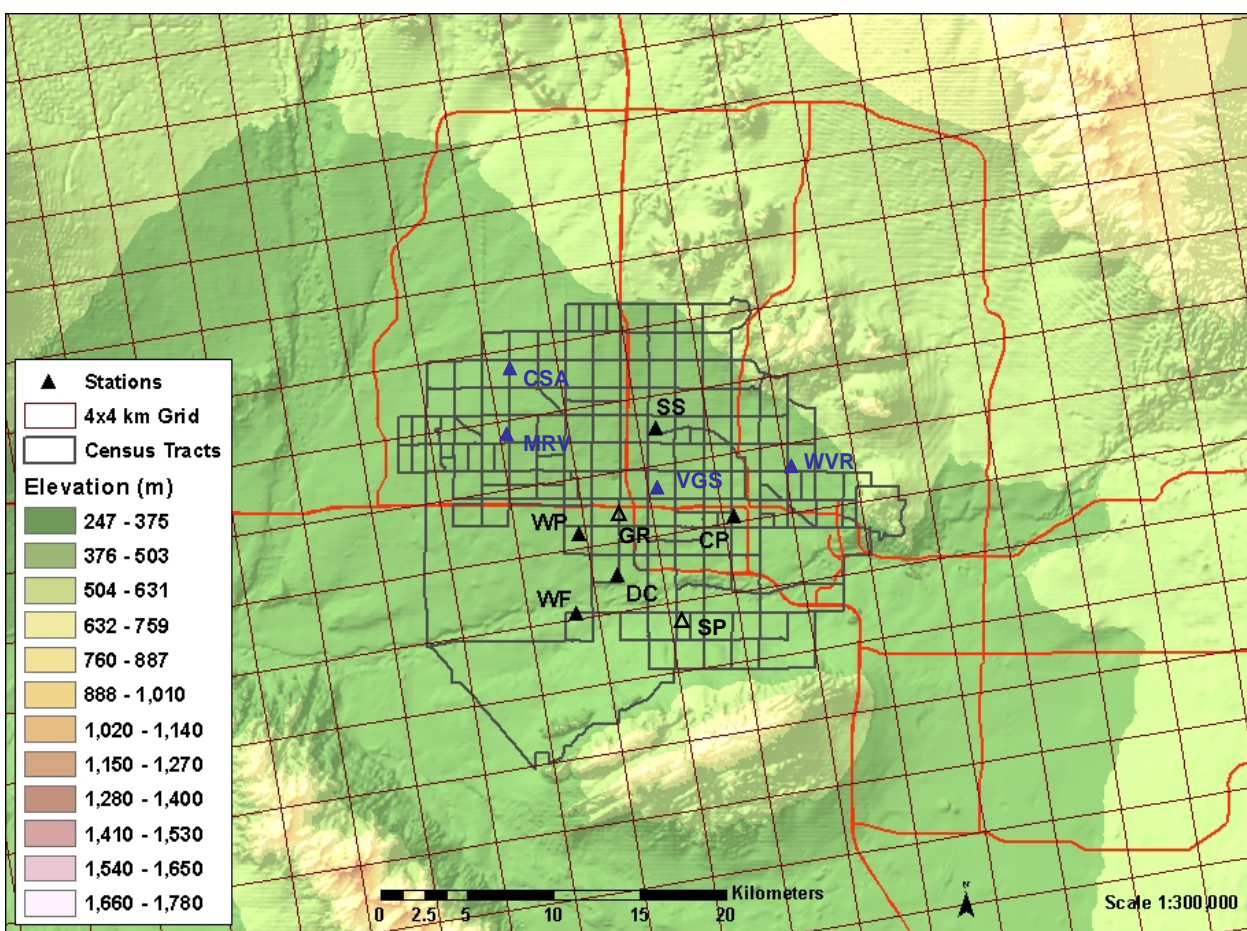
Figure 2.1. PM$_{10}$ monitoring sites with elevations for the Children's Health Project. The permanent monitors are black, the temporary – blue.

The PM$_{10}$ variation among all of the metropolitan sites can be seen in their 2006 annual averages, given in Table 2.2 and also expressed as a percentage of the lowest urban concentration site, Mesa. The central city sites, from WF to CP, have concentrations considerably higher than Mesa's (from 38 to 162% higher), varying widely among themselves. The PM$_{10}$ gradients are steepest here, tapering off in the more outlying portions of the central city.

Shown in Figure 2.2, these concentrations have their highest values and steepest gradients in south-central Phoenix, with almost all of the highest ones being south of I-10. As one moves west of 75th Ave, north of Bethany Home Rd, east of 36th St., and south of Dobbins Rd, the prevailing concentrations generally fall to the mid to low 30's, or even lower in the case of the Phoenix Mountain Preserve of the South Mountains. Because measured PM$_{10}$ concentrations exhibit high sensitivities to localized emissions; however, elevated concentrations can occur in the vicinity of such sources as major earthmoving projects or intensively tilled agricultural lands. Two such examples of these PM$_{10}$ discontinuities in metropolitan Phoenix are Higley in the southeast and Buckeye in the far west. The former's concentrations are elevated above the values expected with its distance from the city center by emissions from major earthmoving activities from road construction, commercial building, and residential housing developments, as well as from continued farming. The latter's concentrations are elevated from the same source categories, with the agricultural activities being the most influential. The greatest uncertainty in this concentration field lies to the west, but even this has been diminished by including measurements from a discontinued

county site called "Maryvale", at 61st Avenue and Encanto Boulevard, normalized to those of Central Phoenix (the former is 1.7% higher than the latter).

Table 2.2. Annual average (2006) PM_{10} concentrations ($\mu g/m^3$)
(bold sites used in the present work)

Symbol	Site name	Location or type	$[PM_{10}]$	% from Mesa
WF	**West 43rd Avenue**	Central	79.9	162
DC	**Durango Complex**	Central	69.2	127
HI	Higley	Suburban	60.6	99
SP	**South Phoenix**	Central	55.0	80
BU	Buckeye	Urban fringe	53.2	74
GR	**Greenwood**	Central	51.7	70
WP	**West Phoenix**	Central	49.8	63
MV[1]	Maryvale	Central	42.7	40
CP	**Central Phoenix**	Central	42.0	38
GL	Glendale	Suburban	36.3	15
SSC	South Scottsdale	Suburban	35.0	19
NP	North Phoenix	Suburban	34.4	13
SS[2]	**Supersite**	Central	32.9	8
DY	Dysart	Urban fringe	32.3	6
ME	Mesa	Suburban	30.5	0
ES[3]	Estrella Park (1995-2004)	Urban fringe	30.2	-1
AJ[4]	Apache Junction	Urban fringe	23.6	-23
PV[5]	Palo Verde (1997-2004)	Urban fringe	21.9	-28
AO[6]	Ajo (1995 – 2003)	Remote small town	20.2	-34
OP[7]	Organ Pipe (1995-2004)	Background	10.6	-65

1. MV, Maryvale, a discontinued county site at 61st Avenue and Encanto Blvd. The 2006 annual average is estimated by the MV/CP long-term average.
2. SS, Supersite, 2006 average was estimated by the SS/CP long-term average.
3. ES, Estrella Park, a discontinued ADEQ site, near Estrella Parkway and the Gila River, 18 mi (29 km) west-southwest of downtown (Van Buren, Grand, 7th Avenue intersection)
4. AJ, Apache Junction, a Pinal County site, 32 miles (51 km) east of downtown
5. PV, Palo Verde, a discontinued ADEQ site, 43 mi (69 km) west of downtown
6. AO, Ajo, Arizona, an ADEQ site, 83 mi (133 km) south-southwest (SSW) of downtown
7. OP, Organ Pipe National Monument, a National Park Service site, 105 mi (169 km) SSW of downtown

Although the two highest concentration sites, West 43rd Avenue (WF) and the Durango Complex (DC) garner most of the regulatory attention, the Greenwood site deserves special mention, as well. Unlike the top two, whose elevated concentrations can in part be attributed to the somewhat localized windblown and mechanically generated PM_{10} emissions along the Salt River, Greenwood, named for the cemetery across the street, is situated in a residential neighborhood with little in the way of fugitive dust emissions. Instead, this monitor is affected by heavy traffic on nearby paved roads. (Traffic on paved roads generates PM_{10} emissions by resuspending soil particles from the road surface and by exhaust emissions, with the former having ten times the weight of the latter.) From the monitor inlet it is 10 meters east to the busy arterial of 27th Avenue (19,000 vehicles on an average weekday (ADT)), 905 m east to I-17 (112,000), and 85 m north to Interstate 10 (229,000 ADT). PM_{10} concentrations from this monitor, with suitable adjustments for wind direction and traffic volume, could be assigned to all of the freeway corridors in the central city.
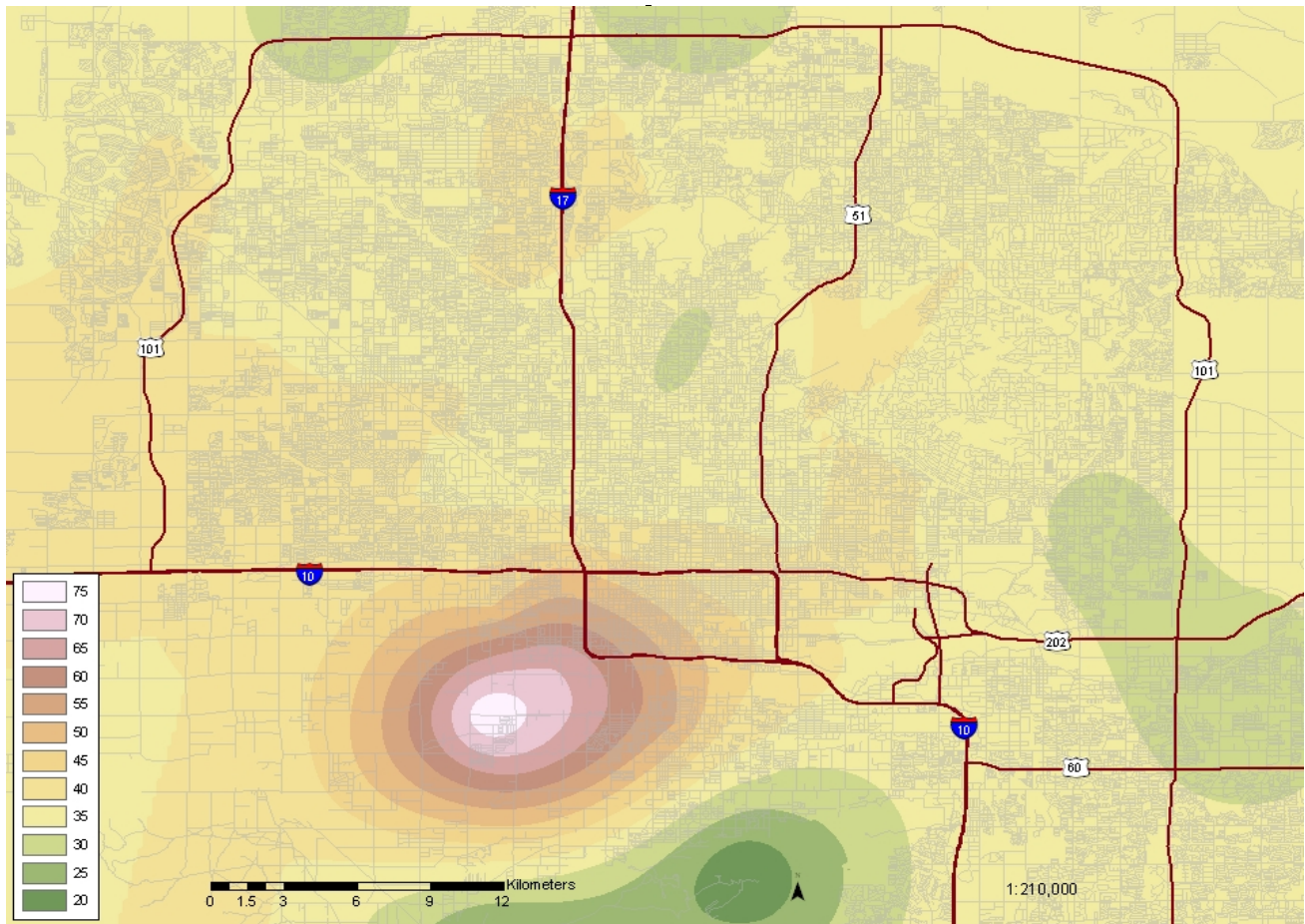
Figure 2.2. Spatial distribution of annual PM_{10} concentrations –central Phoenix for 2006

Temporary PM_{10} sites for this project

Given the five permanent monitoring sites with complete records in 2005 – 2006, and considering that the Greenwood and South Phoenix continuous PM_{10} monitors began operation after 2005, additional continuous PM_{10} monitors were thought desirable for this project. ASU and ADEQ staff established four temporary sites and operated them from November 2007 through March 2008. These additional concentrations, with the Greenwood and South Phoenix sites included as well, provided the 11 points required for the more sophisticated interpolation technique called "ordinary kriging" (the simpler technique is inverse distance weighting, or IDW). The temporary sites were chosen to fill the gaps in the geographic coverage of the permanent PM_{10} network and to be placed in areas with moderate to high numbers of asthma cases. These four temporary sites are shown as three-initial labels in Table 2.1 and Figure 2.1, with additional details given in Appendix A. Even though the PM_{10} concentration fields built with the 11 monitors did not differ much from those based on the original five, the efforts involved were considered well worth while. Without these six additional sites, the fidelity of the interpolated fields based on only the five permanent monitors would have remained too uncertain for comfort.

The PM_{10} concentrations at these four temporary sites were generally lower than those at the permanent sites (Table 2-3).

Table 2.3. December 2007 PM_{10} monthly average concentrations ($\mu g/m^3$)

Label	Name	Type	[PM10]
DC	Durango Complex		49.6
WF	West 43rd Avenue		46.1
GR	Greenwood	Permanent	42.9
SP	South Phoenix		39.6
WP	West Phoenix		38.2
CSA	CSA of Glendale	Temporary	33.7
CP	Central Phoenix	Permanent	32.8
VGC	Valley Garden Center	Temporary	31.4
MRV	Maryvale		28.5
SS	Supersite	Permanent	28.3
WVR	Weaver's Auto Service	Temporary	21.8

Chapter 3 Interpolation methods

Introduction

Interpolating air pollutant measurements to produce spatial concentration fields has a rich history on all scales -- urban, regional, and global. What distinguishes the present work is the nature of the pollutant. Instead of gaseous air pollutants or fine particles that mimic gases (particles 2.5 microns and smaller, "$PM_{2.5}$"), this project concerns particles 10 microns and smaller, or "PM_{10}". In metropolitan Phoenix the coarse fraction of the aerosol (2.5 – 10 microns) comprises two thirds of the mass of PM_{10} and consists of particles that are 90% geological. Even the fine fraction has an appreciable geological component (20%), in addition to the usual secondary and combustion particles. Speciated aerosol measurements show that somewhat less than one fourth of the regulated PM_{10} comes from the better understood and more homogeneously distributed emission sources such as fuel combustion from motor vehicles, industrial combustion, and food cooking, as well as the secondary components of nitrate and sulfate. Most of the remaining three quarters, virtually all geological, comes from paved road dust, construction dust, windblown dust, and unpaved road dust. It is precisely this geological, or "soil", or "crustal" component that defies efforts to build precise emission inventories, and, with a few notable exceptions, including the present work, makes it difficult to simulate with numerical models on an urban scale. Because the continuous $PM_{2.5}$ monitoring network in 2005-2006 was limited to two stations, PM_{10} was the choice for this project.

Practical constraints make it impossible to obtain data at every desired point. Thus, interpolation is important and fundamental to graphing, analyzing and understanding the spatial distribution of air pollution throughout a metropolitan area. Interpolation methods selected in this study were inverse distance weighting and ordinary kriging, the former with the five permanent PM_{10} sites in 2005-2006; the latter, with the expanded network from December 2007 – February 2008. Hourly concentrations were converted to daily 24-hour averages for the daily spatial concentration fields. In addition, select hours were also examined on a case by case basis. Some consideration was given to using emission or traffic estimates to adjust the interpolated values, but this was rejected.

Inverse distance weighting

Inverse distance weighting (IDW) is one of the simplest interpolation methods. A neighborhood in the vicinity of the interpolated point is identified and a weighted average is taken of the observation

values within it. The weights are a decreasing function of distance. The user has control over the mathematical form of the weighting function, the size of the neighborhood (expressed as a radius or a number of points), in addition to other options. In this project, IDW was used to interpolate the PM_{10} concentrations of 2005-2006 from the five permanent monitoring sites with an automated function in Geographic Information Systems (GIS). Within ArcGIS 9.2 software, the Spatial Analyst extension tool was used to create IDW interpolations within the study area. Within Spatial Analyst, a pull-down menu is found in which the user can input the specific information pertaining to the dataset utilized. In the pull-down menu, default input parameters were selected. This included selecting PM_{10} for the z-value, a power value of two, a variable search radius with 12 points, and the search radius distance value unspecified. Once the proper data files were selected in the pull-down menu, the GIS software then automatically created a temporary interpolation raster, based on the PM_{10} value at each of the five monitor sites on the specific day or hour selected. (A "raster" is a scanning pattern of parallel lines that form the display of an image projected on a display screen.) Next, the temporary interpolation raster files were made permanent by saving each hourly file in the table of contents section of ArcMap, the principal graphical user interface to create maps in ArcGIS. Finally, the interpolated surface value tables were aggregated by census tracts in Excel. Census tract shapefiles, containing the new information from these interpolations, were then finalized as graphics in ArcMap.

Ordinary kriging

Ordinary kriging is a geostatistical approach to modeling. Instead of weighting nearby data points by some power of their inverted distance, it relies on the spatial correlation structure of the data to determine the weighting values. This is a more rigorous approach than IDW, as correlation between data points determines the estimated value at an unsampled point. Ordinary kriging makes the assumption of normality among the data points, as well as an unknown constant trend. This is unlike simple or universal kriging, which assume a known constant trend and/or model.

The word "kriging"is synonymous with "optimal prediction". Kriging methods, including ordinary kriging, utilize a variogram model to express the spatial variation of data points, and then minimize their error.

For this project, the Spatial Analyst extension in ArcGIS (the same used for IDW analysis) was chosen as the optimal automated method to create kriged surfaces of PM_{10}. After selecting an hourly file containing PM_{10} for the z-value, the spherical semivariogram model was selected in the pull-down menu as the best way to create a kriged surface with the least amount of error. The advanced parameters tab, which allows for input on the lag size, major range, partial sill, and nugget size, was not used. Default options, including a variable search radius with 12 neighbors, and an unspecified search distance, were used to create temporary interpolated raster files. As was the case with IDW, interpolated files were first made permanent, and were then aggregated into census tract shapefiles in Excel and ArcMap, to create maps of kriging values within study area census tracts.

Comparison between IDW and ordinary kriging

Each interpolation method has its advantages and disadvantages. Although ordinary kriging is more rigorous and better at predicting surfaces at a distance from known data points, IDW can be utilized with fewer data points. For example, ordinary kriging performs best with a large number of data points, ideally above 50, although as few as 10 can be used. IDW on the other hand, can create a prediction surface, though based mainly on nearest neighbors, with as few as 3-4 points within a given area. Figure 3.1 illustrates results from the two methods. Five PM_{10} station values were used in IDW on the left; 11 stations were used in ordinary kriging on the right. Figure 3.2 shows the

percentage differences between the two methods $(PM10_{IDW}-PM10_{KR})/PM10_{IDW}$. In Figures 3.3 and 3.4, statistical comparisons between the two interpolation methods reveal better agreement close to the central part of the study area, in close proximity to the five permanent PM_{10} monitors. Greater disagreement between the two models occurs in the outer edges of the study area, in census tracts close to the temporary PM_{10} monitors.
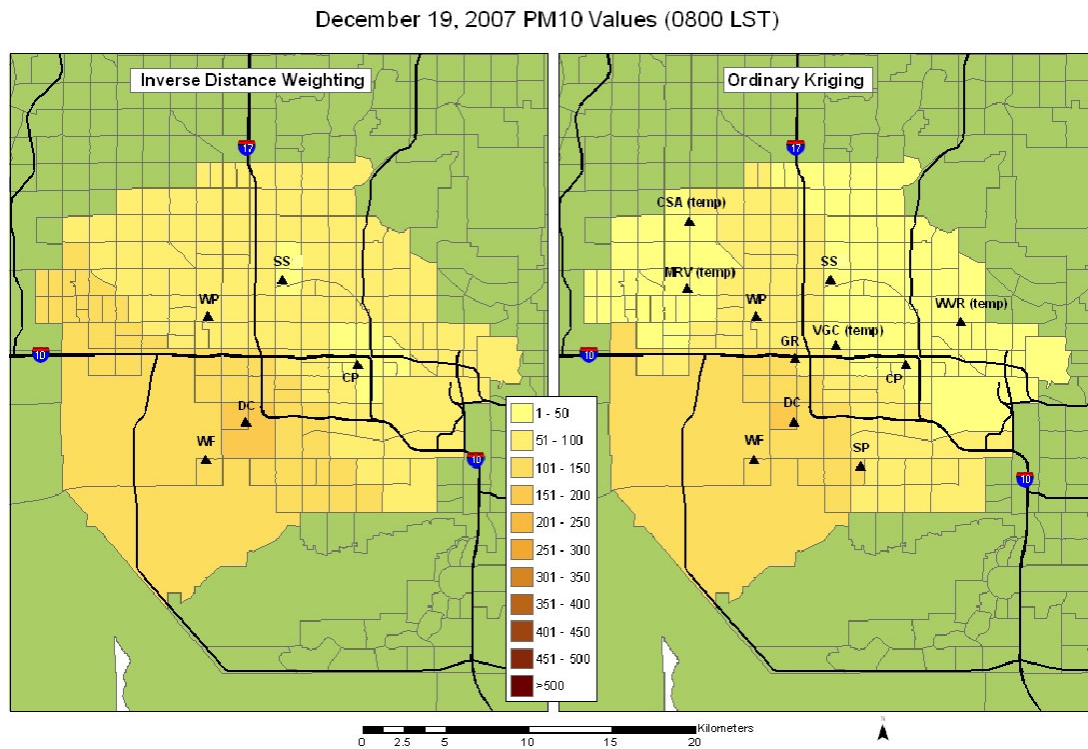
Figure 3.1. Comparison between IDW and Ordinary Kriging methods
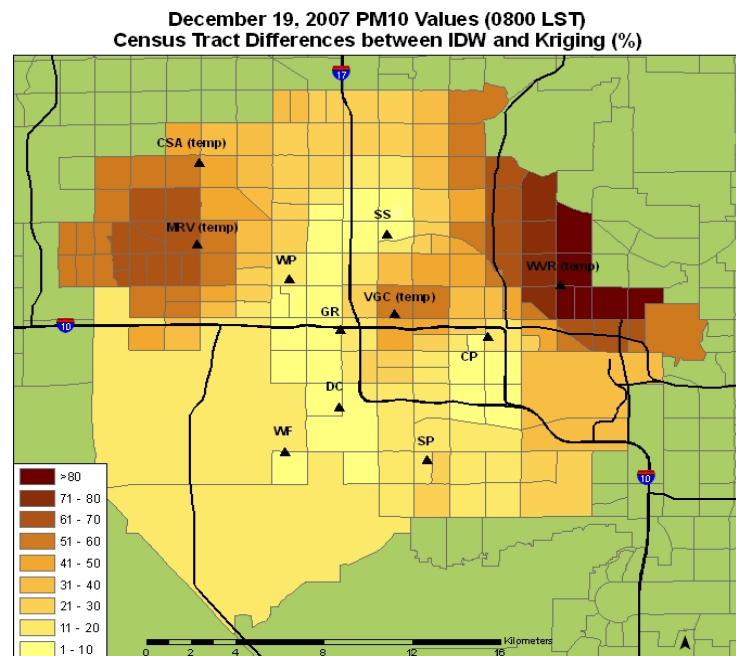
Figure 3.2. Percentage differences $\dfrac{PM10_{IDW} - PM10_{KR}}{PM10_{IDW}} * 100$ between IDW and Ordinary Kriging methods – December 19, 2007, 8am

15
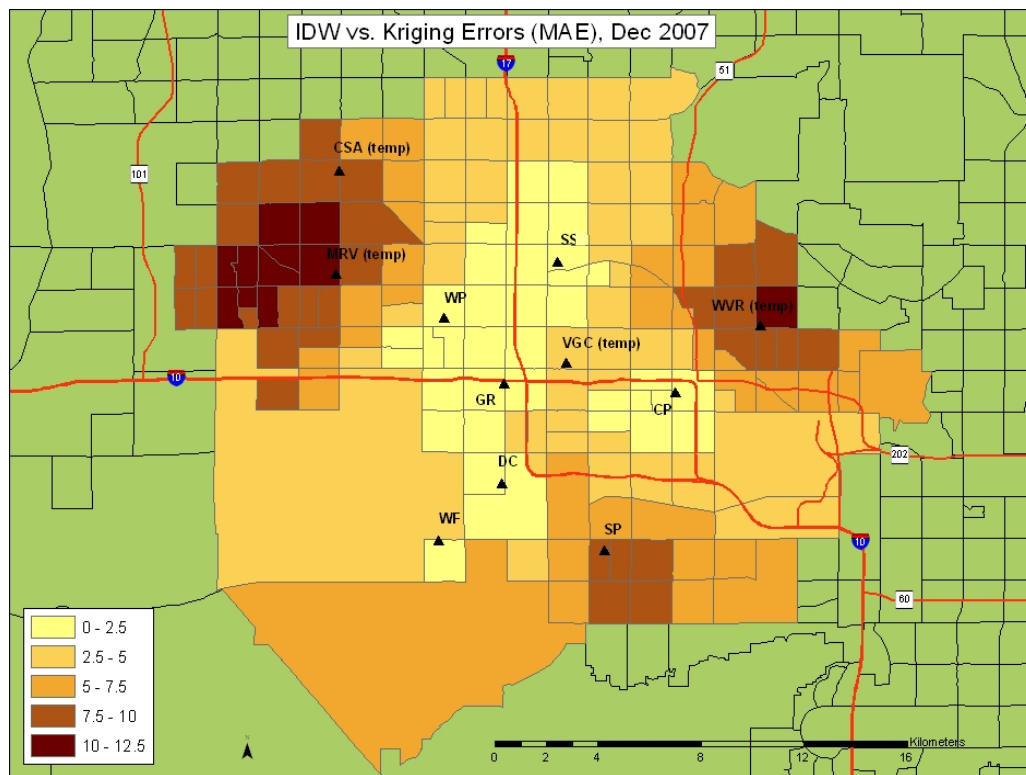
Figure 3.3. Mean Absolute Errors (MAE) for December between IDW and Ordinary Kriging methods – based on daily maps
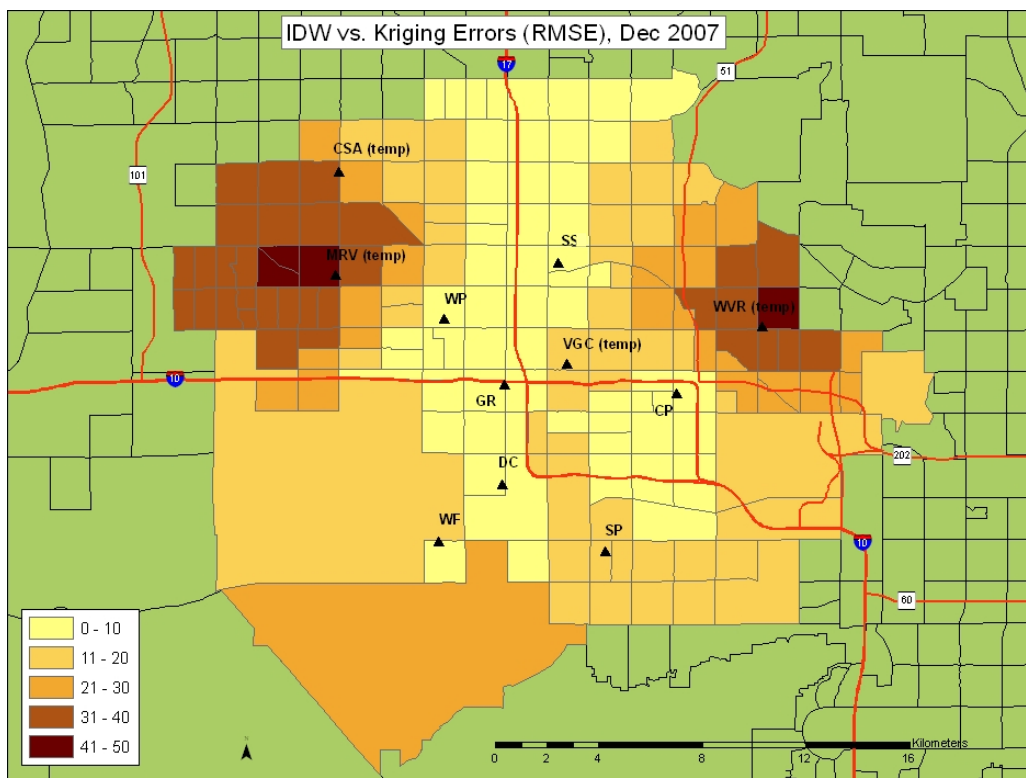
Figure 3.4. Root Mean Square Error (RMSE) for December between IDW and Ordinary Kriging methods – based on daily maps (see Appendix D for mathematical definitions of MAE and RMSE)

Chapter 4 Neural network

Introduction

Traditionally, the term "neural network" referred to a circuit of biological neurons. The modern usage of the term often refers to networks made up of artificial neurons or "nodes." These networks consist of interconnecting artificial neurons such as programming constructs that mimic the properties of biological neurons. Neural networks have been developed and used widely in both applied mathematics and applied science, including predictive modeling based on a time series of measurements – its application in the present work. Other application areas include system identification and control (vehicle control, process control), game-playing and decision making (backgammon, chess, racing), pattern recognition (radar systems, face identification, object recognition), sequence recognition (gesture, speech, handwritten text recognition), medical diagnosis, financial applications, data mining, and e-mail spam filtering. These networks are always imbued with the capability of "learning" through "training," with a variety of different methods employed. Although this may appear somewhat metaphysical, it really boils down to a set of data and predictive equations, which, exercised daily, acquires "knowledge" and an improved predictive ability through the simple acquisition and prediction of additional data. In this project the neural network's application was limited to the prediction of historical PM_{10} concentrations. An operational neural network, on the other hand, would make the daily predictions of tomorrow's air pollution. This network would acquire more "skill" with time as additional daily relationships between PM_{10} concentrations and meteorological variables were encountered, processed, and predicted.

In the present work, an artificial neural network called "EnviNNet" was developed and applied to the PM_{10} monitoring record at the Central Phoenix (CP) site, with the goal of constructing an air pollution predictive system that might complement the deterministic system of the grid-based air quality model, discussed in Chapter 5. Four steps were necessary:

1. Assemble hourly records of PM_{10} and meteorological variables from one monitoring site, preferably for three years or more (only one year was examined in this project).

2. Derive and calculate statistical relationships between the PM_{10} concentrations and the meteorological measurements.

3. Run a meteorological predictive model such as MM5 (see Chapter 5) for each day of the historical record examined, determining quantitatively how well its predictions matched the measurements.

4. Build the artificial neural network and the meteorological modeling system such that predictions of PM_{10} are forthcoming for each day of the historical record. Compare these predictions with the measurements.

Should an organization wish to apply the neural network in a genuine air pollution predictive system, then the requisite software would need to be installed, the data gathering mechanisms built, the meteorological model would be set up for daily operational forecasts, and considerable staff training would have to take place. The remainder of this chapter discusses some aspects of these artificial neural networks and describes how the EnviNNet was built.

Considering its wide usage in atmospheric applications (Gardner and Dorling 1998), a type of neural network called "Multi Layer Perceptron (MLP)" was employed. The MLP structure consists of an interconnected system of nodes (neurons) within a hidden layer that employs non-linear

continuous transfer functions connecting input and output vectors. (Appendix B provides more details.)

Phoenix case study

As the first step, PM_{10} and meteorological data from the Central Phoenix (CP) monitoring station were assembled. EnviNNet was trained using a selected set of appropriately pre-processed historic time series data at CP, whereupon it was used to predict PM_{10} in the hindcasting mode. The input vector is made of the following variables:

1. *Pollution data* - These constitute the endogenous component of the NN (A component or variable is called **endogenous** if it is explained within the model in which it appears). Time lags are selected by optimizing the data reconstruction efficiency of the NN, so as to achieve the best trade-off between sensitivity and specificity. Since these are multi-step operations, the measured pollutant levels are used in a rolling mode to generate the reconstructed values.

2. *Meteorological measurements* - These comprise the exogenous component of the NN, and have a modulating effect on PM_{10} concentrations (**exogenous** refers to an action or object coming from outside a modeling system). The time lags were selected as before, and the balance between data reconstruction efficacy and network efficiency was optimized.

3. *Statistical and descriptive indicators* - These represent the behaviour of the "Central Phoenix" neighbourhood via classes of input parameters that account for aggregated homogeneous spatio-temporal bands of microclimatic factors and air pollutant concentrations. The latter are dependent on the wind velocity, wind direction, and emissions specified as either weekday or weekend/holidays.

The meteorological and emissions characteristics of low, moderate, and elevated PM_{10} concentrations at CP have to be accounted for in developing the NN, which makes the training strategy critical for reliable predictions. Since daily PM_{10} concentrations vary widely throughout the month and year, specific input models had to be built by combining time section data of different years to make the NN robust and adaptive to the local climate. The data for training came from selected four-to-six-month windows, as well as from time periods that show noteworthy patterns such as exceptional events.

Input variables selected for training are:

- Historical series of PM_{10} and meteorological data collected at CP during 2005-2006, prior to the dates selected for hindcasting;

- A selection of days based on analysis and correlations of historical series representing PM_{10} trends in the time window selected;

- Noteworthy patterns observed outside the time window of training (e.g. significant PM_{10} peaks representative of exceptional events).

In this phase, the intrinsic parameters of the NN were estimated by numeric optimization until a satisfactory convergence was obtained. The weights and time lags so identified naturally depend on the site (e.g. local weather and neighbourhood emission characteristics). The most important aspect of this particular training is to obtain a non-linear dynamic relationship that connects input data with PM_{10} output so that the NN can be operated in the hindcasting mode.

Results

The neural-network system gave dependable results for the Central Phoenix monitoring site. These results, compared with those of CMAQ in Chapter 6, are illustrated in Figure 4.1. PM_{10} predictions in arid climates are difficult and a correlation coefficient of 0.38 is better than average.
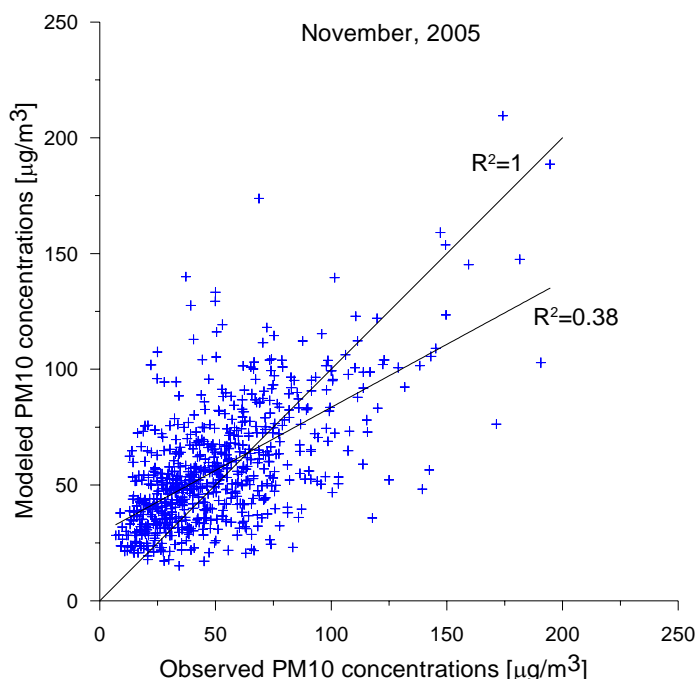
Figure 4.1. 24-hour average PM_{10} predictions from the neural network versus observations at the Central Phoenix site for 2006

Chapter 5 Air Quality Modeling

Introduction

This chapter describes the deterministic, grid-based numerical models employed in simulating the central Phoenix PM_{10} concentrations. The three kinds of models are meteorological, emissions, and air quality. In addition, near the chapter's end, the air quality model results are discussed in light of the interpolated concentration fields of Chapter 3.

The MM5/SMOKE/CMAQ modeling system was employed to simulate PM_{10} concentrations in central Phoenix. This widely used, sophisticated platform has been adopted as a regulatory tool. The predictive system consists of three integrated models: the Pennsylvania State University and National Center for Atmospheric Research (NCAR) Mesoscale Meteorological Model - MM5 v3.7 (Grell and Dudia, 1994) for simulating the weather, the Sparse Matrix Operator Kernel Emissions – SMOKE v2.2 model for emissions processing (Carolina Environmental Program, 2005). and the Community Multiscale Air Quality Model – CMAQ v.4.5 (Byun and Ching, 1999) for simulating pollutant concentrations.

MM5 is a terrain-following model that simulates mesoscale atmospheric circulation. It has been applied to a broad spectrum of studies, including land-sea breezes, mountain-valley circulation, and real-time weather forecasting. The data for model initialization and lateral boundary conditions were obtained from the operational NCEP/Eta model (40km grid resolution) and NCEP global surface and upper air observations every three and six hours, respectively. ("NCEP" is the National

Weather Service's National Center for Environmental Prediction and "Eta" is one of the global weather models.) Three-dimensional analysis and surface nudging with observed data were used to generate grid-based meteorological fields. MM5 provided the meteorological input to CMAQ. Appendix C contains further modeling details.

The SMOKE model produces gridded, hourly emissions for CMAQ, using meteorological fields from MM5 and a host of emission estimating techniques. Temporally, spatially, and chemically resolved model-ready emissions were prepared using the recent Western Regional Air Partnership (WRAP) emissions inventory (including the BRAVO-1999 study for the Mexico emissions inventory).

Developed by EPA in the 1990s, CMAQ is a multi-pollutant, multi-scale air quality model that contains techniques for simulating all atmospheric and land processes that affect the transport, chemical reactions, and deposition of atmospheric pollutants and/or their precursors on both regional and urban scales. It is designed as a science-based modeling tool for handling all the major pollutants such as ozone and particulate matter. This "Eulerian" or grid-based model produces hourly concentrations of a number of pollutants in the frame of a fixed, three-dimensional grid with uniformly sized horizontal grid cells and variable vertical layer thicknesses. This model has undergone numerous applications and performance evaluations, in Phoenix, in Arizona (Yuma and Douglas), in the Western United States, and throughout the world.

Modeling domains

The modeling domain was based on a Lambert Projection centered at (97°W, 40°N), with three nested domains having 36, 12 and 4km grids to predict meteorology, emissions, and air quality, respectively. In the nested simulations, the results obtained from the outer domain were used as initial and boundary conditions for the inner domain (Figure 5.1). Vertically 29 levels were specified with the layer closest to the ground being seven meters thick to capture boundary-layer processes. The inner domain with 4x4km grids was centered in the Salt River Valley in central Phoenix.
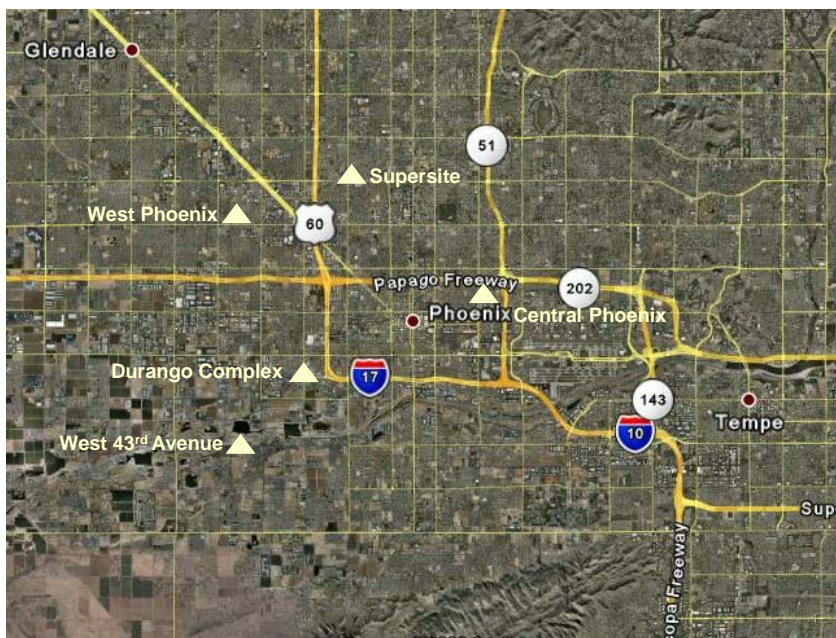
Figure 5.1. Modeling domains for MM5/SMOKE/CMAQ simulations

Modeling periods

The modeling periods selected were constrained by the available air quality and health data in 2004-2006. As was described in Chapter 2, there are five monitors in the study area with hourly PM_{10} concentrations, but only two with hourly $PM_{2.5}$ concentrations. Therefore, the study examined only the PM_{10} concentrations. One part of the project was to develop and test different interpolation techniques to build spatial concentration fields. These interpolation methods require from five to ten monitoring sites, another reason that the $PM_{2.5}$ data could not be used. In 2004 the sites of West Phoenix and West 43rd Avenue had incomplete records, restricting the analysis to 2005 and 2006. The 24-hour averages of PM_{10} are shown for the five monitors in Figure 5.2, whose names and designations are given below:

CP – Central Phoenix
DC – Durango Complex
WF – West 43rd Avenue
WP – West Phoenix
SS – Supersite

Different periods with high and low pollution levels were selected for analysis.

- **High pollution** (above the National Ambient Air Quality Standard of 150μg/m^3 for a 24-hour average); November 2005; December 12-19, 2005; January 10-20, 2006; November 2-16, 2006

- **Low pollution** (less than 75μg/m^3); September 3-15, 2005; August 2005; March 11 - April 9, 2006; August, 2006
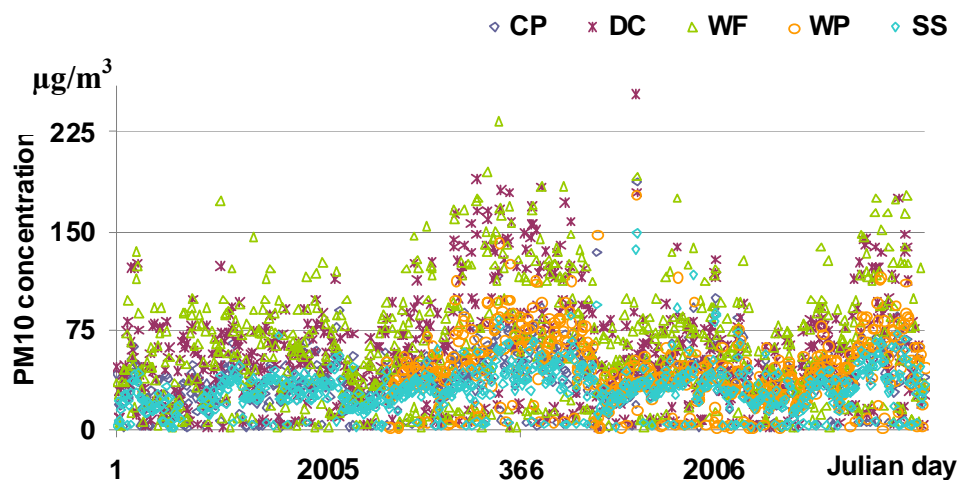
Figure 5.2. 24-hour averaged PM_{10} observations for 2005-2006

The daily counts of emergency department visits and hospital admissions with an asthma diagnosis in Maricopa County, shown in Figure 5.3, were divided into four categories:

- **Worst**: greater than the sum of the average and the standard deviation;

- **Bad**: between the annual average and the sum of the average and the standard deviation;

- **Moderate**: between the average and the difference between this average and the standard deviation;

- **Good**: less than the difference between the average and the standard deviation.
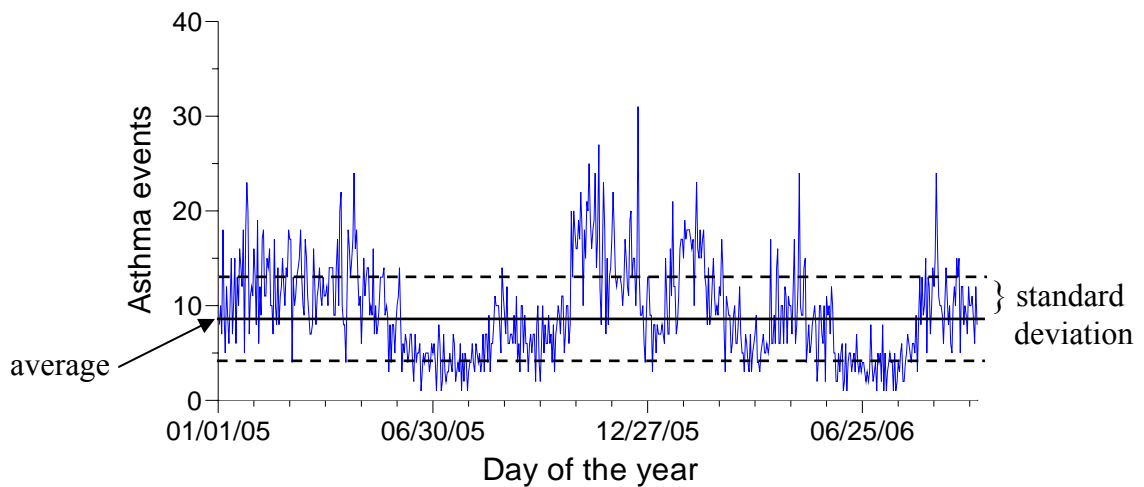
Figure 5.3. Daily emergency department visits and admissions to hospitals of children ages 0-17 in Maricopa County with an asthma diagnosis for 2005 – 2006

The average number of daily asthma visits is 9 with a range from 1 to 31. The seasonal pattern is virtually identical for both years. The good category occurs almost exclusively in July; the worst category is mostly limited to a period from the last week of October until March 1, with a hiatus from December 20 to January 20, when the level of admissions stays in the moderate range.

Simple statistical analyses of the 24-hour PM_{10} concentrations and daily asthma visits were carried out to help select the modeling periods. Curves in Figure 5.4 illustrate the variations throughout the two years, with a seasonal periodicity in both PM_{10} and asthma being quite evident. The periods when the two data sets diverge are well displayed. The highest number of asthma incidents and elevated PM_{10} concentrations occurred together in November 2005 through January 2006. A decrease in asthma incidents near the end of December, while PM_{10} concentrations remain elevated, may be due to behavioral changes during the Christmas holidays. November 2005 had the highest number of asthma incidents; this month was selected to represent "high pollution" conditions. It was more difficult to select the period of low pollution because of incoherence in both data sets. The lowest PM_{10} concentrations were recorded in August, while the lowest numbers of asthma incidents came in July. One period with both low PM_{10} levels and low numbers of asthma cases was found in March-April 2006. This period was chosen to represent "low pollution" conditions.

The modeling was conducted for the two selected periods:

- November 2005, with high pollution, and
- March 11 - April 9, 2006, with low pollution.

Modeling runs were carried out with 31 hours of spin-up time for the weather predictions and 24 hours for the air quality modeling. "Spin-up" time means that the model run is begun before the day (or period) of interest. This allows its calculations to begin before the period of interest, reducing the influence of the initial conditions on the model results.

22
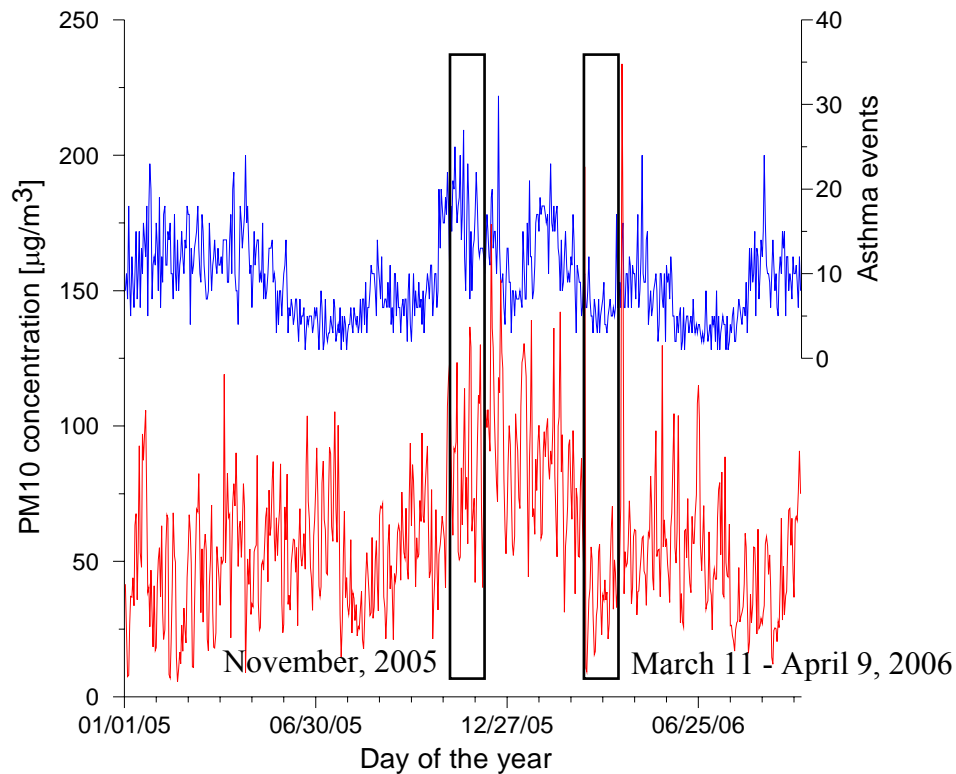
Figure 5.4. PM_{10} concentrations and asthma events (2005-2006)

Modeling results and discussion

Numerical simulations were carried out with the MM5/SMOKE/CMAQ modeling system for both high and low pollution periods and were compared with observations from the five permanent air monitoring stations. This model validation was necessary to estimate the model's performance in the study region. Air pollutant concentrations depend on meteorological conditions such as wind and rainfall, as well as on the strength and patterns of air pollutant emissions. Consequently, in any air quality model's performance evaluation, one must take into account the uncertainties in both the emission and meteorological models.

Model runs for two time periods: November 2005 and March 11 - April 9, 2006, show reasonable results in comparison with the observations. The scatter plots of simulated hourly PM_{10} concentrations versus the observations at all five locations in central Phoenix are shown for both periods with their corresponding regression coefficients (Fig. 5.5).

CMAQ generally overestimated the low (<50μg/m³) and underestimated the elevated (>150μg/m³) observed PM_{10} concentrations for both periods, with better correspondence between observed and modeled data for the high pollution period. Elevated PM_{10} levels were a frequent occurrence at the Durango Complex (DC) and West 43th Avenue (WF) sites, well above the other three sites in winter. For this reason the model results were also compared with the measurements in two groups:

- CP, WP, and SS, the three lower concentration sites, and

- DC and WF, the two higher concentration sites (Figure 5.6).
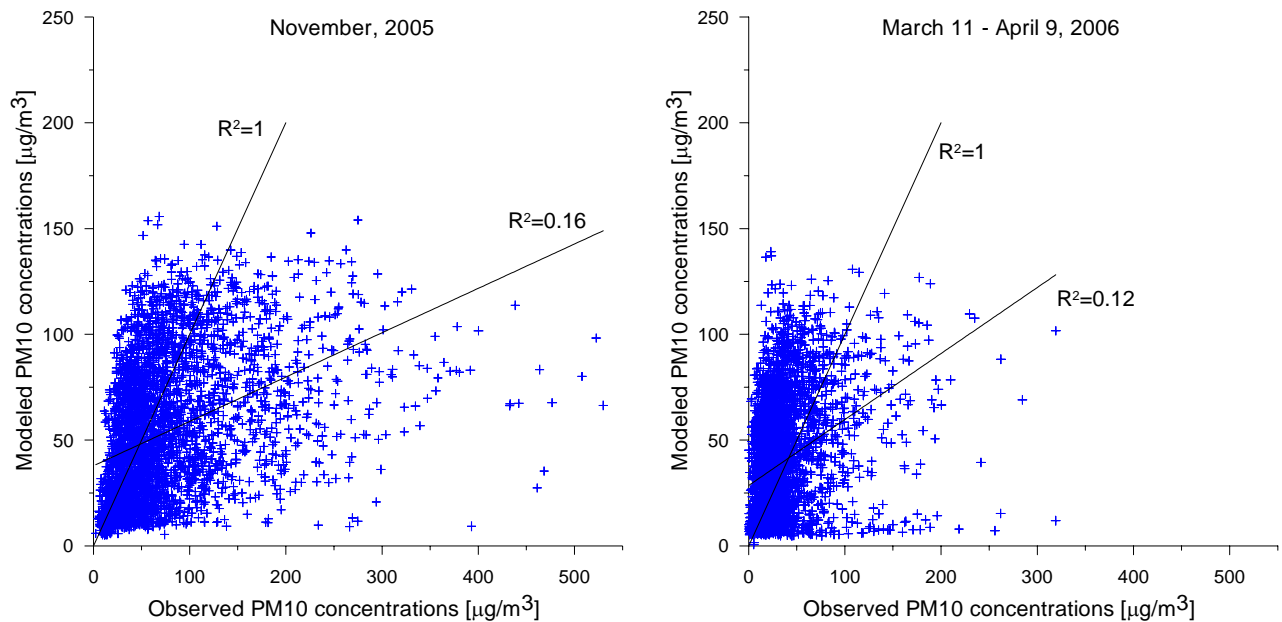
Figure 5.5. Simulated and observed hourly PM_{10} concentrations in central Phoenix for periods of high pollution (left) and low pollution (right) – from all five monitors

The coefficients of determination, which quantify the goodness of the fit and are 1.0 for perfection, were less than 0.2 for all five sites within the study domain with the 4km grids. Perhaps this level of performance can be attributed to various inadequacies of the emissions inventory. Even a perfect description of the boundary layer air flow from the meteorological model would not produce excellent modeled air pollutant concentrations as long as the estimated PM_{10} emissions were inaccurate in magnitude, space, and time. As the WRAP emission inventories came in 36 and 12km grids, the 4km emissions for the central Phoenix model runs were obtained by setting them equal to one ninth of the 12km emissions (there are nine 4km grids within a 12x12km square).
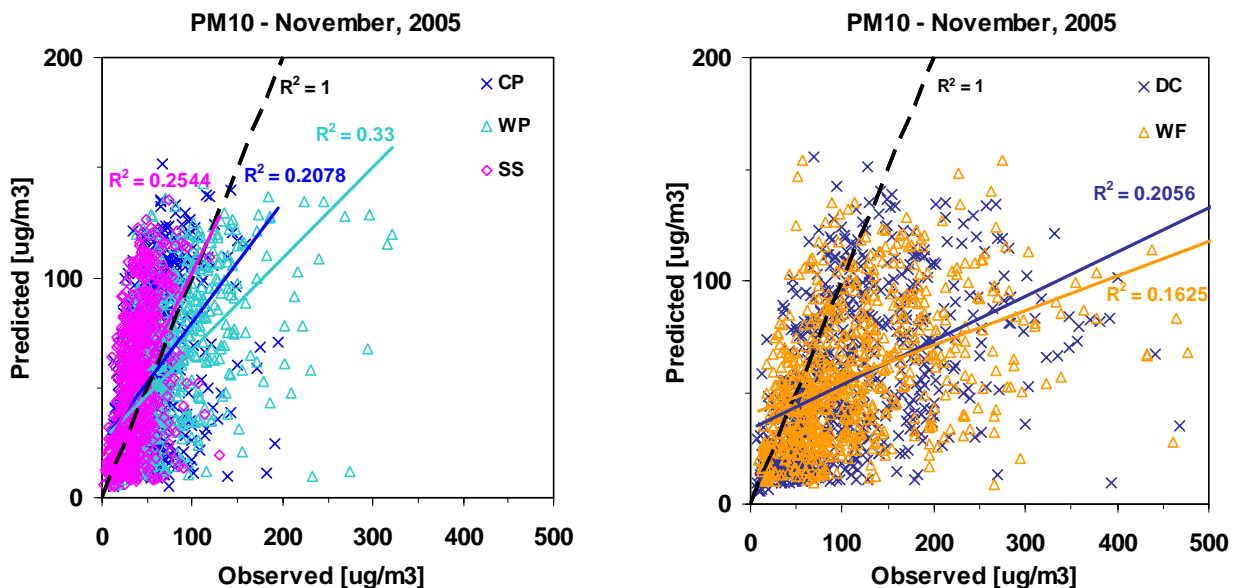
Figure 5.6. Predicted and observed hourly PM_{10} concentrations in central Phoenix for the two sets of monitors shown separately – high pollution period (November 2005)

24

One explanation for the elevated PM_{10} concentrations measured at the DC and WF monitors is that weekday "industrial" and roadway emissions add to the concentration loading already high from urban transport. The air quality model's inability to simulate these higher concentrations, demonstrated by the near-horizontal angle of the DC and WF regression lines in the right figure above, may lie with an insufficient emission inventory. One should keep in mind that while CMAQ has produced excellent simulations for ozone and chemically speciated fine particulates, whose atmospheric behavior mimics that of gaseous pollutants its ability to simulate PM_{10} has not been so good. The reasons for this lack-luster performance are many, and include:

- a single, spatially uniform emission value throughout a single grid – at complete odds with the spatial variability of real-world emissions;

- deposition phenomena that depend on the particle size distribution, as different emission sources produce particles with different distributions; The average particle size of the total mass of PM_{10} in central Phoenix is from five to seven microns, large enough to be deposited somewhat rapidly to the ground, in contrast to the smaller particles comprising the fine fraction (smaller than 2.5 microns), which remain suspended considerably longer.

- the sporadic and unknown temporal distribution of most fugitive sources that cannot be captured by any emissions inventory; and

- the heterogeneous spatial distribution of ambient PM_{10}, exemplified by monitors influenced by localized emissions that vary widely in their distance from the monitor, in their timing, in their release height, and in their magnitude.

Despite its shortcomings, a deterministic model such as MM5/CMAQ offers three advantages over its statistically based competitors, providing:

1. nearly complete geographic coverage, albeit limited to the size of the grid, and adequate temporal coverage in the form of hourly averages, with simulated values of both meteorological variables and air pollutant concentrations calculated for each and every grid cell;

2. air quality predictions years or decades into the future, necessarily dependent on the reliability of a future-year emissions inventory; and

3. a way to quantify the benefits of specific air pollution control strategies, accomplished by modifying a future, base-case emissions inventory to reflect the anticipated emission reductions from the controls.

While only the first advantage is of relevance to the Children's Health project, the other two should be considered in any general assessment of the utility of deterministic models.

A disadvantage of CMAQ is that, as a deterministic model, it has none of the interpolation techniques that could better fit its output to the observed data. Furthermore, the emissions data and meteorological data that drive CMAQ each have considerable uncertainties, the former to a far greater degree than the latter. These uncertainties, as well as those inherent in its embedded science, cause it to predict better for longer time scales (monthly, annual) than for shorter times (1-hour or 24-hour); and to be the most error prone with smaller grid cells. The "soccer goal" plot, recommended by USEPA (Guidance on the Use of Models, 2007), is a convenient way to visualize

model performance, as both bias and errors are shown on a single plot. Two statistics -- the Mean Fractional Error and the Mean Fractional Bias -- for both the high and low pollution periods are plotted for the different sites in Figure 5.7. As bias and error approach 0, the points are plotted closer to or within the "goal" represented here by the dashed boxes. (See Appendix D for the mathematical definitions of these and other statistics.) The plot shows reasonable model performance, with only a single site being out of the goal area -- West 43th Avenue for the high pollution period.
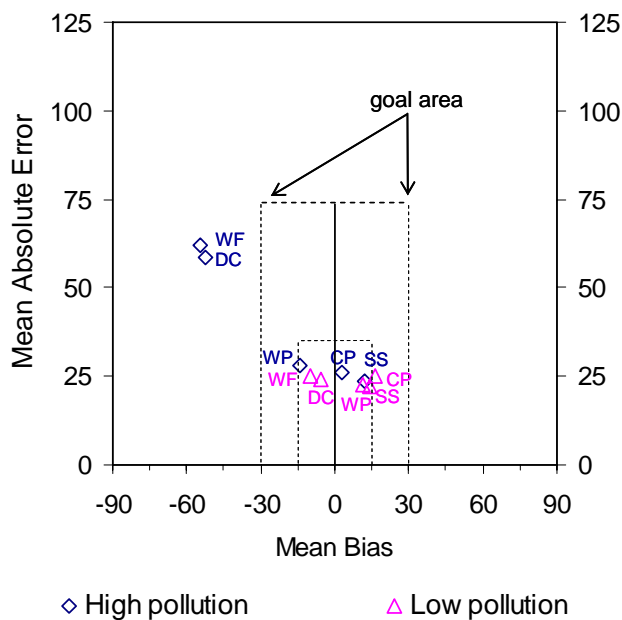
Figure 5.7. The "soccer goal" plot measures both bias and error for central Phoenix

In addition to this visual estimate of performance, the different statistics that were calculated to estimate the model performance for the study periods also show reasonable model performance (Table 5.1).

Of all these statistics, perhaps the most telling one is the Index of Agreement (IA): its values range from 0.46 to 0.72, with perfect agreement being 1.0. The best IA was achieved at WP during the winter and at DC during the spring. The better known Coefficients of Determination (RSQ), also known as the linear "correlation coefficient" abbreviated as "R^2, ranges from 0.10 to 0.33, indicative of a slightly positive correlation. This weak correlation is often found in matching numerically modeled concentrations with the measured ones in air pollution studies, especially for PM_{10}. The Mean Absolute Errors (MAE) are all less than 30 except for DC and WF in November 2005. The local emissions not taken into account with sufficient spatial and temporal accuracy in the emissions inventory contribute to this disagreement. CMAQ overestimated the PM_{10} concentrations at CP and SS: the Modified Coefficient of Determination (RSQ*) is greater than 1; but it underestimated the observations at WF and DC, where RSQ* is less than 1 for both high and low pollution periods. At West Phoenix (WP) the model under-estimated the higher concentrations measured in November 2005 but over-estimated the lower ones in March-April 2006. The Root Mean Square Errors (RMSE) ranged from 26 to 42, except for the two problematic sites of WF and DC in November 2005, which had anomalously high values about 90.

26

Table 5.1. Statistical measures in comparing model-predicted hourly PM_{10} concentrations to observations for both study periods at different sites

Monitor	MAE	RMSE	RSQ	RSQ*	IA
Perfect agreement	0	na	1.00	na	1
November 2005					
Central Phoenix	26.12	34.39	0.21	1.45	0.68
West Phoenux	27.81	41.99	0.33	0.60	0.72
Super Site	23.48	30.06	0.25	3.30	0.62
West 43rd Avenue	62.21	89.85	0.16	0.06	0.51
Durango Cpmplex	58.49	85.80	0.21	0.68	0.55
March 11- April 9, 2006					
Central Phoenix	25.00	33.06	0.10	4.28	0.46
West Phoenux	22.78	30.25	0.16	2.39	0.59
Super Site	22.19	27.15	0.12	5.01	0.47
West 43rd Avenue	25.31	26.47	0.17	0.42	0.60
Durango Cpmplex	23.94	35.86	0.25	0.54	0.68

Abreviation: MAE - Mean Absolute Error; RMSE - Root Mean Square Error; RSQ - Coefficient of Determination (aka R^2); RSQ* - Modified Coefficient of Determination[2]; IA - Index of Agreement
[2]Modified Coefficient of Determination: values greater than 1 mean the model overestimated (orange); values less than 1 mean the model underestimated (green)

The health data are available only on a daily basis, and consequently, the prediction of accurate 24-hour averages of PM_{10} was of greater importance than the hourly values. Figure 3 shows the 24-hour averaged Mean Bias for both high and low pollution periods. The difference between daily calculated and observed concentrations can be substantial. While the average MB for 30 days was in the range of -15 to 15, except at WF and DC in November (see Fig. 5.7), the 24-hour averaged MB doubled for some days and is almost zero for the others, as can be seen from Figure 5.8.

The model underestimations (the negative MB) were most pronounced at Durango Complex and West 43rd Avenue, and a weekly periodicity can be found for the MB. The weekday industrial and roadway emissions add to already-high concentration loading from urban transport. These two regulatory problematic sites, which represent the worst PM_{10} air quality in metropolitan Phoenix, have relatively high frequencies of violations of the NAAQS, in part because of somewhat dense localized emissions from the extractive and material handling industries along the Salt River. Some of these sporadic and unknown temporally distributed fugitive sources cannot be captured by an emissions inventory, and they contribute to the heterogeneous spatial distribution of ambient PM_{10} and hence to prediction errors. The average particle size of the total mass of PM_{10} in central Phoenix is from five to seven microns, large enough to be deposited on the ground somewhat rapidly, in contrast to the smaller particles comprising the fine fraction (smaller than 2.5 microns) that remains suspended for considerably longer times. The aerosol module in CMAQ considers both $PM_{2.5}$ and PM_{10}, but represents the particle size distribution as the superposition of three lognormal sub-distributions called modes. The model takes into account only one mode of the "coarse particles" (2.5-10μm) and assigns the same deposition velocity.
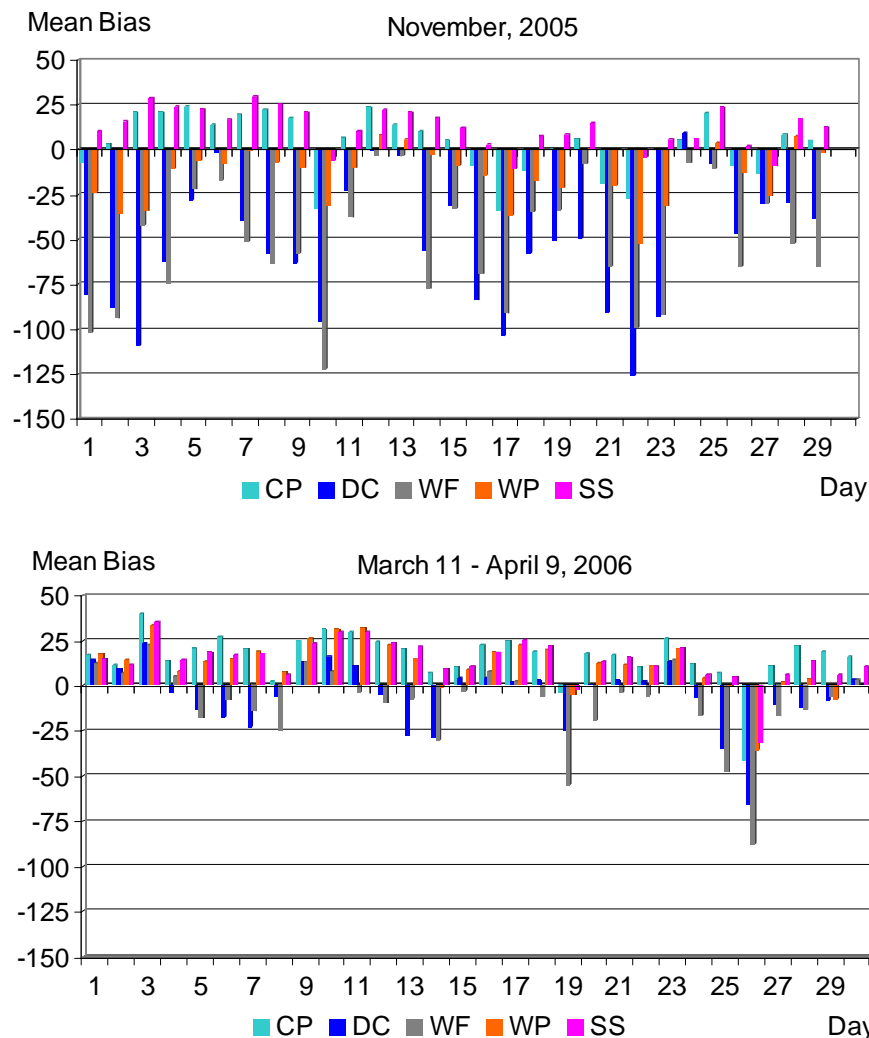
Figure 5.8. Daily Mean Bias for high pollution conditions (top) and low pollution

Figures 5.9 and 5.10 show the CMAQ predictions compared with 24-hour averaged observations for both high and low pollution periods. The calculated data were extracted from the grid cell where the corresponding monitor is located. A good correspondence between observed and calculated data for WP and CP sites can be found in November 2005 (Fig. 5.9). The model overestimates the 24-hour averaged observed values at SS and strongly underestimates the values at WF and DC sites. The same behavior can be found for the low pollution case (Fig. 5.10). CMAQ overestimates the 24-hour averaged measured values at SS, CP, WP and underestimates the values at WF and DC sites for several days. Nonetheless, the model's predicted values generally follow the trends of the observations. In spite of MM5's inability to simulate the higher wind speeds for several days, the model did predict some higher wind speeds, reflected by the low PM_{10} concentrations calculated by CMAQ for 11, 26-27 of November 2005, March 30, and 2, 5-6 of April, 2006.
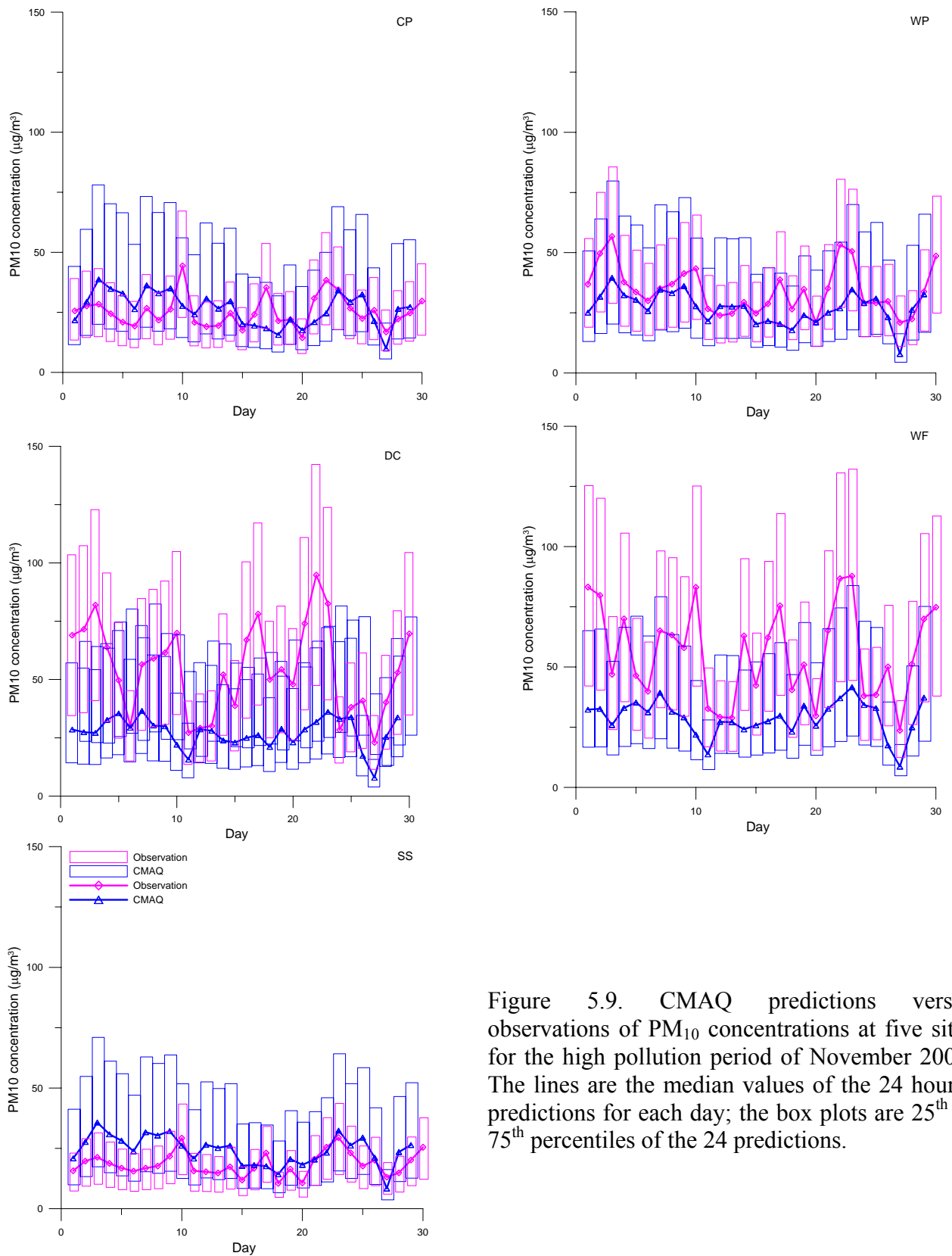
Figure 5.9. CMAQ predictions versus observations of PM_{10} concentrations at five sites for the high pollution period of November 2005. The lines are the median values of the 24 hourly predictions for each day; the box plots are 25th to 75th percentiles of the 24 predictions.
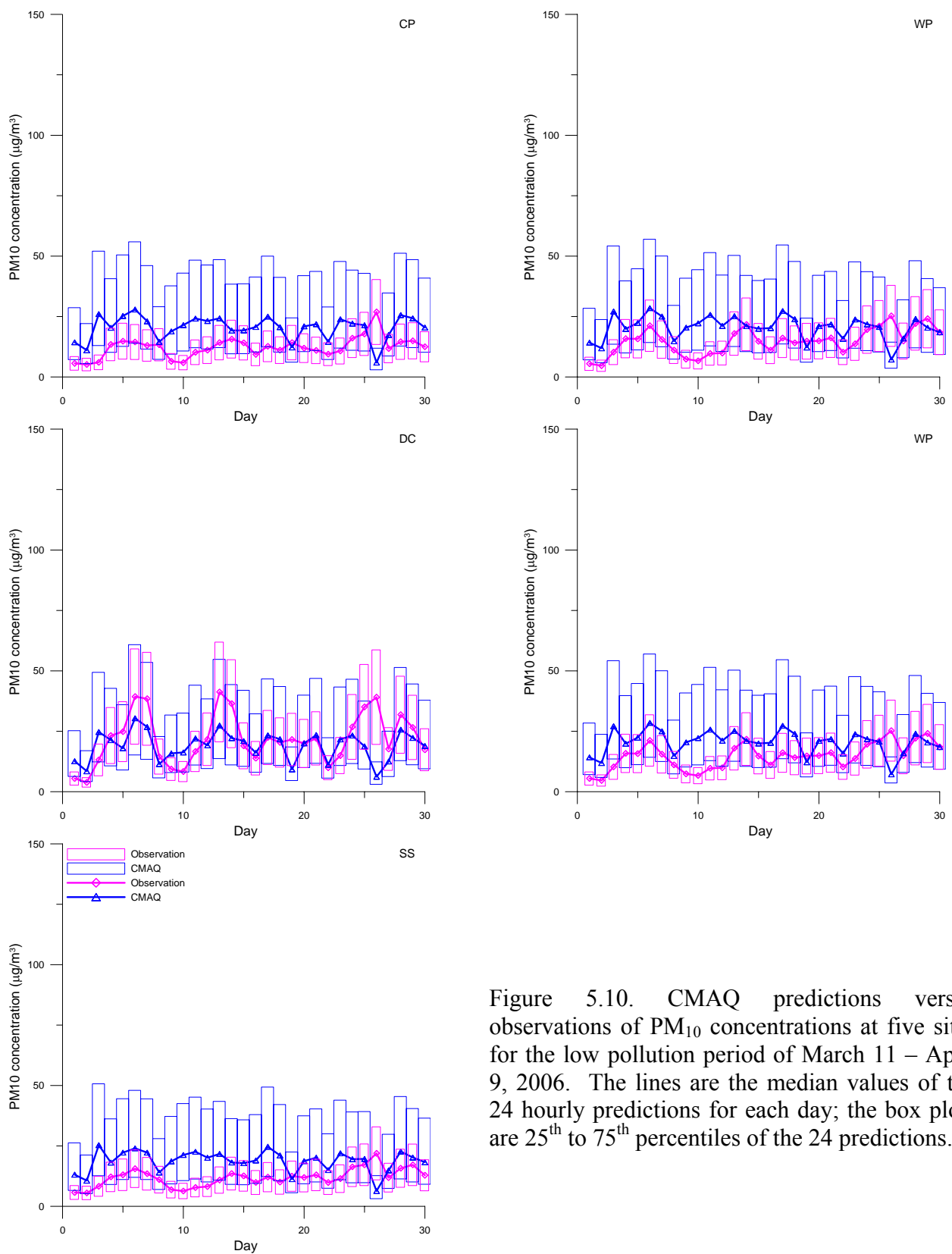
Figure 5.10. CMAQ predictions versus observations of PM_{10} concentrations at five sites for the low pollution period of March 11 – April 9, 2006. The lines are the median values of the 24 hourly predictions for each day; the box plots are 25th to 75th percentiles of the 24 predictions.

The PM_{10} concentrations were averaged for the five sites for the entire period for every hour. Figure 5.11 presents the averaged concentrations from the five monitors in central Phoenix with the spatially-averaged PM_{10} concentrations from the numerical modeling.
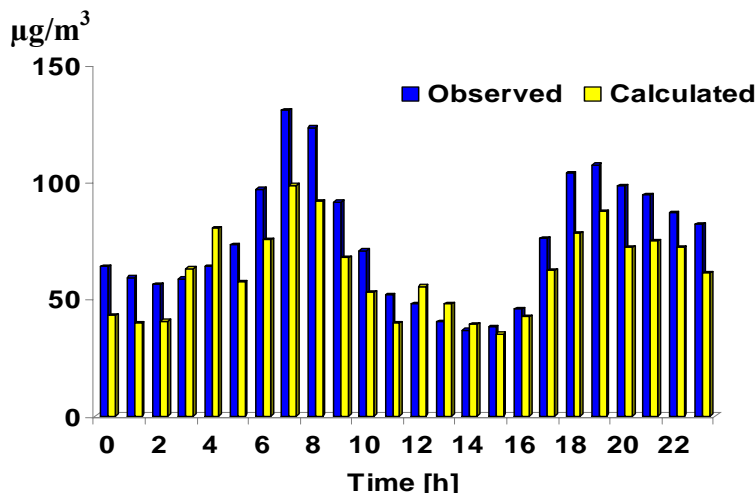
Figure 5.11. Hourly variation of the five-site averages, calculated and observed PM_{10} concentrations for November 2005

The model is able to produce the morning and evening maxima at the right times, in agreement with the observations, but it underestimates the magnitude of the peaks. There are at least two explanations for this lack of agreement. First, consider the weather-predicting MM5 model, which is in need of some modifications itself. Its predicted wind fields have speeds considerably higher than the measured values during the morning and evening transitions (for more details see Appendix C). Provided that the wind speeds remain below the dust resuspension threshold - roughly 15 to 20 miles per hour (7 to 10 meters per second) - higher wind speeds generally lead to lower PM_{10} concentrations; hence, the underestimation. Second, consider that MM5 does not differentiate among the various types of urban land surface. The treatment of urban land in modeling grids results in too uniform a surface roughness and other properties, which are not representative of the local-scale variation. Sub-categories are needed for the so called "urban" land characteristics. These unrealistic uniformities can cause incorrect transport of pollutants, as well as too little or too much vertical mixing, both of which affect their resultant concentrations. Especially for stable conditions, which can last for several days, improvements in the application of this model to metropolitan Phoenix would be helpful.

CMAQ contains "accurate" and "state-of-the-science" parameterizations of atmospheric processes affecting transport, transformation, and deposition of pollutants. Process analysis is a useful tool for understanding the contributions of different physical processes to the total PM_{10} concentrations. Through process analysis the contribution that each phenomenon makes to the resultant PM_{10} concentration can be quantified (Fig. 5.12). The emissions (EMIS), dry deposition (DDEP), and vertical diffusion (VDIF) give a joint contribution ten times greater than the combined contributions of advection (horizontal HADV + vertical VADV), horizontal diffusion (HDIF), atmospheric chemistry (CHEM), aerosol composition (AERO), and cloud chemistry (CLDS) combined. Inadequate parameterizations of both the diffusion and the depositional processes in the planetary boundary layer, combined with uncertain emission inventories, may be responsible for the model's performance.

Process Analysis - November 7-9, 2005

Legend: DDEP, EMIS, VDIF, AERO, CLDS, HADV, VADV, HDIF, CHEM, PM10

EMIS, DDEP, VDIF

Process Analysis - April 1-3, 2006

Legend: DDEP, EMIS, VDIF, AERO, CLDS, HADV, VADV, HDIF, CHEM, PM10
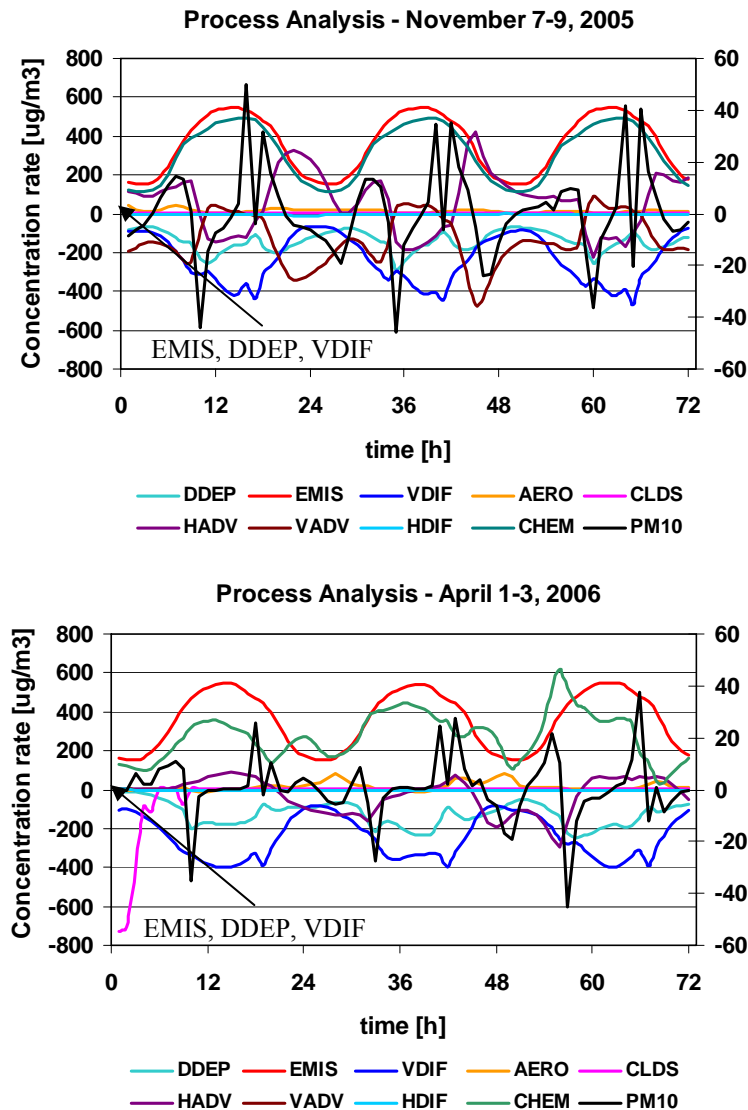
EMIS, DDEP, VDIF

Figure 5.12. Contributions of different processes to PM_{10} concentrations for 3-days periods in November 2005 and April 2006: the values are averaged from several grid cells in central Phoenix, with EMIS, DDEP, and VDIF plotted on the left Y-axis, with all others on the right

One reason for the differences between the modelled and observed PM_{10} concentrations is that measured point values cannot represent the larger grid-based volumes of 36, 12, or 4 km surrounding the monitoring sites, given the large spatial inhomogeneities already noted. The spatial distribution of the Index of Agreement (IA) between the interpolated and modeled PM10 concentrations is shown in Figure 5.13 for November 2005. The interpolated surfaces were constructed from the observations and mapped into census tract concentrations, from which the average value for each modeling grid cell was calculated. The map shows the IA between the interpolated PM10 concentrations from the IDW and the CMAQ estimates for each 4 km grid cell. A very good correspondence can be found with the IA greater than 0.5 for the whole domain. The modeled data fit very well to the interpolated surfaces (IA between 0.6 - 0.7) in the northeast part (WP, CP, SS) and some disagreement can be seen at the south-west (less than 0.5). The CMAQ model overestimates the PM10 concentrations in the northeast around CP and SS, unlike in the

southwest around WF and DC, where it generally underestimates the observations, as can be seen from the map of Mean Bias for November 2005 (Figure 5.14).
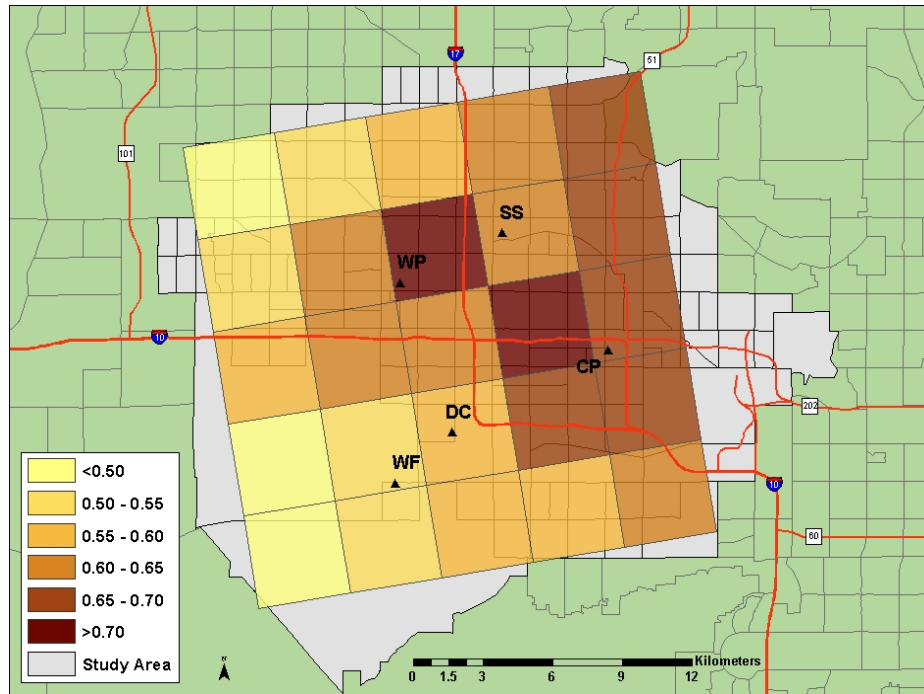
Figure 5.13. The spatial distribution of the Index of Agreement between CMAQ and Inverse Distance Weighting (IDW) interpolated surfaces
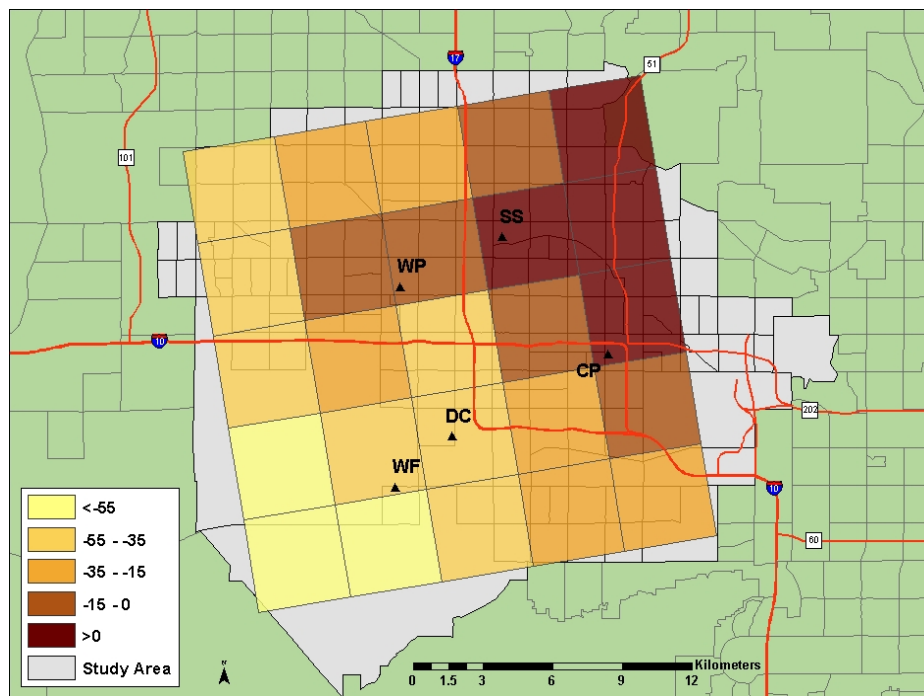
Figure 5.14. The spatial distribution of Mean Bias between CMAQ and Inverse Distance Weighting (IDW) interpolated surfaces

One way to improve the numerical predictions for the central part of the study area would be to combine CMAQ and IDW surfaces. Application of the Daily Mean Biases to CMAQ predictions produces a more realistic pattern of PM_{10} concentrations and reduces the disagreement between calculated and observed data. Examples of this technique are shown in Figures 5.14-5.18 for all five permanent sites for November 2005.
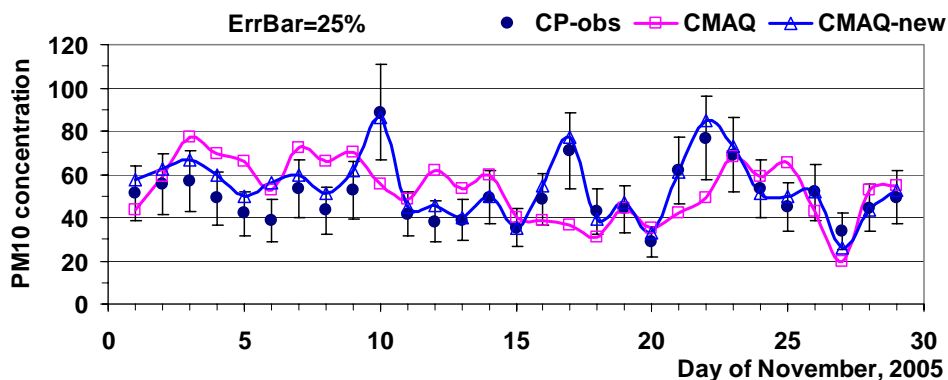
Figure 5.15. Comparison of the daily, "simulated" PM_{10} concentrations with the observations at Central Phoenix: violet is straight CMAQ; blue is "CMAQ-new" - CMAQ combined with interpolation
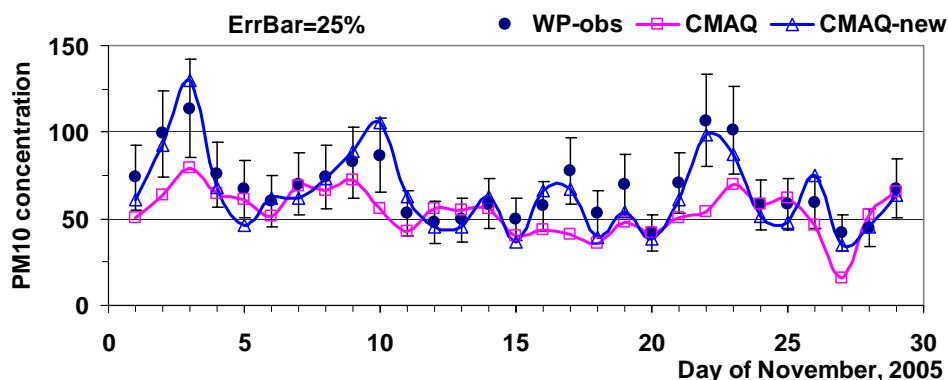
Figure 5.16. Comparison of the daily, "simulated" PM_{10} concentrations with the observations at West Phoenix (WP): violet is straight CMAQ; blue is "CMAQ-new" - CMAQ combined with interpolation
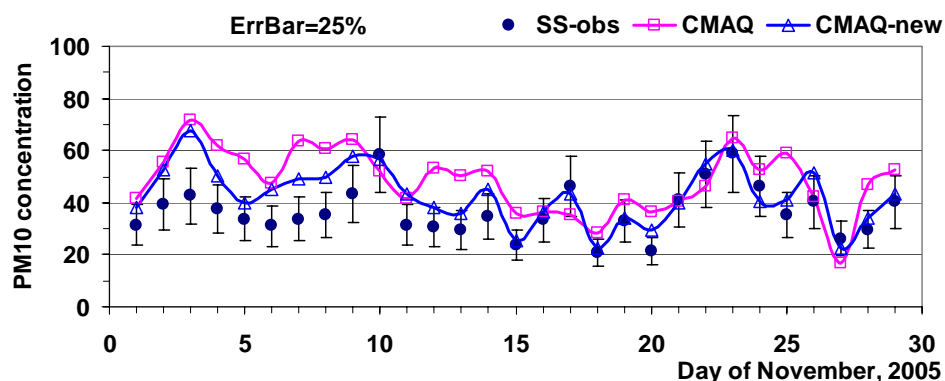
Figure 5.17. Comparison of the daily, "simulated" PM_{10} concentrations with the observations at Supersite (SS): violet is straight CMAQ; blue is "CMAQ-new" - CMAQ combined with interpolation.
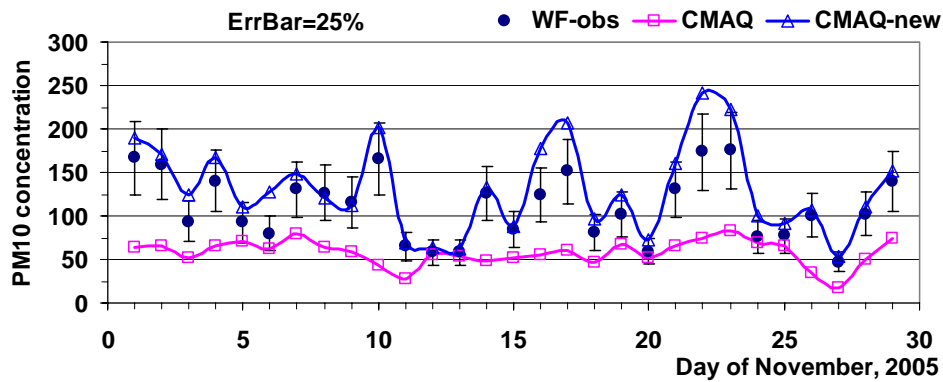
Figure 5.18. Comparison of the daily, "simulated" PM_{10} concentrations with the observations at West 43rd Avenue (WF): violet is straight CMAQ; blue is "CMAQ-new" - CMAQ combined with interpolation
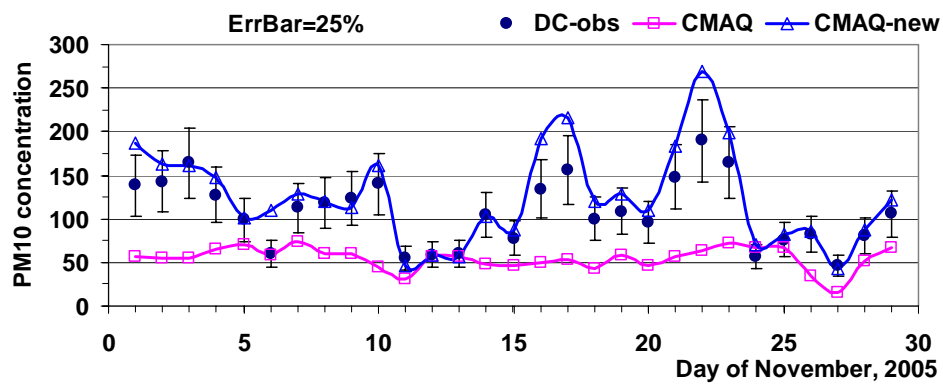
Figure 5.19. Comparison of the daily, "simulated" PM_{10} concentrations with the observations at Durango Complex (DC): violet is straight CMAQ; blue is "CMAQ-new" - CMAQ combined with interpolation

Although this "nudging" technique can be applied to historical periods, it cannot be of help in forecasting, as the observations that would provide the interpolated surfaces are yet to be made. Any improved health warning system would have to rely either on a statistical-based prediction such as the neural-network EnviNNet or on CMAQ or another deterministic model prediction driven by the meteorological model's predicted weather for the next day.

Conclusions

  For the meteorological fields:

- MM5 fails to predict high wind speeds, perhaps due to the inconsistency in global model predictions used as input and boundary conditions.

- MM5 slightly overestimates the low wind speeds during the generally stable conditions of the night and early morning; furthermore, it cannot faithfully simulate rapid changes of wind direction.

- MM5 does accurately simulate the temperature field, albeit with slight underestimates of nocturnal temperatures.

For the PM$_{10}$ concentration fields:

- CMAQ generally underestimates the higher observed PM10 concentrations and overestimates the lower ones.

- CMAQ captures the diurnal variation of PM10 concentrations.

- CMAQ especially underestimates the ately simulates accurate such as the neural-network based EnviNNet or on a CMAQ or CMAQ-type deterministic model driven byelevated PM10 concentrations at West 43rd Avenue and the Durango Complex in November 2005. Dust emissions in the vicinity of the monitors, but inadequately accounted for in the emissions inventory, are the likely explanation.

- CMAQ adequately simulates the surface PM10 distribution in the central Phoenix study area for the needs of this project.

Three difficulties plague the application of a deterministic system such as MM5/SMOKE/CMAQ to air quality surveillance and management:

- First, these models need precise initial conditions, boundary conditions, and emissions to provide reasonable predictions;

- Second, they are computationally demanding and somewhat labor-intensive to operate, troubleshoot, update, and maintain; and

- Third, the meteorological model MM5 is actually designed to predict larger-scale, regional phenomena, not the more local-scale characteristics that prevail in and around specific urban air pollution monitoring sites.

As done in this project, the importance of the initial conditions can be reduced through spin-up times. As also done in this project, the importance of boundary conditions can be diminished through choosing larger modeling domains. The importance of spatially and temporally accurate hourly emissions, however, cannot be overlooked: their   contribution to the performance of air quality model predictions is paramount. In particular, airsheds in arid and semiarid areas, including most of the southwestern U.S. and much of its intermountain West, are subject to pervasive fugitive emissions of dust under all meteorological conditions and to windblown dust under more turbulent and stormy conditions. Locally suspended dust from widespread fugitive emissions is a major component of everyday particulate matter concentrations in this region. Production of soil dust aerosols depends on the nature of the mechanical disturbance, the wind energy, and the soil surface properties. Improvements in quantifying both human-caused, mechanically generated emissions, as well as windblown dust emissions, would improve deterministic model performance in the study area.

The computational demands of deterministic models cannot be casually dismissed, in spite of the recent, substantial improvements in speed and power stemming from parallelization and other techniques. Accurate weather forecasting on the synoptic scale of one to five days is now a facet of our daily lives; still, the computational time needed for more precise predictions on the local scale remains about equal to the typical real-world time of the local phenomena themselves. These phenomena include thermally driven upslope and valley winds, stagnation, extremely low wind speeds, stratification, and canalization effects – all of which last for hours and require equal hours of simulation. Considering human exposure, in spite of the general lack of short-term health

standards (let's say from one to six hours), the higher concentrations occurring in a few to several hours may be as important or even more so than the exposures of 24 hours or longer.

Meteorology's critical control of air pollutant concentrations is well known: the emission and chemical transformation of particles, their transport and dispersion – both horizontal and vertical -- and their loss through dry and wet deposition are all consequences of the weather. During the meteorological simulations of this project, it has become evident that the MM5 model would benefit from a number of modifications. For example, disagreements between a measured wind vector (speed and direction) and the MM5 volume-averaged predictions for the 36, 12, or 4 km grids are commonly encountered. MM5 is not scientifically formulated to reproduce the exact wind speed and direction at each measurement point; rather, it has been designed to generate sub-regional and regional wind, temperature, and moisture fields that are internally consistent and strictly satisfy the laws of mass, momentum, and energy conservation. Conversely, local wind measurements are seldom sited in such a manner as to be representative of a large volume of space surrounding the observation site. In the complex terrain of metropolitan Phoenix and its surrounding mountains, because of terrain forcing and orographic effects, the MM5 volume-averaged meteorological estimates have greater uncertainties than in flat terrain.

Chapter 6 Neutral Network versus CMAQ Predictions

For these comparisons November 2005 was selected, considering that the late fall and winter months tend to have the highest PM_{10} concentrations and the most hospital visits for respiratory illnesses. EnviNNet predictions were limited to a single site, Central Phoenix. Furthermore, this November has both high and low PM_{10} days, including two periods of elevated PM_{10} – November 10 and November 22-23, for which statistics and graphics have been produced. The daily averaged values are presented first, given that the health data for comparison with PM_{10} are available on a daily basis and that the National Ambient Air Quality Standard is expressed as a 24-hour average, midnight to midnight. The data are from the Maricopa County Air Quality Department, whose staff has verified their accuracy through quality control procedures and has reported them to EPA's AIRS system. Figure 6.1 shows the time series of these daily predictions by EnviNNet and CMAQ in comparison with the daily observations; Figure 6.2 presents comparisons of the hourly observations from November 2005 with the two models.
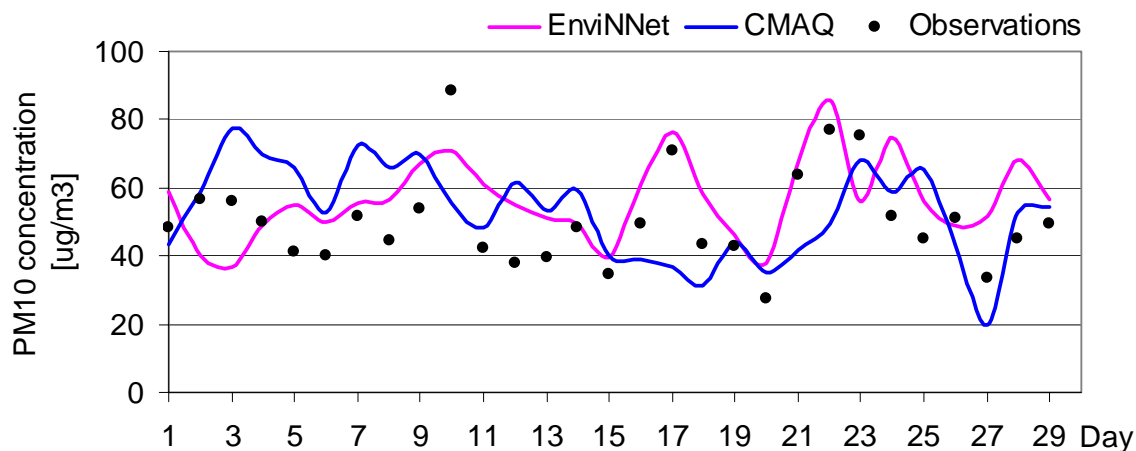
Figure 6.1. Time series of 24-hour average PM_{10} concentrations predicted by CMAQ and EnviNNet with observations at the Central Phoenix site
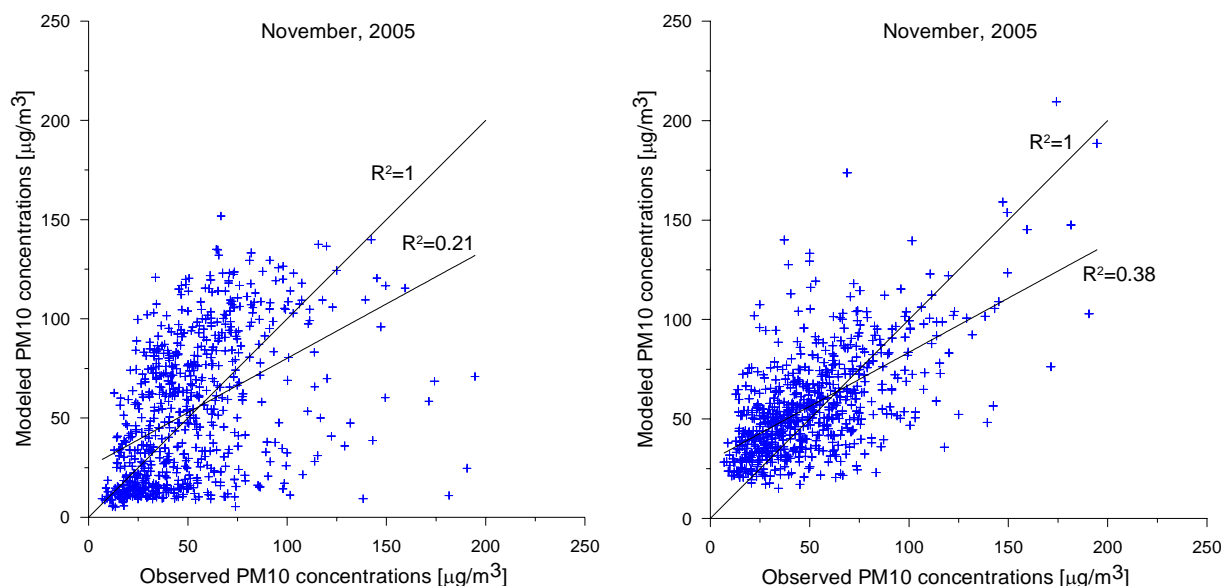
Figure 6.2. Scatter plots of hourly PM_{10} concentrations predicted by CMAQ (left) and EnviNNet with observations: November 2005, Central Phoenix site

Predicting the higher PM_{10} concentrations well is more important than doing well on the low ones. To this end the model's predictions for elevated PM_{10} concentrations were evaluated for the two high pollution periods of November 6-10 and November 22-26. The results are shown in Figures 6.3 and 6.4; the performance measures for the three time periods and the two models are in Table 6.1, are defined in Appendix D, and are discussed below.

The calculations were made for one month and for the two five-day periods with elevated PM_{10} concentrations. The Index of Agreement (IA) is greater than 0.6, which shows good correspondence between the calculated and observed data. Generally, EnviNNet gives better IA in comparison with CMAQ for all periods considered here. The Mean Absolute Errors (MAE) are less than 32 for CMAQ and less than 24 for EnviNNet. The Root Mean Square Errors (RMSE) are in the range of 25 – 40 for different periods. The statistical model EnviNnet yields smaller errors than CMAQ.

Table 6.1. Statistics of CMAQ and EnviNNet predictions of hourly PM_{10} concentrations at the Central Phoenix site

Model	MAE	RMSE	RSQ	RSQ*	IA	Period
CMAQ	26.12	34.40	0.21	1.45	0.68	November
EnviNNet	19.01	25.02	0.39	0.82	0.77	November
CMAQ	32.24	40.18	0.14	1.05	0.61	6-10 Nov.
EnviNNet	20.39	28.04	0.42	0.75	0.79	6-10 Nov.
CMAQ	29.33	39.17	0.10	1.19	0.60	22-26 Nov.
EnviNNet	24.26	34.01	0.13	0.78	0.61	22-26 Nov.

Abreviation: MAE - Mean Absolute Error; RMSE - Root Mean Square Error; RSQ - Coefficient of Determination (aka R^2); RSQ* - Modified Coefficient of Determination[2]; IA - Index of Agreement
[2]Modified Coefficient of Determination: values greater than 1 mean the model overestimated (orange); values less than 1 mean the model underestimated (green)
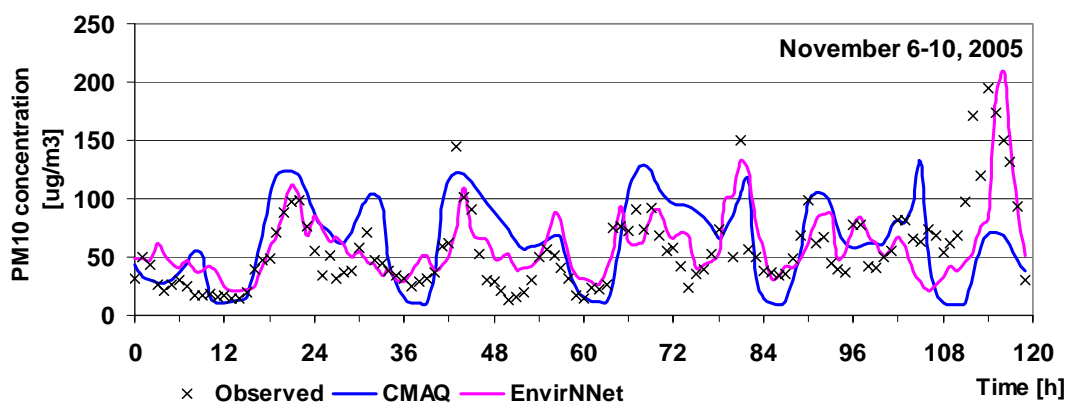
Figure 6.3. Comparison of hourly PM_{10} concentrations predicted by Models 3 and EnviNNet with the observations of November 6-10, 2005, Central Phoenix site
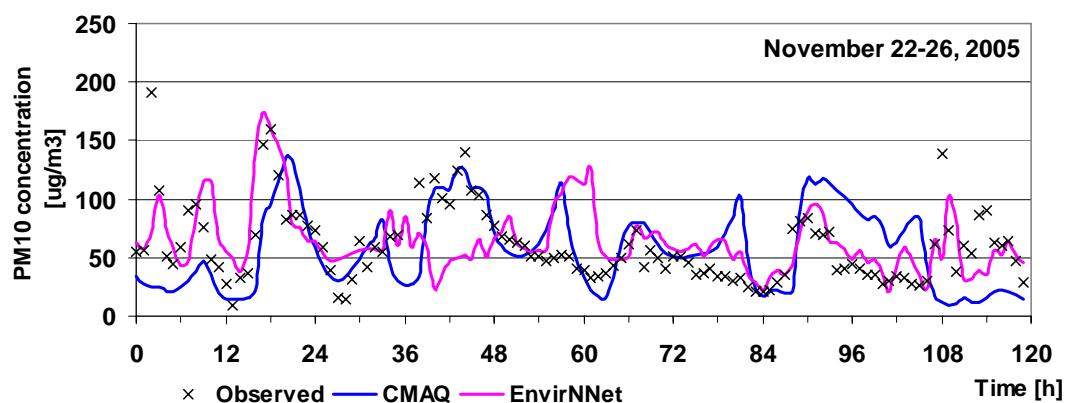
Figure 6.4. Comparison of hourly PM_{10} concentrations predicted by CMAQ and EnviNNet with the observations of November 22-26, 2005, Central Phoenix site

The neural network satisfactorily predicts the PM_{10} peaks in contrast to CMAQ, which has problems capturing them satisfactorily. Although the deterministic model may have given much better predictions under ideal initial, boundary and pollution inventory conditions with all scales of motion fully resolved, the present status of the model is far from this state. In addition, CMAQ cannot resolve scales smaller than the size of the grid, which in this case is 4x4 km.

Conclusions

As a workable alternative to the deterministic MM5/CMAQ, the neural network proved to be somewhat better than CMAQ in predicting the moderate to high PM_{10} concentrations. Its principal advantage in an asthma warning system is that it would not require an emissions inventory or the daily computational and staff demands of the grid-based, deterministic modeling system. The neural network is much easier and quicker to use than CMAQ and could be partially automated for issuing health warnings. Its shortcoming lies in its limited geographical coverage, especially for pollutants with steep concentration gradients such as PM_{10}. In addition, only one site was examined, suggesting that similar work at additional sites would be advisable before any claims of area-wide viability could be supported.

Chapter 7 Linking asthma with PM$_{10}$ concentrations

Introduction

The goal of the health effects analysis is to determine whether asthma incidents (primarily emergency department (ER) visits and hospital admissions with a diagnosis of asthma) can be quantitatively linked to the air quality measurements obtained from Maricopa County, ADEQ, and ASU monitoring sites. The primary health data are the asthma incident reports from the Arizona Department of Health Services (ADHS). This data includes hospitalization admissions and emergency room visits from throughout the state as well as patient demographics e.g., gender, age, etc.

The health effects analysis was conducted by the Center for Health Information & Research (CHIR), part of the School of Computing and Informatics in Arizona State University's Ira A. Fulton School of Engineering. CHIR is a multidisciplinary team whose interests are health care, clinical quality, the health care workforce, occupational illness and injury, medical malpractice, health care economics, and disability. CHIR is home of the Arizona Health Query (AZHQ), a community/university database effort. More than fifty organizations voluntarily share their data with ASU to create this integrated database. Each partnership is governed by contracts that comply with the federal Health Insurance Portability and Accountability Act (HIPAA), and stringent security is maintained to avoid unauthorized disclosures. AZHQ contains health information on millions of Arizona adults and children and provides the unique capability of tracking patients across health care systems and over time. As the data system continues to expand to include more services, CHIR efforts are focused on building additional partnerships with large employers, third party administrators, and physician groups. The ADHS routinely reports its data to the AZHQ.

AZHQ data has already been utilized to study the respiratory effects of agricultural burning in northern Mexico and southwest Arizona on Yuma County, AZ children study funded by the Southwest Center for Environmental Research and Policy (SCERP). Using AZHQ, we examined the frequency of health care visits, emergency department utilization' and hospitalizations for respiratory illnesses for children ages 0-17 during the burning and compared this frequency with the prevalence of respiratory illness before and after exposure to agricultural burning. A separate study was conducted that linked asthma incidents to air quality in the Casa Grande area of Pinal County, AZ.

Data

In the present work, the ADHS and CHIR conducted a high-level scan of air quality monitoring data for PM$_{10}$ and asthma incidents from hospital discharge data [and ER admission data] to determine the relationship, if any, between poor air quality and higher rates of asthma admissions. Preliminary analyses also helped researchers define the demographic groups, sample size, and data cleaning strategies that were subsequently applied in the final analyses of the work being reported here. Based on these preliminary results and discussions, research focused on ADHS asthma incident data occurring within the 168 census tract areas of central Phoenix from January 1, 2005 through December 31, 2006, a period for which complete air monitoring records were available. All asthma events within five miles of a continuous PM10 monitor were included.

In addition to the standard cleaning applied by CHIR to correct errors, additional cleaning steps were taken. For example, there were cases where the same patient went to an emergency room and was later admitted to the hospital. This single patient had multiple records on the same day with his

status changing from emergency to inpatient. Such redundant records were deleted to leave but a single asthma incident. Also, those subsequent medical encounters occurring sufficiently long after the initial visit were considered to be a distinct incident. This time period is commonly referred to as a "washout" period. We explored several washout periods in this study. Figure 7.1 shows the change in the number of reported incidents for selected washout periods. As the incident changes are small for washout periods of seven days or greater, we selected a washout period of seven days in this work. If the same person had multiple records within the seven days, only the initial record was kept.
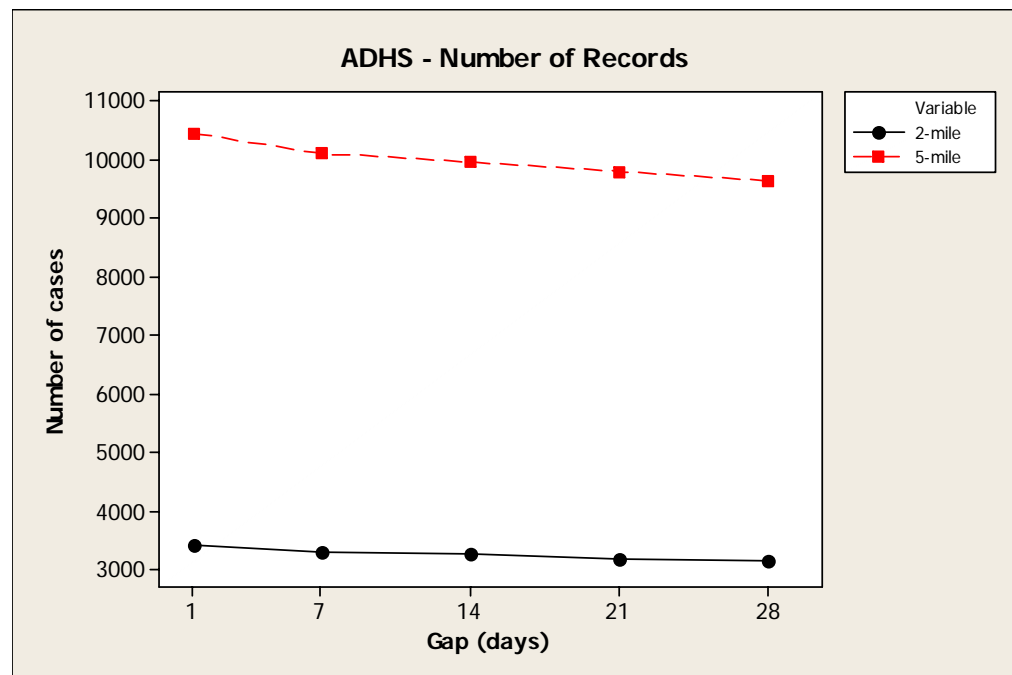
Figure 7.1. Washout periods for asthma incidents within two and five miles of a continuous PM_{10} monitor

Asthma incidents were described by age group, day of the week, month, and place of service (emergency department and inpatient admission), resulting in a dataset containing about 2,000 events for the two-mile radius and 6,000 events for the five-mile radius for children aged 0-17 years. See Figures 7.2 - 7.5.
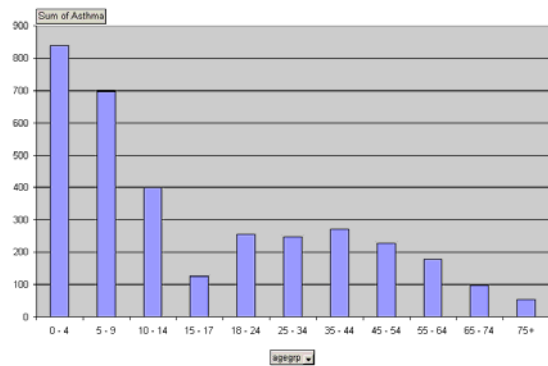
(a) Asthma incidents by age group
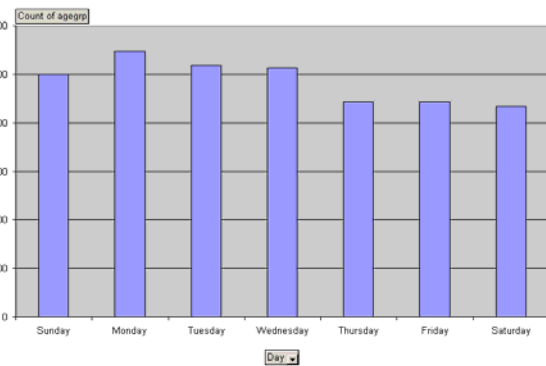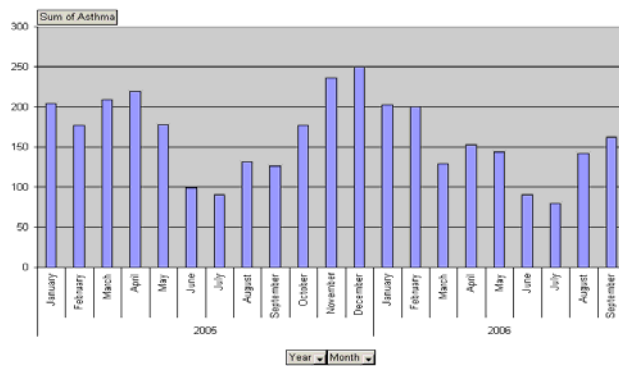
(b) Asthma incidents by day of week

(c) Asthma incidents by month
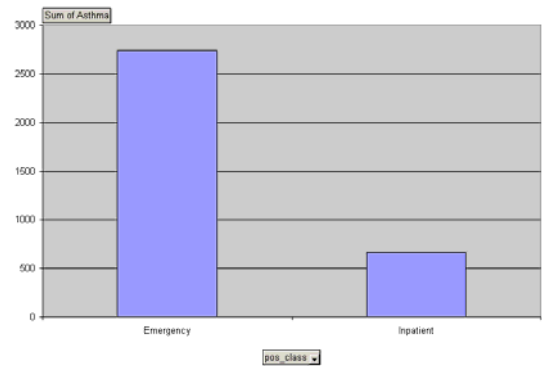
(d) Asthma incidents by place of service
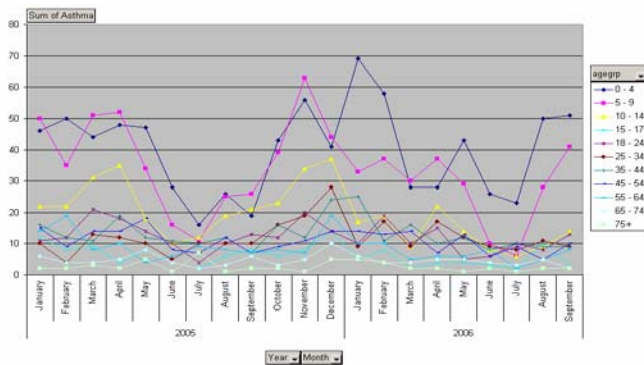
(e) Asthma incidents by age group and time

Figure 7.2. Asthma incidents by different characteristic within two miles of PM_{10} monitoring sites
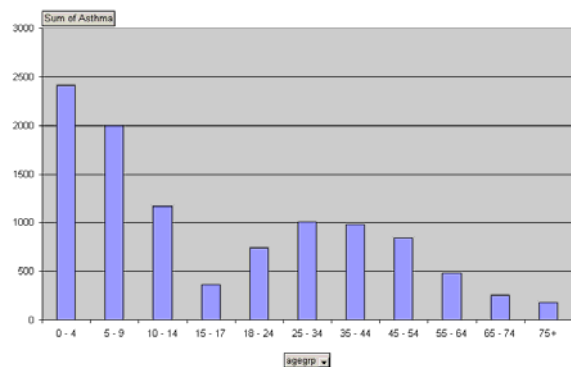
(a) Asthma incidents by age group
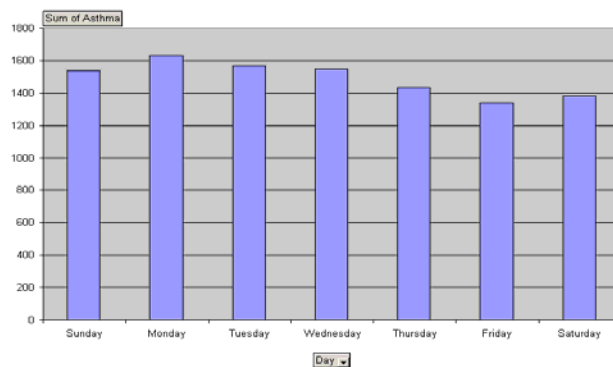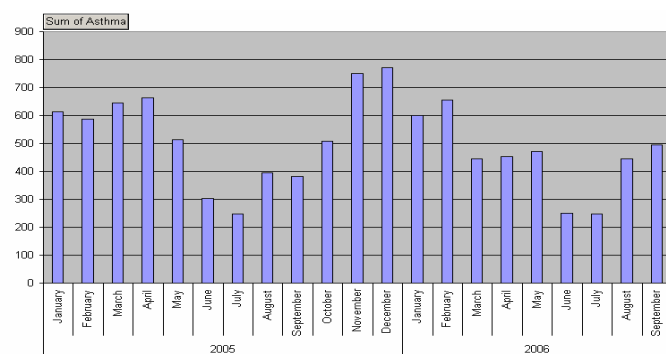
(b) Asthma incidents by day of week

(c) Asthma incidents by month
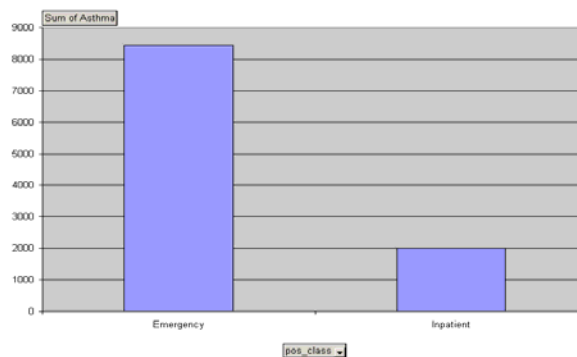
(d) Asthma incidents by place of service
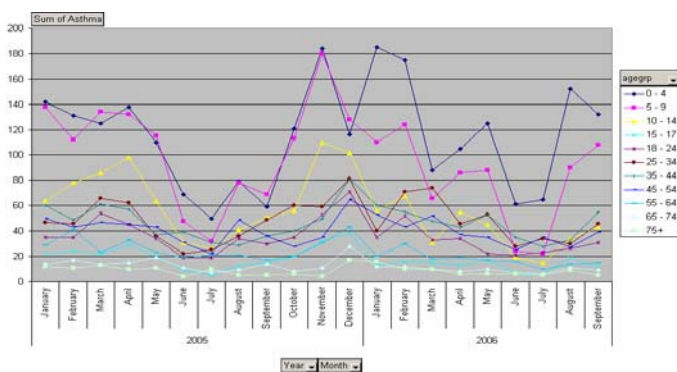
(e) Asthma incidents by age group and time

Figure 7.3. Asthma incidents by different characteristic within five miles of PM_{10} monitoring sites

No.	ZIP	ADHS	AZHQ
1	85003	118	180
2	85004	83	83
3	85006	514	642
4	85009	722	1281
5	85019	415	486
6	85031	419	748
7	85041	718	1064
8	85043	265	375
9	85339	146	361
	Total	3400	5220

(a) Asthma incidents by zip code

ZIP	Ambulatory		Emergency		Inpatient		Missing		Other	
	AZHQ	ADHS	AZHQ	ADHS	AZHQ	ADHS	AZHQ	ADHS	AZHQ	ADHS
85003	108	-	47	93	23	25	-	-	2	-
85004	54	-	15	61	13	22	-	-	1	-
85006	441	-	145	428	54	86	-	-	2	-
85009	938	-	257	594	79	128	3	-	4	-
85019	347	-	100	326	32	89	-	-	7	-
85031	546	-	131	336	55	83	5	-	11	-
85041	753	-	218	553	79	165	12	-	2	-
85043	267	-	69	218	32	47	2	-	5	-
85339	278	-	54	108	27	38	1	-	1	-
Total	3732	-	1036	2717	394	683	23	-	35	-

(b) Asthma incidents by zip code and place of service

Age Group	Ambulatory		Emergency		Inpatient		Missing		Other	
	AZHQ	ADHS	AZHQ	ADHS	AZHQ	ADHS	AZHQ	ADHS	AZHQ	ADHS
0 - 4	810	-	184	685	95	155	1	-	4	-
5 - 9	868	-	185	580	57	117	7	-	3	-
10 - 14	574	-	107	338	29	64	3	-	5	-
15 - 17	184	-	47	115	6	11	2	-	3	-
18 - 24	173	-	110	222	25	33	-	-	1	-
25 - 34	192	-	113	216	27	32	4	-	2	-
35 - 44	262	-	120	227	34	45	4	-	4	-
45 - 54	211	-	73	160	48	69	1	-	5	-
55 - 64	176	-	51	94	35	85	1	-	5	-
65 - 74	99	-	22	57	17	41	-	-	-	-
75+	183	-	24	23	21	31	-	-	3	-
Total	3732	-	1036	2717	394	683	23	-	35	-

(c) Asthma incidents by age group and place of service

Figure 7.4. Asthma incidents by zip code within two and five miles of PM_{10} monitoring sites

No.	ZIP	ADHS	AZHQ
1	85003	118	180
2	85004	83	83
3	85006	514	642
4	85007	331	461
5	85008	1049	1205
6	85009	722	1281
7	85012	102	323
8	85013	231	342
9	85014	325	423
10	85015	596	993
11	85016	421	434
12	85017	578	736
13	85018	310	389
14	85019	415	486
15	85031	419	748
16	85033	821	1213
17	85034	224	226
18	85035	633	1018
19	85040	624	1022
20	85041	718	1064
21	85043	265	375
22	85301	788	1509
23	85339	146	361
	Total	10433	15514

(a) Asthma incidents by zip code

ZIP	Ambulatory		Emergency		Inpatient		Missing		Other	
	AZHQ	ADHS	AZHQ	ADHS	AZHQ	ADHS	AZHQ	ADHS	AZHQ	ADHS
85003	108	-	47	93	23	25	-	-	2	-
85004	54	-	15	61	13	22	-	-	1	-
85006	441	-	145	428	54	86	-	-	2	-
85007	302	-	112	269	41	62	1	-	5	-
85008	806	-	265	861	114	188	10	-	10	-
85009	938	-	257	594	79	128	3	-	4	-
85012	257	-	42	72	23	30	-	-	1	-
85013	195	-	102	195	42	36	-	-	3	-
85014	251	-	105	274	63	51	1	-	3	-
85015	647	-	246	514	86	82	2	-	12	-
85016	308	-	78	332	38	89	2	-	8	-
85017	494	-	175	473	59	105	1	-	7	-
85018	262	-	67	235	56	75	1	-	3	-
85019	347	-	100	326	32	89	-	-	7	-
85031	546	-	131	336	55	83	5	-	11	-
85033	891	-	240	663	64	158	7	-	11	-
85034	161	-	49	184	13	40	-	-	3	-
85035	757	-	191	534	58	99	3	-	9	-
85040	713	-	207	508	86	116	7	-	9	-
85041	753	-	218	553	79	165	12	-	2	-
85043	267	-	69	218	32	47	2	-	5	-
85301	1031	-	343	602	115	186	7	-	13	-
85339	278	-	54	108	27	38	1	-	1	-
Total	10807	-	3258	8433	1252	2000	65	-	132	-

(b) Asthma incidents by zip code and place of service

Age Group	Ambulatory		Emergency		Inpatient		Missing		Other	
	AZHQ	ADHS	AZHQ	ADHS	AZHQ	ADHS	AZHQ	ADHS	AZHQ	ADHS
0-4	2456	-	533	1966	301	446	2	-	6	-
5-9	2387	-	479	1006	157	167	12	-	14	-
10-14	1572	-	320	332	90	34	7	-	16	-
15-17	513	-	134	663	17	78	5	-	11	-
18-24	496	-	308	899	64	112	4	-	5	-
25-34	631	-	445	815	86	165	13	-	12	-
35-44	794	-	414	584	129	256	10	-	28	-
45-54	786	-	311	1674	151	323	7	-	15	-
55-64	554	-	149	278	122	202	3	-	12	-
65-74	314	-	86	139	68	113	1	-	4	-
75+	304	-	79	77	67	104	1	-	9	-
Total	10807	-	3258	8433	1252	2000	65	-	132	-

(c) Asthma incidents by age group and place of service

Figure 7.5. Comparison of AZHQ and ADHS asthma incidents within two and five miles of PM_{10} monitoring sites

Analysis Objectives

The processed asthma incidence data by census tract were linked with the PM_{10} concentrations interpolated from the five continuous monitors. In addition to the daily PM_{10} concentrations on the asthma "event" day, 24-hour averages of PM_{10} from one to seven days before the event were also examined in the statistical analysis (these variables are referred to as "lags"). To detect the effects of PM_{10} for each asthma incident while accounting for the confounding variables of seasonality, day of the week, patient-level covariates (e.g., age, gender, ethnicity), and the presence of other air pollutants, a case-crossover analysis was conducted. This type of analysis associates a reference time period as a referent (or control) for each case. Consequently, each patient was treated as a matched case-referent pair with control exposures obtained from the same patient in different time periods. The time-stratified design used a 28-day period or "stratum size" with three referents selected from the same day of the week as the case. With an appropriate time-stratified period, the case-crossover analysis controlled for long-term trends, seasonal effects, and various epidemiologic covariates that change slowly with time by design (e.g., lifestyle behaviors, diet).

Analysis Methods

Background

The case-crossover design, similar to a crossover and matched-pair case-control studies, was developed to study transient short-term exposure effects on the risk of rare acute events (Maclure, 1991). The case is a person with the event of interest at a certain time called the "hazard period", while the control (called the referent) is the same person at a different time called the "control period." The key feature of this design is that each case serves as its own control. The exposure information for each subject during the hazard period is compared to the exposure information during the control period, defined as the referent period for that event. With an appropriate referent

period, the case-crossover analysis controls for long term trends, seasonal effects, epidemic, and other covariates that change slowly with time by design.

In the bidirectional approach Bateson and Schwartz (1999, 2001) have examined methods to sample for the referent to reduce the bias by selecting from either side of the event Also, disjoint referent periods have been recommended for bias concerns (Levy et al., 2001). With a control close in time to the event, these methods avoid much of the confounding due to subject differences and other long-term effects such as seasonality. However, a balance must be maintained between a control too close in time that generates autocorrelation and a control too far apart which confounds the long-term effects. Previous work considered alternatives within a few weeks of the event. Neas et al. (1999) studied daily mortality in Philadelphia where the case period was the 48 hour period ending at midnight on the day of death (Schwartz and Dockery, 1992) and the control period was the day of week seven, 14, or 21 days before and after the case period. Medina-Ramon et al. (2006) used a matching scheme from Bateson and Schwartz (1999, 2001) and a time-stratified partition by Lumley and Levy (2000) that chose control days only in the same month as the hospital admission for chronic obstructive pulmonary disease (COPD). Lin et al. (2005) calculated a one to seven day exposure average ending on the admission date as the exposure in the case period with control periods of two weeks before and after the admission date. Peel et al. (2005) studied the hospital admissions associated with ambient air pollution levels and respiratory health effects. The case period of three-day moving averages of pollutant concentration was selected within two weeks of the case period. The average was the average of pollutant concentrations on the same day as the visit, one day before, and two days before.

Method of the present work

We chose to select the reference period based on a time-stratified scheme because it can control confounding effects from seasonality and time trends. The referents are also selected within a 28-day stratum at seven, 14, and 21 days before or after the case, provided they occur in the same stratum shown in Figure 7.6. Each case has three controls.

Table 7.1. Referent selection based on time-stratified scheme within a 28-day stratum

Day	1	2	3	4	5	6	7	8	9	10	11	12	13	14	15	16	17	18	19	20	21	22	23	24	25	26	27	28
Stratum	S	M	T	W	TH	F	SA	S	M	T	W	TH	F	SA	S	M	T	W	TH	F	SA	S	M	T	W	TH	F	SA
1				■							▨							▨							▨			
2					▨							■							▨							▨		
3		▨							▨							▨							■					

■ Event Day = Case   ▨ Referent Day = Control

While the case-crossover method has been widely used to examine a transient effect of an intermittent exposure on an infrequent acute disease, the same problem can be analyzed by other methods. Szyszkowicz (2006) applied a generalized linear mixed models (GLMM) and used days of the week to construct clusters to study the effects of air pollution on daily emergency department (ED) visits in Vancouver, Canada. Each cluster contained four or five days of the same day of the week. We conducted preliminary analyses with this approach but did not find it as effective as the case-crossover method. Mathematical details of the case-crossover method employed in the present work can be found in Appendix B.

Results

In the analysis, we considered many potential effects. The first primary effect was the 24-hour average PM_{10} concentration from the Inverse Distance Weighting (IDW) interpolation of the observations on the day of the asthma event. The second primary effect, called the "lag", was the PM_{10} concentration two to six days before the event, the "lag" being the delay in days between the

exposure and the health effect. For example, a two-day lag is the average PM_{10} of the previous two days, abbreviated as "lag_2".

Secondary effects were the covariates of age, gender, ethnicity, and place of service. Place of service is a categorical variable with two values: emergency and inpatient. Age is encoded into four categories: 0 - 4, 5 - 9, 10 - 14, and 15 -17 years. Ethnicity followed U. S. Census Bureau definitions. Preliminary analysis detected no differences between places of service; therefore, this variable was not considered further. Even though the case-crossover design does control for the main effects of these patient-level covariates, we nonetheless also considered the interactions of these covariates with the event-day PM_{10} concentration and its various lags. For example, we considered interactions such as:
age*event day PM_{10},
age*$meanlag_2$,
age*$meanlag_3$,
age*$meanlag_4$,
age*$meanlag_5$,
age*$meanlag_6$,
gender*event day PM_{10},
gender *$meanlag_2$,
gender *$meanlag_3$,
gender *$meanlag_4$,
gender *$meanlag_5$,
and gender*$meanlag_6$.

The analysis considered all subsets of these covariates through conditional logistic regression. The event day PM_{10}, also called "Dailymean", and all lag variables were highly correlated as shown in the scatter plots of Figure 7.7 and the statistics of Table 7.1. These and the other statistics that appear in the remainder of this chapter are explained below, as the relationships between an increased probability of an asthma incident and PM_{10} :

- Variable

- Coefficient

- Chi Square

- p-value

- Standard Error (SE)

- Adjusted Odds Ratio (Adjusted OR*)

- 95% Confidence Interval (95% CI)

- Interquartile Range (IQR)

Variable:
The mean PM_{10} concentration on the day of the asthma incident, or the average concentration of the "lag" days before the incident.

Coefficient:
The slope of a line obtained using linear least squares fitting is called the regression coefficient, or, for short, just "Coefficient". In Table 7.1 the first five coefficients are similar, indicative of

generally similar relationships between the "Dailymean PM_{10}" and the lagged PM_{10}. The last variable, "Lag6", has a coefficient different from the others, suggesting a different least squares relationship. In Tables 7.2 – 7.5 the "Coefficient" has a similar meaning, although it comes from the more complex "conditional logistic regressions" of the case-crossover method. These coefficients do vary considerably – from 0.0016 to 0.0055 – indicating somewhat different relationships between the increased probability of an asthma event and the event-day PM_{10} concentrations among the four different cases.

Chi Square:
Generally speaking, the chi-square test examines whether two variables are independent: in the case of Table 7.1, the two variables are:

1. the PM_{10} concentration on the day of the asthma incident, and

2. the average concentration of the "lag" days before the incident.

The "Chi Square" values of Table 7.1 exceed the five percent significance level of 3.84, meaning that with an uncertainty of five percent, the effects of the lags differ insignificantly from the effects of the PM_{10} concentration on the day of the asthma incident (called "Dailymean" in the table).

p-value:
In statistical hypothesis testing, the **p-value** is the probability of obtaining a result at least as extreme as the one that was actually observed, given that the null hypothesis is true. Generally, one rejects the null hypothesis if the p-value is smaller than or equal to the significance level. If the level is 0.05, then the results are only 5% likely to be as extraordinary as just seen, given that the null hypothesis is true. In Table 7.1 the p-values are all less than the significance level of 0.05; thus, the null hypothesis that the lagged concentrations differ from the event-day concentrations is rejected. In Tables 7.2 – 7.5, all p-values are also less than the significance level of 0.05, indicating that the PM_{10} concentration on the day of the asthma incident was significantly associated with it.

Standard Error (SE):
The **standard error** of a statistical analysis is the estimated standard deviation of the error in that analysis. Specifically, it estimates the standard deviation of the difference between the measured or estimated values and the true values. Notice that the true value of the standard deviation is usually unknown and the use of the term **standard error** carries with it the idea that an estimate of this unknown quantity is being used. It also carries with it the idea that it measures not the standard deviation of the estimate itself but the standard deviation of the error in the estimate, and these can be very different. Standard errors of the first three cases in Tables 7.2 – 7.4 are similar, but the one for the fourth case – the ambulatory events excluding preschoolers – is roughly twice that of the first three, indicating more uncertainty for this case.

Adjusted Odds Ratio (Adjusted OR*):
While its mathematical form is in Appendix E, this odds ratio can be readily interpreted as a measure of how likely or unlikely it is for an asthma incident to be associated with a Dailymean PM_{10} concentration. Odds ratios greater than 1.0 mean that the asthma event is more likely to be associated with the PM_{10} concentration; less than 1.0, less likely; and 1.0, equally likely.

95% Confidence Interval (95% CI):
In statistics, a **confidence interval (CI)** is an interval estimate of a population parameter. Instead of estimating the parameter by a single value, an interval likely to include the parameter is given.

Thus, confidence intervals, such as the 95% confidence interval from the case-crossover statistical analysis of the present work, indicate the reliability of a estimate: the wider the interval, the lower the confidence.

Interquartile Range (IQR):
The difference between the 75th and 25th percentiles of the daily mean PM_{10} concentrations in $\mu g/m^3$.
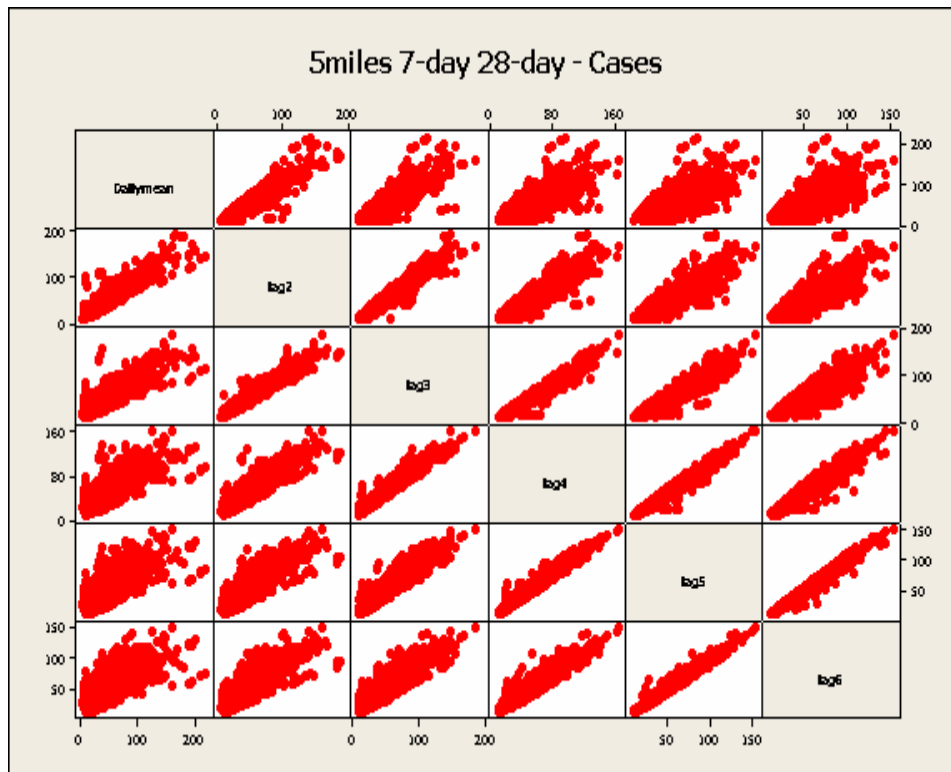
Figure 7.6. Correlation matrix among Dailymean PM_{10} and lag variables

Table 7.2. Model statistics for each main effect (preschool age group omitted)

Variable	Coefficient	Chi Square	P-Value
Dailymean	0.00331	11.7859	0.0006
Lag2	0.00350	9.3428	0.0022
Lag3	0.00303	5.7093	0.0169
Lag4	0.00312	5.0621	0.0245
Lag5	0.00380	6.4476	0.0111
Lag6	0.00465	8.4119	0.0037

Case-crossover: final results

The case-crossover statistics are now presented and discussed for four different samples of the childhood asthma population:

1. all events, ages 0 -17,

2. events excluding ages 0-4, the preschool group,

3. all ambulatory events, ages 0 – 17, and

4. ambulatory events excluding ages 0-4, the preschool group.

All events, ages 0 -17

Because of the high positive correlations between the Dailymean and its lags, further analysis was restricted to the Dailymean as the principal covariate of PM_{10}. All subsets regression indicated that the Dailymean alone was a sufficient covariate for asthma incidents. A statistically significant relationship was detected between Dailymean and asthma incidents. The adjusted odds ratio and 95% confidence interval are shown in Table 7.2

Table 7.3. Results for all asthma incidents

Variable	Coefficient	Standard Error	p-value	Adjusted OR*	95% CI
Dailymean PM_{10}	0.00248	0.0007507	0.0010	1.093	(1.061, 1.153)

Adjusted OR is the odds ratio adjusted by the approximate interquartile range of 36: $(Q_3 - Q_1) \approx (71-35) \approx 36$ µg/m^3

The change in daily average PM_{10} from the 25th to 75th percentile is the interquartile range (IQR). For the data analyzed here the IQR = 36 µg/m^3. Every additional 36 µg/m^3 of daily mean PM_{10} increases the odds ratio of an asthma incident for a person under 18 years old by 9. The 95% confidence interval suggests that there could be as little as 6% or as high as 15% increased risk of an asthma incident.

There was also evidence of an interaction between age and Dailymean. The research group considered an analysis to compare the 0-4 age group to the others because asthma is more difficult to detect in the youngest age group. Further analysis detected a stronger relationship between Dailymean and asthma incidents when the 0-4 age group "preschoolers") was excluded.

Events excluding ages 0-4, the preschool group

The preschool (0-4 years old) group was excluded and the analysis was repeated. All subsets regression again indicated that Dailymean alone was a sufficient covariate for asthma incidents. The adjusted odds ratio and 95% confidence interval are shown in Table 7.3

Table 7.4. Results for asthma incidents excluding the preschool group

Variable	Coefficient	SE	p-value	Adjusted OR*	95% CI
Dailymean PM_{10}	0.00331	0.0009629	0.0006	1.127	(1.053, 1.206)

Adjusted OR is the odds ratio adjusted by approximate interquartile range of 36: $(Q_3 - Q_1) \approx (71-35) \approx 36$ µg/m^3

Every additional 36 µg/m^3 of daily mean PM_{10} increases the odds ratio of an asthma incident for a person between 5 to 17 years old by 13%. The 95% confidence interval suggests that there could be as little as 5% or as high as 21% increased risk of an asthma incident.

All ambulatory events, ages 0 – 17

The ADHS data base contains emergency and inpatient records. There are also a large number of asthma incidents by ambulatory place of service in the AZHQ database. We conducted an analysis from the AZHQ database with only ambulatory data to compare to the previous ADHS results. The adjusted odds ratio and 95% confidence interval are shown in Table 7.4

Table 7.5. Results for ambulatory events only

Variable	Coefficient	SE	p-value	Adjusted OR*	95% CI
Dailymean PM_{10}	0.00163	0.0008124	0.0448	1.060	(1.001, 1.123)

Adjusted OR is the odds ratio adjusted by the approximate interquartile range of 36: $(Q_3 - Q_1) \approx (71\text{-}35) \approx 36\ \mu g/m^3$

The adjusted odds ratio is 1.060. The confidence interval suggests that there could be as little as 0.1% or as high as 12% increased risk of an asthma incident. The results from AZHQ and ADHS showed similar effects.

Ambulatory events excluding ages 0-4, the preschool group

The analysis of the AZHQ ambulatory events was repeated excluding the preschool (0-4 years old) group. The odds ratio and 95% confidence interval are shown in Table 7.5

Table 7.6. Results for ambulatory events without the preschool group

Variable	Coefficient	SE	p-value	Adjusted OR*	95% CI
Dailymean PM_{10}	0.00551	0.00172	0.0013	1.219	(1.080, 1.377

Adjusted OR is the odds ratio adjusted by the approximate interquartile range of 36: $(Q_3 - Q_1) \approx (71\text{-}35) \approx 36\ \mu g/m^3$

The adjusted odds ratio is 1.219. The confidence interval suggests that there could be as little as 8% or as high as 38% increased risk of an asthma incident. The results from AZHQ and ADHS data were similar.

Case-crossover summary

Assembled in Table 7.6, the results from the four childhood asthma populations exhibit certain differences. That the coefficients vary considerably indicate four somewhat different relationships between asthma and event-day PM_{10} concentration. As the standard errors are all similar except for the fourth case, this case is considered the most uncertain by this criterion. Among the p-values, however, it is the third case that is the most uncertain, although still statistically significant at the five percent confidence level. The adjusted odd ratios show that in all four cases the risk of asthma increases with an increase in PM_{10} concentration of 36 $\mu g/m^3$. The increased risk is highest for the case of ambulatory events excluding preschoolers and lowest for all ambulatory events, but these are the two cases of greatest uncertainty, based on the standard error of the former and p-value of the latter. Of greater importance in this work, the adjusted odd ratios of the first two cases -- all events with and without preschoolers – are accompanied by low standard errors and by p-values far less than the significance level of 0.05. The increased risk of asthma from an incremental gain of 36 $\mu g/m^3$ of daily-averaged PM_{10} is 9% for all children 0-17 years of age and 13% for children 5-17 years of age.

Table 7.7. Case-crossover statistics relating asthma incidents to PM_{10} concentrations in central Phoenix

Case	Variable	Coefficient	Standard Error	p-value	Adjusted OR*	95% CI
All events	Dailymean PM_{10}	0.0025	0.00075	0.0010	1.093	(1.061, 1.153)
All events w/o ages 0-4	Dailymean PM_{10}	0.0033	0.00096	0.0006	1.127	(1.053, 1.206)
Ambulatory events	Dailymean PM_{10}	0.0016	0.00081	0.0448	1.060	(1.001 1.123)
Ambulatory events w/o ages 0-4	Dailymean PM_{10}	0.0055	0.00172	0.0013	1.219	(1.080, 1.377)
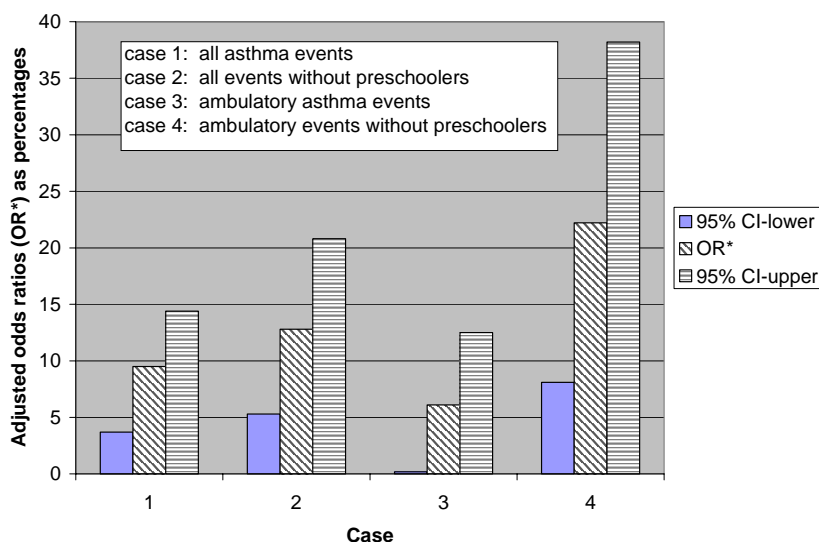
Figure 7.7. Adjusted odd ratios expressed as percentages with 95% lower and upper bound confidence limits for the four asthma populations

Model Validation

The regression analysis is based on a linear relationship between the Dailymean exposure and response. A model without any linear or monotonic assumptions determined the relationship between asthma incidents and Dailymean PM_{10}. Divided into quartiles, the PM_{10} concentrations were linked to asthma events by the indicator variables in the regression models with the first quartile as the baseline. The natural logarithm of the adjusted odds ratio of an asthma incident, "log odds" of the y-axis, plotted against the exposure quartile in Figure 7.8, illustrates the monotonic, nearly linear relationship of the log odds versus the quartiles of the Dailymean PM_{10}.
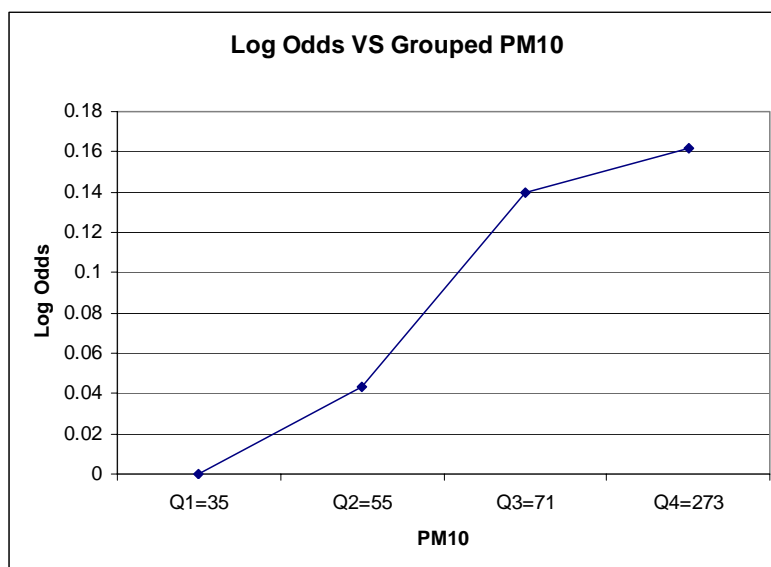
Figure 7.8.   Natural logarithm of the adjusted odds ratio (Log Odds) of asthma incidents versus quartiles of mean PM_{10} concentrations

Chapter 8 Asthma warning systems

Predicting air pollutant concentrations has been one of the mainstays of the Air Quality Division of the Arizona Department of Environmental Quality since the early 1990s. These predictions have been for ozone in Phoenix and for particulate matter in Phoenix and Yuma, with more specialized predictions for various towns and cities during the forest fire and prescribed burning seasons. In general, predictions of this kind can be done in three ways, presented here in hypothetically decreasing degrees of rigor, reliability, and labor:

1. Apply deterministic grid-based meteorological and air quality models, coupled with a complete, model-ready emissions inventory, to predict concentrations of several different pollutants throughout a particular urban area or region. One example of this is a predictive system for the eastern United States for both ozone and fine particulates. Another example is in Seattle, Washington, where predictions of gaseous, particulate, and air toxic pollutants are made throughout the Seattle-Portland region. Predictions for both of these progressive systems are distributed to the news media and are made available through the internet. The predictions are a result of first, having an adequate emissions inventory that is ready for the air quality model; second, running a prognostic meteorological model such as MM5 to predict tomorrow's meteorological fields of temperature, winds, and so forth; and third, running an air quality model such as the Community Multiscale Air Quality system (CMAQ) to provide the grid-based concentrations of pollutants. Among the products of the Seattle system are color-coded concentration maps for the next day's pollutants that can be viewed through the internet on home (and business) computers.

2. Apply a statistical model that relates historical pollutant levels to measured meteorological variables at a specific air pollutant monitoring site to predict tomorrow's air quality. Though neither computationally nor labor intensive as the first method, this system still requires full-scale meteorological modeling with a grid-based prognostic model. This meteorological modeling is first done for the historical period to derive quantitative relationships between the measured and simulated variables such as mixing height, wind

speed, and temperature. In constructing the system as a whole, the next step is to determine from the historical record the statistical relationship between measured meteorological variables and pollutant concentrations at a specific monitoring site. With this relationship, and with the link between the meteorological model's predictive performance and the measured variables, a daily operational system can then be put into place. It works as follows and entails considerable automation. First, the prognostic meteorological model is run for the next day, producing tomorrow's meteorological fields of importance in air pollution. Second, these predicted fields are aligned with those from the historical record and their corresponding air pollutant concentrations. Third, tomorrow's air pollution is predicted statistically from the predicted weather and the correspondence between the historical weather and measured air pollution. Into this system an additional component can be incorporated that adds the daily pollutant-weather measurements and simulated weather to the historical records in such a way that the system *en toto* effectively improves it performance with each additional day's prediction. This last wrinkle is subsumed into a mathematical-statistical construct called a "neural network." As described in chapters 4 and 6 of this report, the historical portion of this work has already been done for PM_{10} for Maricopa County's Central Phoenix monitoring site. Based on one year of measurements, the system's performance for November 2005 PM_{10} concentrations was slightly better than the deterministic CMAQ model's.

3. The third kind of predictive system, and the one employed by Air Quality Division meteorologists for over ten years, can be characterized as "manual forecasting." In this method the meteorologist scrutinizes different National Weather Service and other numerical models that predict a host of variables influencing pollutant concentrations. This scrutiny extends to regional and national weather maps and charts that are of help in predicting long-distance transport. This staff person synthesizes the various predictions, in part based on how well they have performed. The next step is to relate the most recent two or three days' pollutant concentrations to the measured weather variables, and, in many cases, to consult the historical records to understand how these relationships have led to specific levels of an air pollutant. Often pollutant concentrations are assembled from broad swaths of Arizona and southern California, as well as from greater Phoenix. Because the prediction does not have to be made until noon, the staff person will usually examine the morning's hourly concentrations to determine how quickly (or slowly) the present day's air pollution is developing. Finally, with all this information and with genuine seat-of-the-pants knowledge and intuition, the forecaster issues tomorrow's predictions for ozone or particulates.

Since asthma has been clearly linked with PM_{10} concentrations, not only in the present work but also in numerous studies worldwide, an effective asthma warning system would consist of two parts:

- one (or more than one) of the three predictive systems just described, and

- an automated, or semi-automated communication network that would not only advise the news media on tomorrow's PM_{10} outlook but would also send this prediction directly to interested citizens by phone, fax, text, and/or e-mail. These citizens would include parents of asthmatic children, school nurses and other school officials, public health nurses, and, anyone of any age or occupation who wished to receive the notices because of respiratory sensitivity in themselves, their immediate families, relatives, friends, or neighbors.

Chapter 9 Conclusions

Major findings on asthma and PM$_{10}$

- PM$_{10}$ concentrations have a statistically significant association with asthma incidents in central Phoenix at the 95% confidence level.

- For children ages 5-17 an increase in the daily mean PM$_{10}$ from the 25th to the 75th percentile - 36 μg/m^3 in this study - is associated with a 13% increase in the probability of asthma incidents, an effect ***much stronger*** than in previous studies.

- The effects of age and gender were insignificant.

Additional findings

- CMAQ generally underestimated the higher PM10 concentrations and overestimated the lower, with the better correlations for the higher concentrations.

- The better correlations in the higher concentration regimes, despite their under predictions, still bode well for the viability of the predictive tool to warn asthma populations in central Phoenix for these reasons:
    - The under predictions were most pronounced at the two maximum concentration sites of Durango Complex and West 43rd Avenue, which represent the worst PM$_{10}$ air quality in metropolitan Phoenix.
    - Any predictive system that comes close to predicting these peak concentrations provides adequate protection for asthmatic children in the rest of greater Phoenix.

- Despite some shortcomings, the meteorological model MM5 performed adequately for the needs of this project, even though it
    - failed to simulate the higher wind speeds;
    - overestimated the low wind speeds during stable conditions at night and in the early morning;
    - could not capture the rapid changes of wind direction during the morning and evening transitions.

- Because the uncertainty in emissions far exceeds that of the meteorological fields or of the dynamics and chemistry inherent in the model, the construction, maintenance, and periodic updating of an adequate model-ready PM$_{10}$ emissions inventory ought to receive a higher priority and more resources.

- The Neural Network, which proved to be somewhat better than CMAQ in predicting PM$_{10}$ concentrations, might be a complementary system for the "manual forecasting" now in place.

- Because the PM$_{10}$ concentration fields from inverse distance weighting (IDW) and the more sophisticated ordinary kriging were similar, only the former were used to produce the census-tract-specific concentrations for the health analysis.

References

Arizona Department of Environmental Quality (ADEQ), 2008. *2007 Annual Report*. [Online] Available at: http://www.azdeq.gov/environ/air/monitoring/monitor.html [Accessed 27 October 2008]

Bateson, T. and Schwartz, J., 1999. Control for seasonal variation and time trend in case-crossover study of acute effects of environmental exposures. *Epidemiology*, 10(5), pp.539–544.

Bateson, T. and Schwartz, J., 2001. Selection bias and confounding in case-crossover analyses of environmental time-series data. *Epidemiology*, 12(6), pp.654–661.

Byun, D. W. and Ching, J. K. S., 1999. *Science Algorithms the EPA Model-3 Community Multiscale Air Quality (CMAQ) Modeling System*, Washington, DC: U.S. Environmental Protection Agency, Office of Research and Development, EPA-600/R-99/030.

Carolina Environmental Program, 2005. *SMOKE v2.2 User's Manual*, Chapel Hill, NC

Figueiras, A., Carracedo-Martinez, E., Saez, M., and Taracido, M., 2005. Analysis of casecrossover designs using longitudinal approaches: a simulation study. *Epidemiology*, 16(2), pp.239–246.

Gardner, M.W. and Dorling, S.R., 1998. Artificial neural networks (the multilayer perceptron)--a review of applications in the atmospheric sciences. *Atmospheric Environment*, 32(14-15), pp.2627-2736

Grell, G.A. and Dudia, D.R.S., 1994. *A description of the fifth generation Penn State/NCAR Mesoscale Model (MM5)*, Boulder, Colorado: National Center for Atmospheric Research, NCAR/TN-398+STR.

Hosmer, D. and Lemeshow, S., 2000. *Applied Logistic Regression*.2nd ed. John Wiley & Sons.

Kemball-Cook, S., Jia, Y., Emery,C., Morris, R., Wang, Z., Tonnesen, G., 2004. *2002 Annual MM5 36 km simulation to support WRAP CMAQ visibility modeling for the Section 308 SIP/TIP: Preliminary Report on the Initial 2002 36 km MM5 Simulation Performed during 2003*, ENVIRON International Corporation and University of California Riverside.

Lee, S. M., Giori, W., Princevac, M., Fernando, H. J. S., 2005. Implementation of a stable turbulence parameterization for the mesoscale model MM5: nocturnal flow in complex terrain, *Boundary-Layer Meteorology*, 119, pp.109-134.

Levy, D., Lumley, T., Sheppard, L., and Checkoway, H., 2001. Referent selection in casecrossover analyses of acute health effects of air pollution. *Epidemiology*, 12(2), pp.186–192.

Lin, M., Steib, D., and Chen, Y., 2005. Coarse particulate matter and hospitalization for respiratory infections in children younger than 15 years in Toronto: a case-crossover

analysis. *Pediatrics*, 116(2):e235–e240.

Lumley, T. and Levy, D., 2000. Bias in the case-crossover design: implications for studies of air pollution. *Environmetrics*, 11, pp.689-704.

Maclure, M., 1991. The case-crossover design: a method for studying transient effects on the risk of acute events. *American Journal of Epidemiology*, 133(2), pp.144–153.

Maricopa County Department of Air Quality (MCDAQ), 2007. *2007 Air Monitoring Network Review.*
[Online]
Available at: http://www.maricopa.gov/aq/divisions/monitoring/network.aspx
[Accessed 27 October 2008]

Medina-Ramon, M., Zanobetti, A., and Schwartz, J., 2006. The effect of ozone and PM_{10} on hospital admissions for pneumonia and chronic obstructive pulmonary disease: a national multicity study. *American Journal of Epidemiology*, 163(2), pp.579–588.

Morris, R.E., Koo, B., Lau, S., Tesche, T.W., McNally, D., Loomis, C., Stella, G., Tonnesen, G., Wang, Z., 2004. *VISTAS Emissions and Air Quality Modeling – Task 4cd Report: Model Performance Evaluation and Model Sensitivity Tests for Three Phase I Episode*, ENVIRON International Corporation, Novato, California.

Neas, L., Schwartz, J., and Dockery, D., 1999. A case-crossover analysis of air pollution and mortality in Philadelphia. *Environmental Health Perspective*, 107(8), pp.629–631.

Peel, J., Tolbert, P., Klein, M., Metzger, K., Flanders, W., Todd, K., Mulholland, J., Ryan, P., and Frumkin, H., 2005. Ambient air pollution and respiratory emergency department visits. *Epidemiology*, 16(2), pp.164–174.

Redelmeier, D. and Tibishirani, R., 1997. Association between cellular-telephone calls and motor vehicle collisions. *The New England Journal of Medicine*, 336(7), pp.453–458.

Schwartz, J. and Dockery, D.W., 1992. Increased mortality in Philadelphia associated with daily air pollution concentrations. *American Review of Respiratory Disease*, 145, pp.600–604.

Szyszkowicz, M., 2006. Use of generalized linear mixed models to examine the association between air pollution and health outcomes. *International Journal of Occupational Medicine and Environmental Health*, 19(4), pp.224–227.

U.S. Environmental Protection Agency, Office of Air Quality Planning and Standards, 2007. *Guidance on the Use of Models and Other Analyses for Demonstrating Attainment of Air Quality Goals for Ozone, PM2.5 and Regional Haze*, Research Triangle Park, North Carolina: EPA-454/B-07-002.

Western Governors' Association (WGA), 2006. *Final Report for the Western Regional Air Partnership (WRAP) 2002 Visibility Model Performance Evaluation*, WGA 30203.

Appendix A

PM monitoring sites

Table A-1. Characteristics and images of continuous PM$_{10}$ monitoring sites

Symbol	Name	Objective[1]	Scale[2]	Height[3]	Cover[4]
Permanent sites (all MC, except SS, which is ADEQ)					
WF	West 43rd Avenue	#1 #3	Middle/ Neighborhood	5	Gravel
					Paved
					Desert, bare dirt
DC	Durango Complex	#1 #3	Middle/ Neighborhood	3.9	Paved
					Bare dirt
					Paved, bare dirt, homes, offices
WP	West Phoenix	#2	Neighborhood	3.6	Gravel
					Paved
					Lawns/Houses
CP	Central Phoenix	#2	Neighborhood	11.3	Paved
					Paved
					Commercial & residential
SS	Supersite	#2	Neighborhood	4.4	Gravel
					Lawns
					Homes, apartments
GR	Greenwood	#2	Micro/Middle	4.4	Paved
					Paved, lawns
					Freeways
SP	South Phoenix	#2 #3	Neighborhood	4.0	Paved parking lot
					Pavement, dirt lot
					Commercial & residential
Temporary sites (ASU), November 2007 – March 2008					
MRV	Maryvale	#2	Neighborhood	4.4	Lawn
					Golf Coarse
					Homes
VGC	Valley Garden Center	#2	Neighborhood	2.0	Lawns
					Homes
					Garden Area
WVR	Weaver's Auto Service	#2	Neighborhood	2.0	Paved
					Lawns, homes
					Lawns, apartments
CSA	Community Service AZ	#2	Neighborhood	4.4	Gravel
					Paved
					Homes

1. Objectives

    1. Determine highest concentrations expected to occur in the area covered by the network.

    2. Determine representative concentrations in areas of high population density.

    3. Determine the impact on ambient pollution levels of significant sources or source categories.

2. Choices of spatial measurement scales (radius from site)

    Micro Scale 0 to 100 meters

    Middle Scale 100 to 500 meters

    Neighborhood Scale 0.5 to 4 kilometers

    Urban Scale 4 to 50 kilometers

Regional Scale 10 to 100s of kilometers
Note: In addition to the scales specified in the table, all sites have PM_{10} concentrations with some (unknown) degree of urban contributions from transport and with 10 ug/m3 of desert background on an annual basis.

3. Height of instrument inlet above ground in meters

4. Predominant ground surface in

    (1) immediate vicinity of the monitor (0 – 25 meters);

    (2) 25 – 100 meters; and

    (3) 100 – 500 meters.

Table A-2. Traffic near PM monitoring sites

Symbol	Name	Streets	Distance[1]/ Direction	Traffic[2]
WF	West 43rd Ave.	Broadway Road	37, S	8,000
DC	Durango Complex	27th Avenue	78, E	9,000
		Durango Street	325, N	9,000
WP	West Phoenix	39th Avenue	30, W	2,000
		Earll Drive	25, N	<1,000
		Thomas Road	360, S	32,000
CP	Central Phoenix	16th Street	91, W	24,000
		Roosevelt Street	75, N	12,000
		I-10 – E-W portion	450, N	276,000
		I-10 – N-S portion	865, E	297,000
SS	Supersite	17th Avenue	11, E	<1,000
		15th Avenue	425, E	17,000
		Camelback Road	635, N	40,000
		19th Avenue	370, W	17,000
		I-17	1525, W	208,000
GR	Greenwood	27th Avenue	10, E	19,000
		I-10	85, N	229,000
		I-17	850, E	101,000
SP	South Phoenix	Broadway Road	360, N	25,000
		Central Avenue	200, E	16,000
		7th Avenue	680, W	22,000
MRV	Maryvale	51st Avenue	115, E	30,000
		Indian School Road	300, S	34,000
VGC	Valley Garden Center	15th Avenue	30, W	13,000
		McDowell Road	267, S	21,000
WVR	Weaver's Auto Service	29th Street	33, W	<500
		Thomas Road	75, S	38,000
CSA	Community Service AZ	59th Avenue	36, E	31,000
		Glendale Ave./Grand Ave/59th Ave Intersection	375, NNE	73,000

1 Distance in meters and direction towards the roadway

    2 Average daily traffic for weekdays: vehicles per day
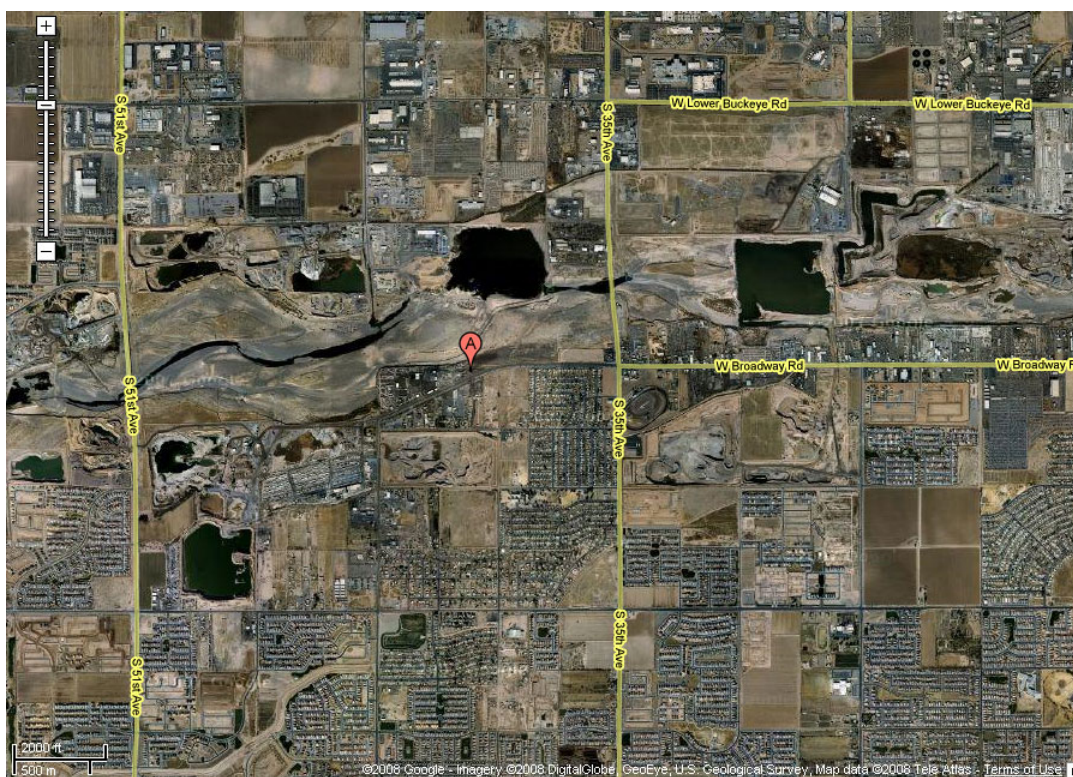
Figure A1.1. West 43rd Avenue PM$_{10}$ monitoring site
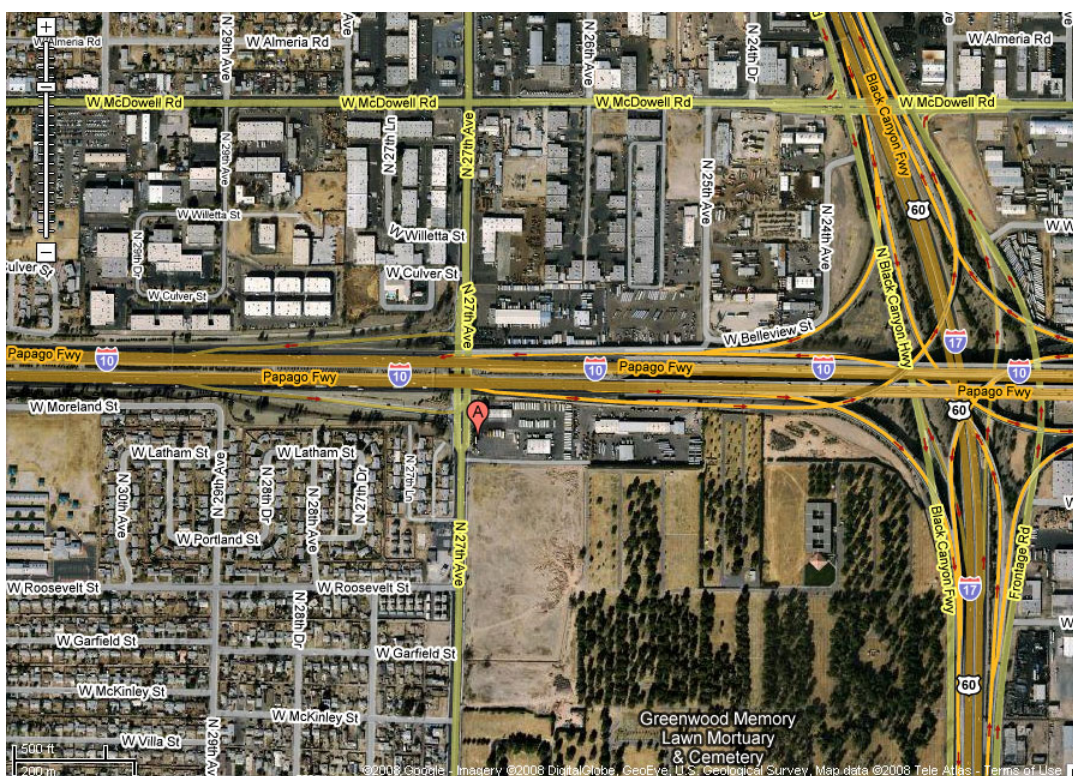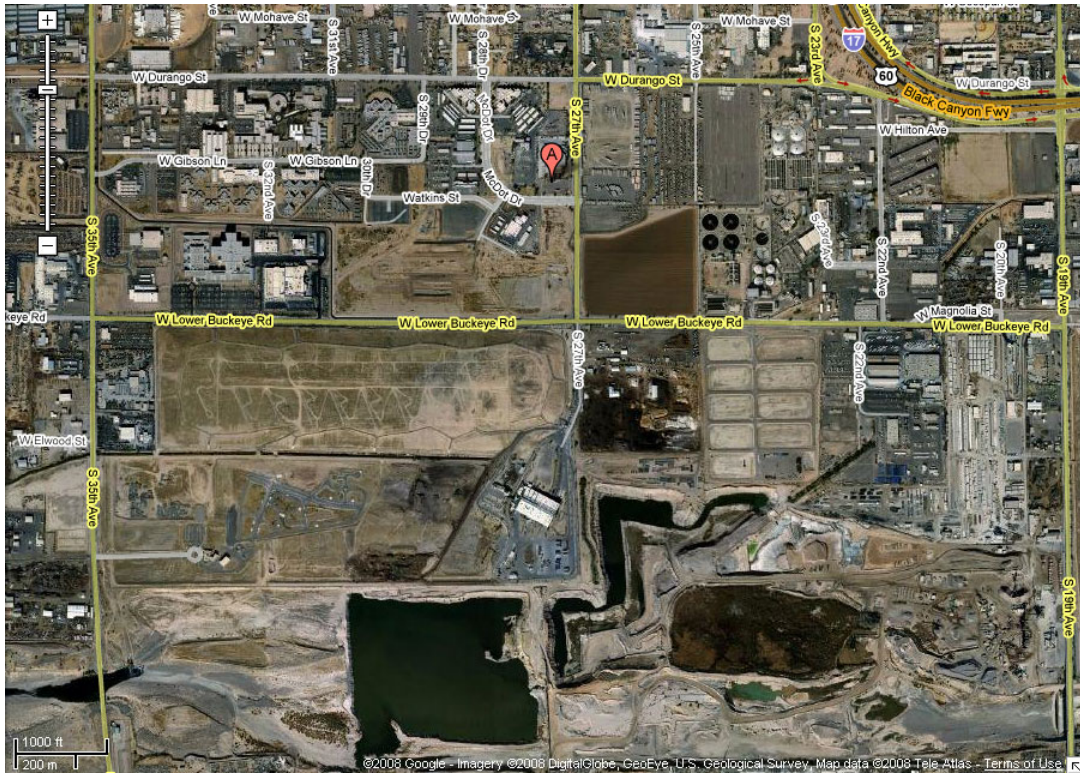

Figure A1.2. Greenwood PM$_{10}$ monitoring site
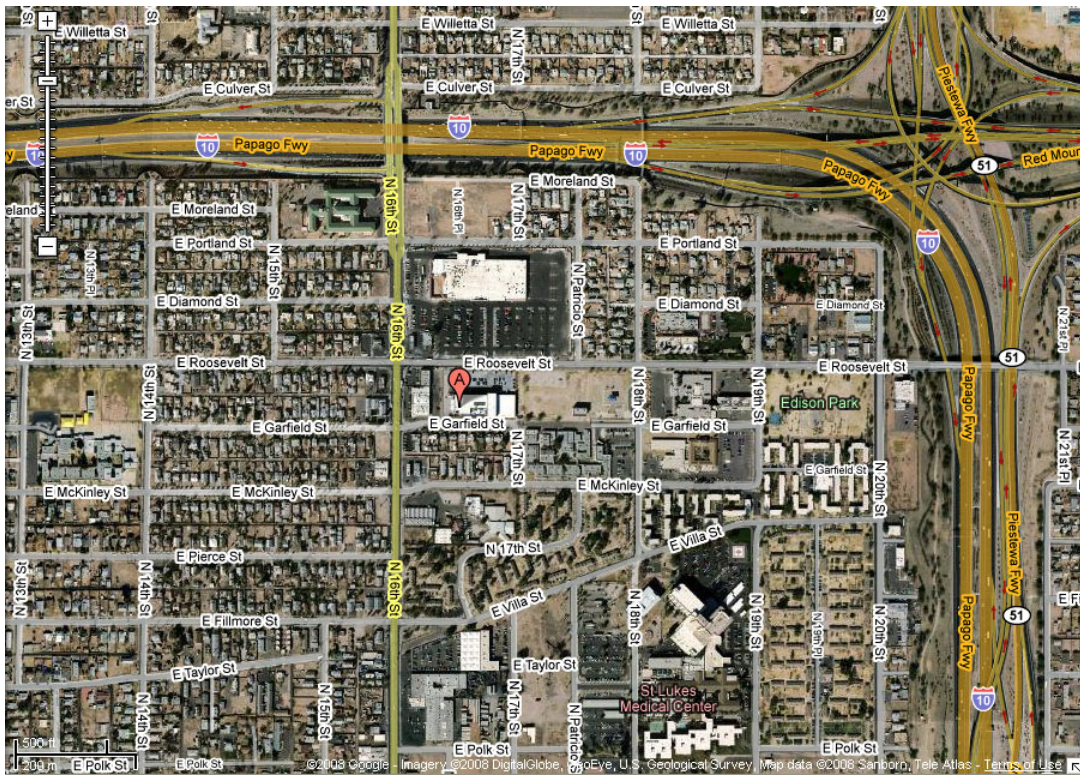
Figure A1.3. Durango Complex PM_{10} monitoring site

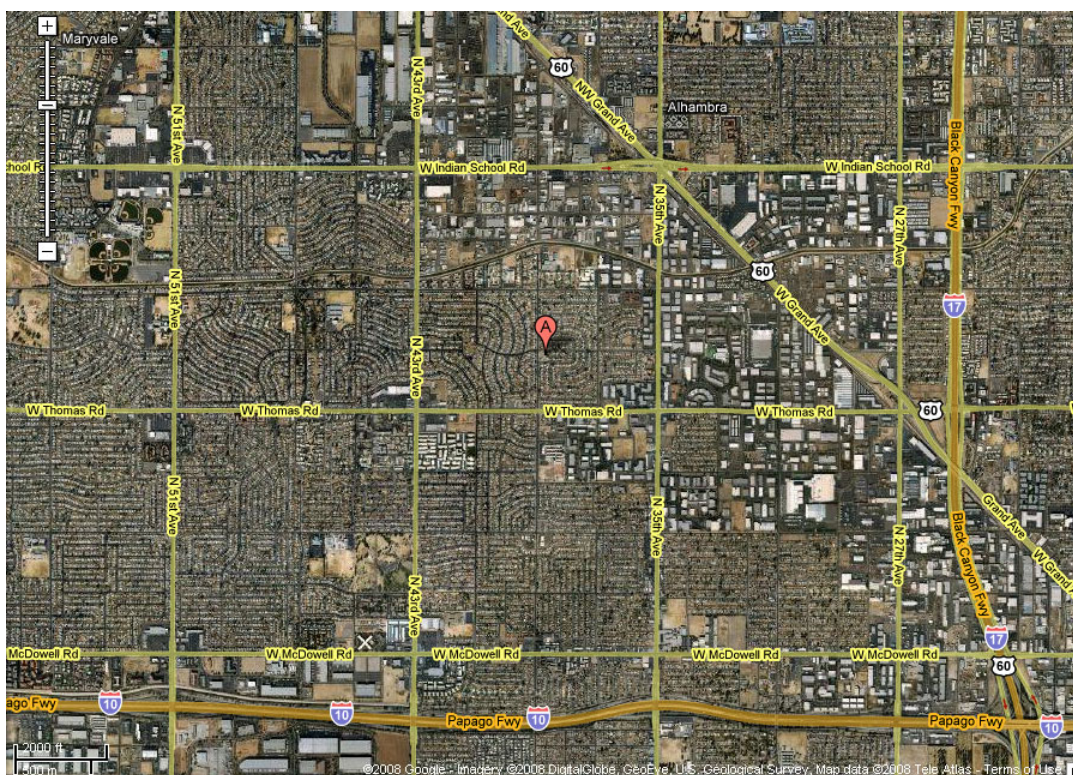Figure A1.4. Central Phoenix PM_{10} monitoring site

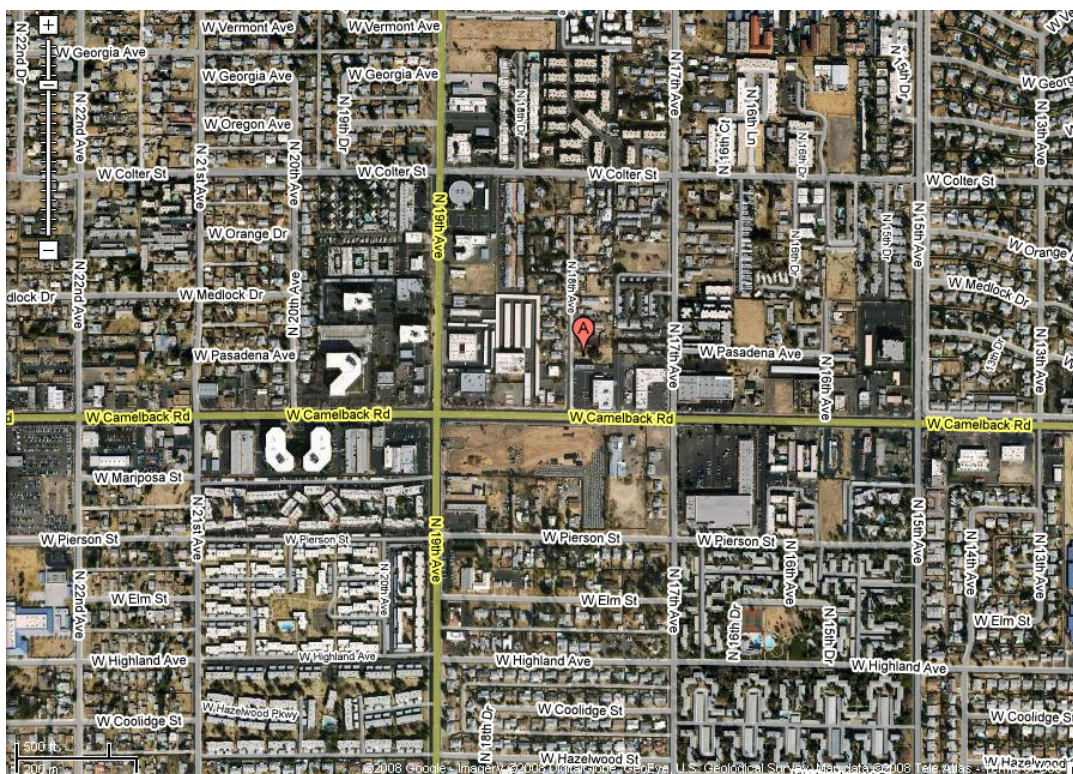Figure A1.5. West Phoenix PM$_{10}$ monitoring site
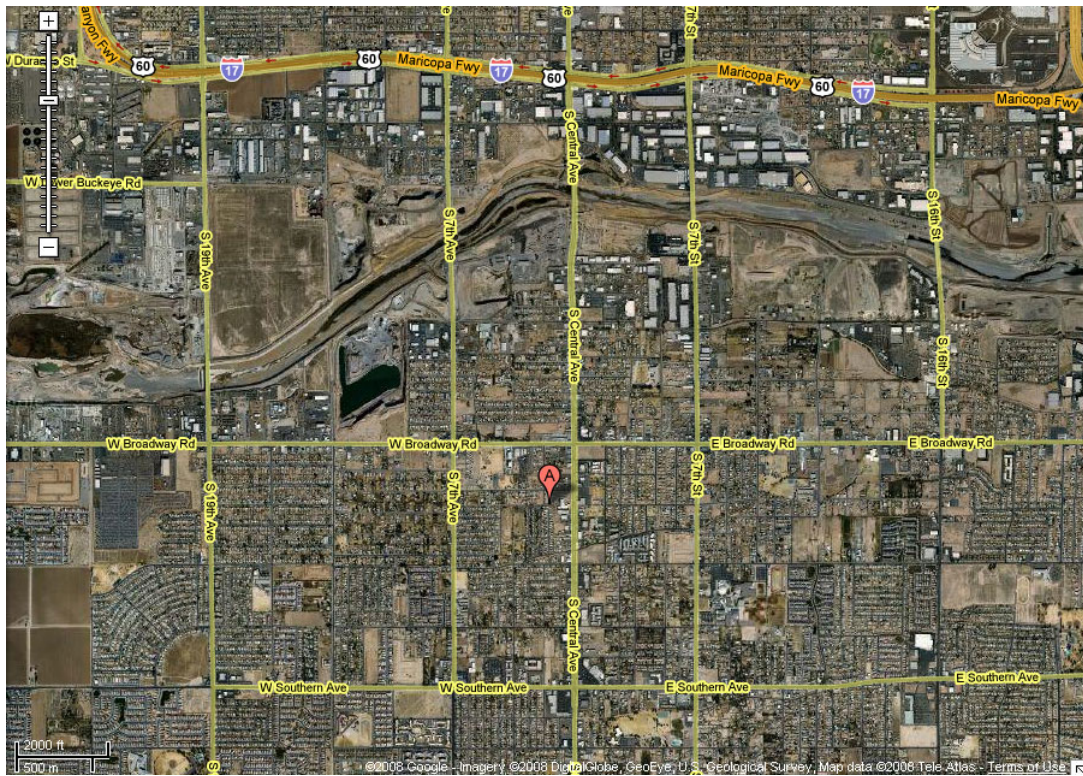

Figure A1.6. Supersite PM$_{10}$ monitoring site

Figure A1.7. South Phoenix monitoring site

Appendix B

Neural Network

This appendix goes with Chapter 4 and explains some of the details of the network's construction.

Bearing in mind that the main purpose of EnviNNet is the prediction of PM_{10}, the following design choices were made:

- *architecture*: three-layer MLP network, with the number of hidden nodes selected to reliably rebuild data from a test data-set;

- *topology***:** full connection between layers and no connection between neurons in the same layer;

- *transfer function*: exponential, to ensure positive functions at the output node, and hyperbolic tangent for hidden nodes, with the latter an excellent compromise for a non-linear function both globally and locally;

- *information flow*: feed-forward;

- *representation of input variables***:** standardization of inputs to eliminate problems due to different measurement scales for different predictors;

- *reconstruction of the output signal*: through linear combination and exponentialization of the outputs of hidden nodes; and

- *training method*: parameters are learned or estimated through the conjugate-gradient method. It is preferred over the back-propagation method as it exploits both first-order (gradient) and second-order (curvature) data during optimization of the objective function.

Mathematically, the three-layer neural network has the following form:

$$y = f\big(\varphi(x, w)\big)$$

where x represents input data, w the coefficients (parameters estimated by learning), f the activation functions from layers 2 to 3 and φ the activation functions from layers 1 to 2. The choice of f and φ determines the output; for example, if φ is hyperbolic tangent and f linear, an input of meteorological and pollution variables are transformed to an output with both negative and positive values, but if f is exponential the output can have only positive values. As such, an exponential function for the output and a hyperbolic tangent activation function for the hidden neurons were selected.

Appendix C

MM5 - modeling results and discussion

This appendix goes with Chapter 5 and explains some of the more detailed aspects of the meteorological modeling.

The modeling domain was based on a Lambert Projection, centered at (97°W, 40°N), and three nested domains with 36, 12 and 4km grids were utilized. In the nested simulations, the results obtained for the outer domain were used as initial and boundary conditions for the inner domain. Vertically 29 levels were applied with the layer closest to the ground being seven meters to capture the surface-layer processes. The parent domain for MM5 covered the entire North American continent with 36km grids, the inner domain with 4x4km grids, was centered in Phoenix and its surrounding mountains (Figure C-1).

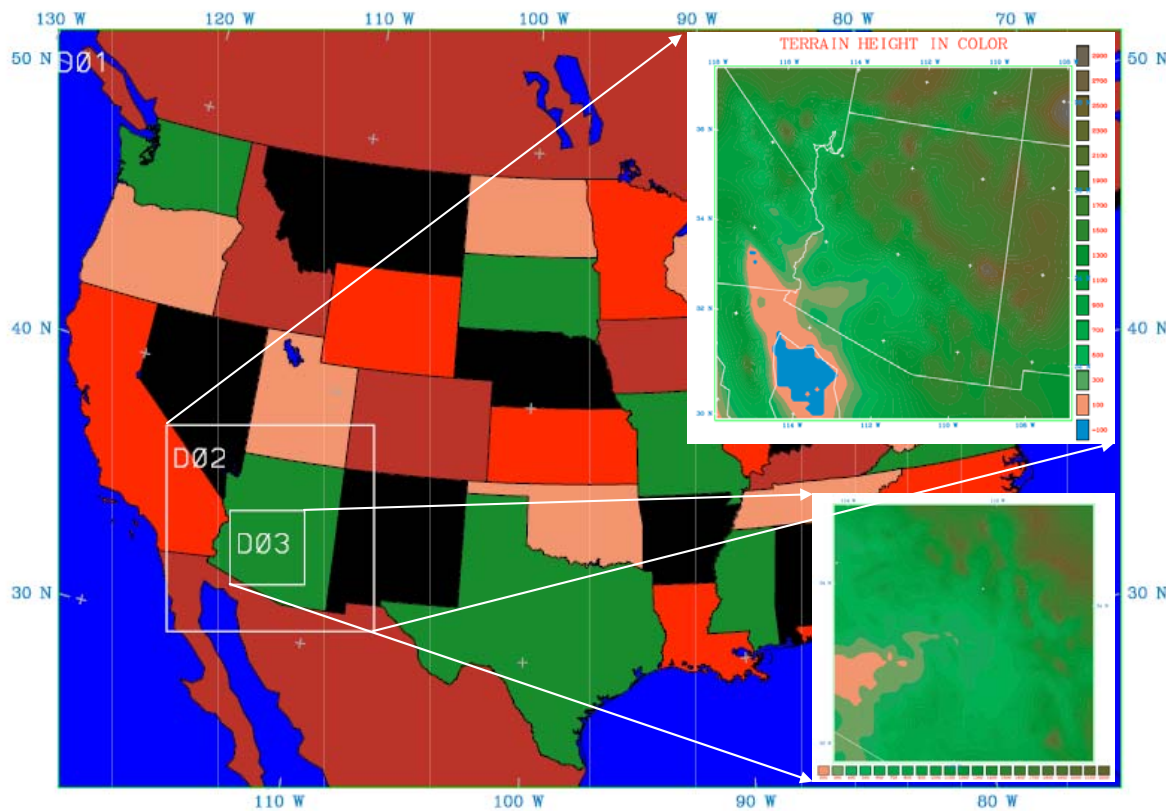Figure C-1. Modeling domains used with weather predicting model MM5

The number of rows (running west-east), columns (running south-north) and the definition of the *x-y* origin (i.e. the southwest corner) are listed in Table C-1. For each domain the values indicated as the *x-y* origin are the distances in meters of the domain's southwest corner from the center of the parent domain (97°W, 40°N).

Table C-1. Grid definitions for MM5 model

Model	Columns Dot (Cross)[1]	Rows Dot (Cross)[1]	South-west corner (in *m*)	
			x Origin	*Y* Origin
MM5 – *36km*	130 (129)	94 (93)	-2304000	-1656000
MM5 – *12km*	77 (76)	77 (76)	-1836000	-972000
MM5 – *4km*	83 (82)	83 (82)	-1648000	-908000

[1]Dot nodes are defined at grid cell vertices; cross nodes – at grid cell centers;

A model validation was necessary to estimate the model performance in the study region. Without a doubt concentration fields depend on the meteorological conditions (wind, temperature, rainfall, humidity, and so forth). So it is very important to have good performance for the meteorological flow field. Several tests were made for different physical components to achieve better model predictions. The sensitivity tests (three days were performed for each case - November 2005 and April 2006) were carried out specifically to solve temperature and humidity problems in the southwestern US. It was found in earlier studies (WGA, 2006; Morris et al., 2004; Kemball-Cook et al., 2004) that the model underestimates the amplitude of the diurnal temperature cycle and greatly overestimates the humidity during the summer. The difficulties associated with the parameterization of turbulence in the stable nocturnal planetary boundary layer (PBL) have been overcome by the use of a modified Medium Range Forecast (MRF) scheme (Lee et al., 2005). MRF is high resolution PBL based on non-local K-theory with an additional counter gradient term that incorporates the contribution of large-scale eddies to the total flux. A unique aspect of this parameterization is its stability-dependant turbulent Prandtl number that allows momentum to be transported by the internal waves, while heat diffusion is impeded by the stratification. The new schemes showed an improvement in predictions, particularly for nocturnal near-surface temperatures. Surface wind predictions also improved slightly, but not to the extent of the temperature predictions. The physical options ultimately chosen are shown into the Table C-2.

Table C-2. MM5 configuration for different domains *

Grid resolution	Radiation	LSM	PBL	Cumulus	Microphysics	Analysis FDDA 3D	Surface
D1 – 36km	RRTM	5 Layers	MRF mod.	Betts-Miller	Mixed Phase	W/T/H	W/T/H
D2 – 12km	RRTM	5 Layers	MRF mod.	Grell	Mixed Phase	W/T/H	W/T/H
D3 – 4km	RRTM	5 Layers	MRF mod.	None	Mixed Phase	W/T/H	W/T/H

* Abbreviations: LSM – land surface model; PBL – planetary boundary layer; FDDA – four dimensional data assimilation; RRTM – rapid radiative transfer model; MRF mod. – Medium Range Forecast scheme - modified; W/T/H – wind/temperature/humidity.

Numerical calculations were completed for both 30-day periods – November 2005 and March 11-- April 9, 2006. The model evaluations have been made for all three domains, but outcomes only for the innermost one are presented in this report. The scatter plots based on hourly wind speeds and temperature are shown for two different cases with high and low pollution (Figures C-2 and C-3) with their corresponding regression coefficients. The conclusion for both cases is that we achieve excellent model performance for temperature but only average predictions for wind fields. The model was not able to capture events with high synoptic wind speeds (Figure C-4), because of the inconsistency of the input data from the operational NCEP/ETA global model. The model predicted wind speeds considerably higher than the measured values during the night and early morning periods (Figure C-5), when stagnation with low wind speeds occurs, especially in the northeast valley. The model was able to predict the wind direction for a strong synoptic wind (Figure C-4), but the disagreement between predicted and observed directions is quite pronounced for the case

with low synoptic wind conditions (Figure C-5). The change in the wind direction with 12 hours periodicity is well displayed within the model predictions (Figure C-5). Mesoscale thermal circulation induced by the diurnal heating-cooling cycle of valley and slope flows, with down-slope/down-valley flows occurring at night and up-valley/up-slope flows during the day, was well simulated by the model, especially under low synoptic wind conditions (Figure C-6).
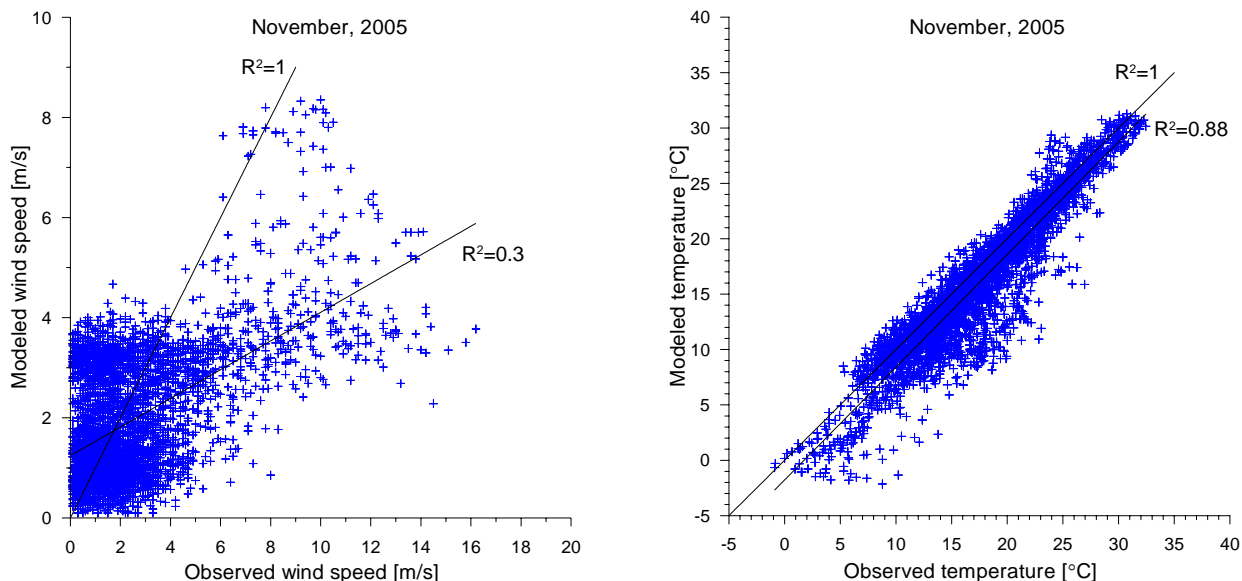
Figure C-2. Scatter plots of wind speed and temperature for all stations for high pollution episode November 2005

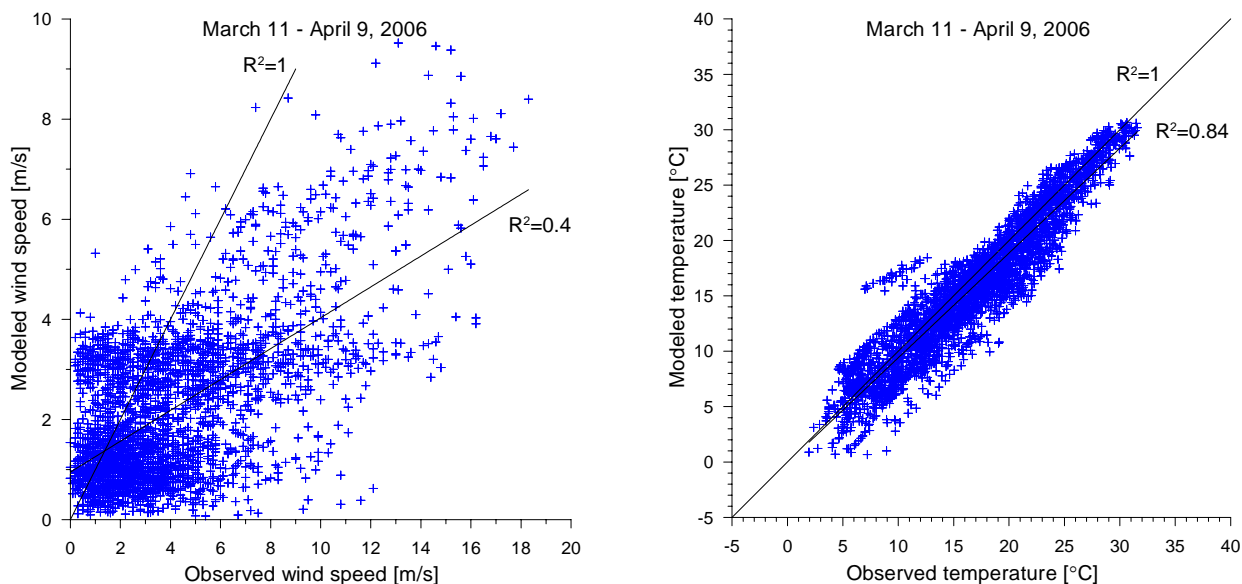Figure C-3. Scatter plots of wind speed and temperature for all stations for the low pollution period of March 11 – April 9, 2006
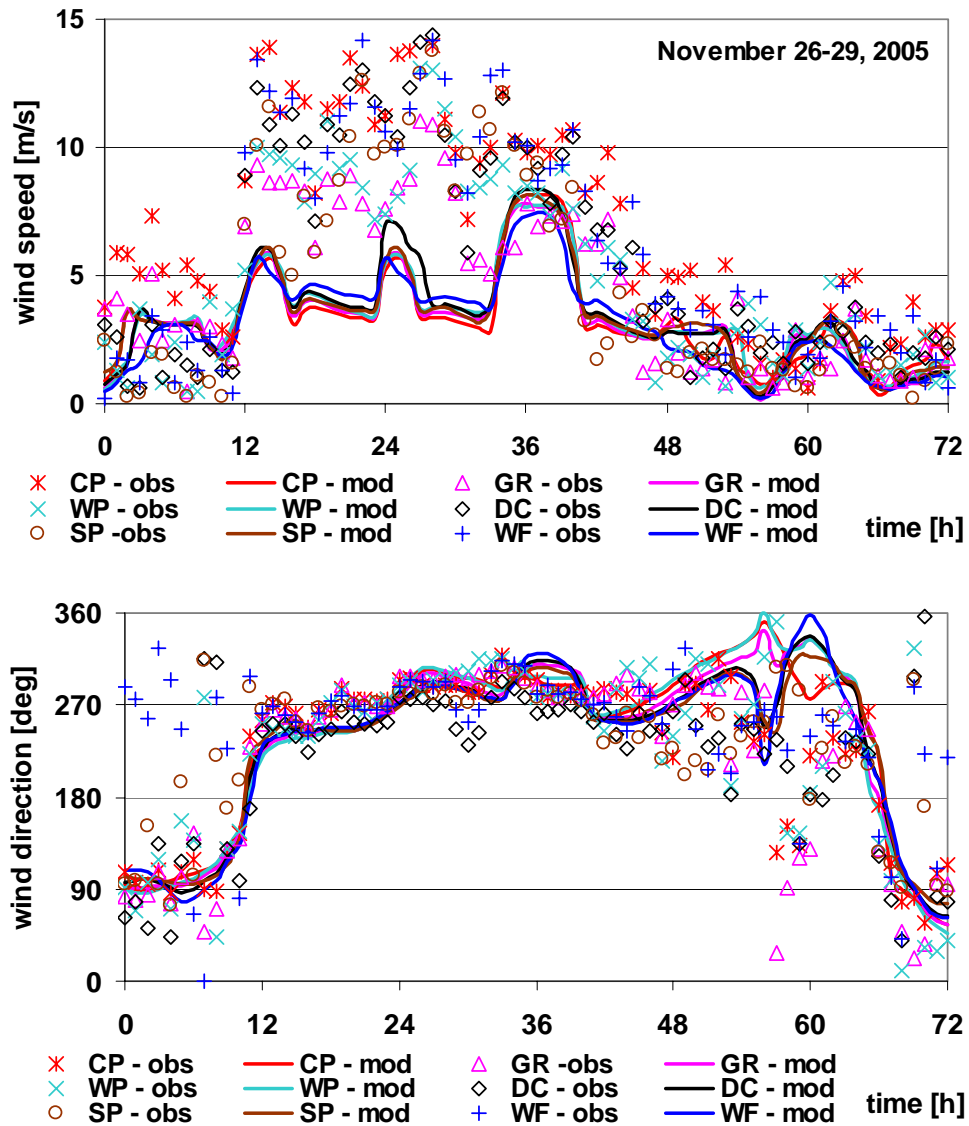
Figure C-4. Comparison between predicted and observed wind speeds and directions at different locations – with strong synoptic winds
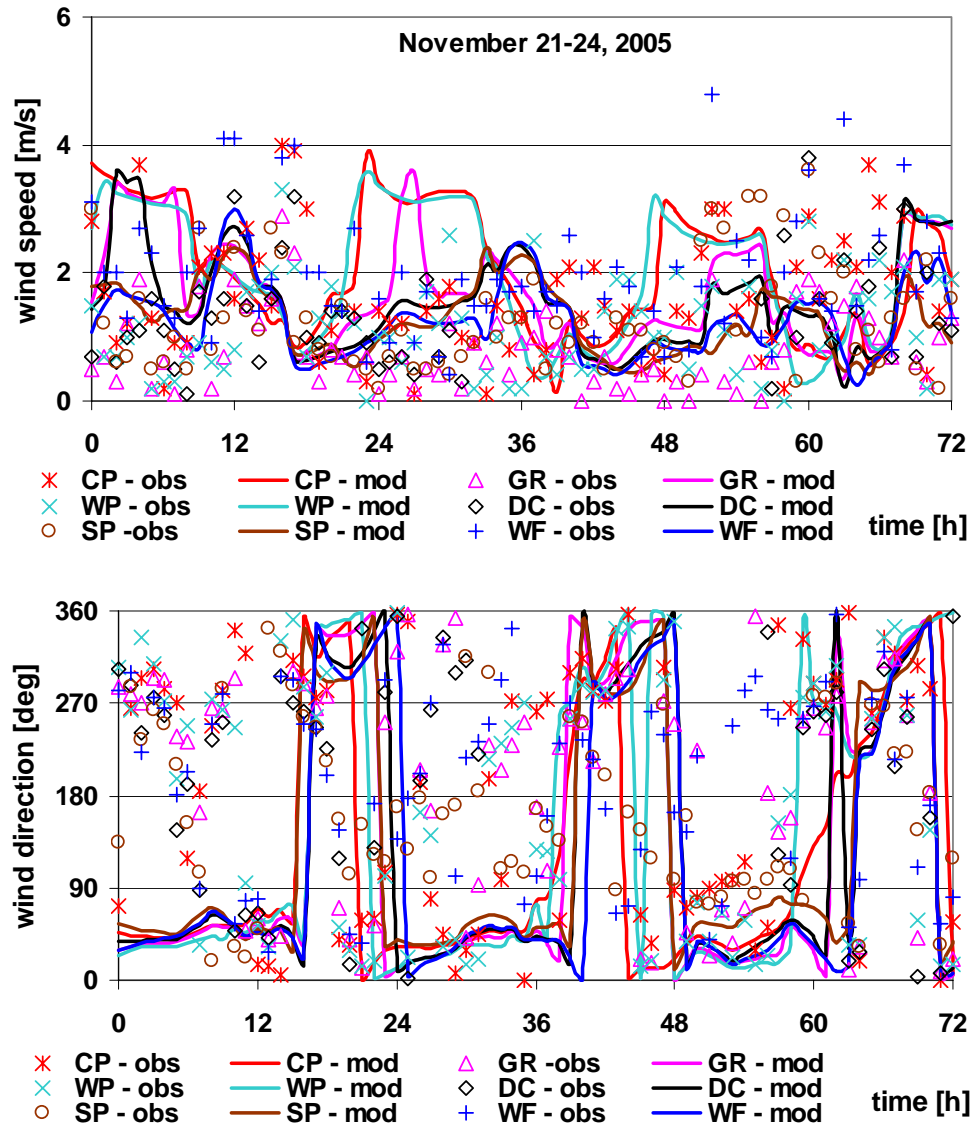
Figure C-5. Comparison between predicted and observed wind speeds and directions at different locations – with calm synoptic conditions
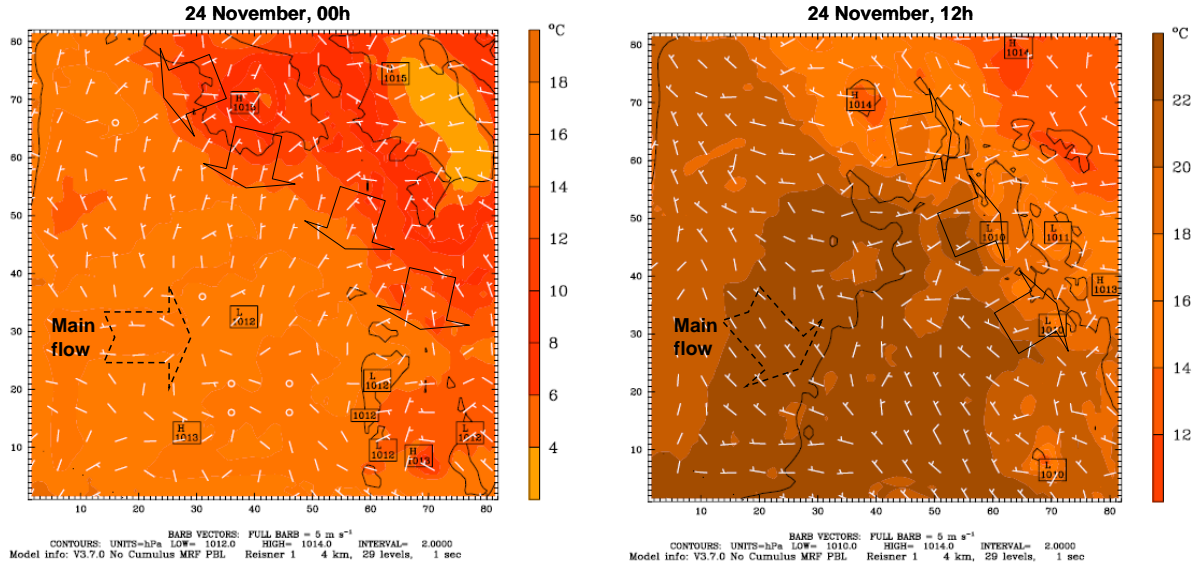
Figure C-6. Simulated horizontal winds at 10m and surface temperature fields during nocturnal (left) and daytime conditions, November 24, 2005

The Root Mean Squared Error (RMSE) is given at different locations within the study domain in Table C-3. The model gives better predictions for wind speeds less than 6m/s but the errors double for the higher wind speeds. The model provides wind flow better in the southern part (DC, SP) than the northern and central parts (CP, WP, GR) of the study domain. The worst model performance is for WF, where the influence of local effects from the Salt River channel and the South Mountains appears to be beyond the model's grasp. The MM5 model gives better performance for the winter period (November 2005) than the spring period (March-April 2006), as the RMSE for the CP and DC sites in the former are twice that of the latter.

Table C-3. RMSE for wind speed at different sites*

Range (m/s)	CP	WP	GR	WF	DC	SP
November, 2005						
All	2.56	3.25	3.1	4.0	1.95	3.32
<6	1.6	1.52	1.56	1.5	1.33	1.34
>6	6.17	4.52	3.87	6.37	4.96	5.13
March 11 – April 9, 2006						
All	5.19	5.18	-	5.21	4.28	-
<6	1.9	1.76	-	1.92	1.78	-
>6	6.1	4.63	-	6.06	5.72	-

* Abbreviations: CP – Central Phoenix; WP – West Phoenix; GR – Greenwood; WF – West 43rd Avenue; DC – Durango complex; SP – South Phoenix.

Additional statistics are shown in Table C-4, giving the model's performance at different locations in central Phoenix for both high and low pollution periods. The following indicators were used for performance evaluation (see Appendix 1 for details).

Table C-4. Summary of statistical measures, in comparing observations to model predictions of wind speed at different sites[*]

Site	MAE	RMSE	RSQ	IA	MFB [%]
			November 2005		
CP	1.02	2.56	0.36	0.55	-25.65
WP	0.12	3.25	0.36	0.67	7.74
GR	0.01	3.09	0.37	0.68	23.17
WF	0.35	3.98	0.38	0.60	-36.36
DC	0.20	1.95	0.34	0.70	-8.81
SP	0.25	3.32	0.33	0.70	5.03
			March 11- April 9, 2006		
CP	2.02	2.56	0.62	0.60	-52.82
WP	1.87	3.25	0.58	0.64	-47.39
WF	1.92	3.98	0.63	0.64	-53.63
DC	1.10	1.95	0.46	0.68	-2.42

* Abbreviations: CP – Central Phoenix; WP – West Phoenix; GR – Greenwood; WF – West 43rd Avenue; DC – Durango complex; SP – South Phoenix; MAE - Mean Absolute Error, RMSE - Root Mean Square Error, RSQ - Coefficient of Determination (aka R2), IA – Index of Agreement, MFB - Mean Fractional Bias

Appendix D

Definitions of statistics:

The following indicators were used for performance evaluation. Here P is the predicted value, O the measured value, and $\overline{P}$ and $\overline{O}$ the mean values.

$$MAE = \frac{1}{N}\sum_{i=1}^{N}|P_i - O_i| \quad \text{(Mean Absolute Error)}$$

$$MB = \frac{1}{N}\sum_{i=1}^{N}(P_i - O_i) \quad \text{(Mean Bias)}$$

$$RMSE = \sqrt{\frac{\sum_{i=1}^{N}(P_i - O_i)}{N}} \quad \text{(Root Mean Square Error)}$$

$$R^2 = \frac{\left[\sum_{i=1}^{N}(P_i - \overline{P})(O_i - \overline{O})\right]^2}{\sum_{i=1}^{N}(P_i - \overline{P})^2 \sum_{i=1}^{N}(O_i - \overline{O})^2} \quad \text{(RSQ Coefficient of determination)}$$

$$R^2 = \frac{\sum_{i=1}^{N}(P_i - \overline{O})^2}{\sum_{i=1}^{N}(O_i - \overline{O})^2} \quad \text{(RSQ* Coefficient of determination)}$$

$$IA = 1 - \frac{\sum(P_i - O)^2}{\sum(|P_i - \overline{O}| + |O_i - \overline{O}|)^2} \quad \text{(IA Index of Agreement)}$$

$$MFB = \frac{2}{N}\sum_{i=1}^{N}\frac{(P_i - O_i)}{(P_i + O_i)}.100\% \quad \text{(Mean Fractional Bias)}$$

$$MFB = \frac{2}{N}\sum_{i=1}^{N}\frac{|P_i - O_i|}{|P_i + O_i|}.100\% \quad \text{(Mean Fractional Error)}$$

$$NMB = \frac{\sum_{i=1}^{N}(P_i - O_i)}{\sum_{i=1}^{N}O_i}.100\% \quad \text{(Normalized Mean Bias)}$$

$$NME = \frac{\sum_{i=1}^{N}|P_i - O_i|}{\sum_{i=1}^{N}O_i}.100\% \quad \text{(Normalized Mean Error)}$$

Appendix E

Mathematics of the case-crossover method

This appendix begins with a general discussion of the "odds ratio", the typical statistic employed in reporting the results from the case-crossover method. The appendix continues with a discussion of conditional logistic regression, and it concludes with the specific mathematical formulation of the odds ratio used in the present work.

The **odds ratio** is a measure of effect size particularly important in logistic regression.

It is defined as the ratio of the odds of an event occurring in one group to the odds of it occurring in another group, or to a sample-based estimate of that ratio. These groups might be men and women, an experimental group and a control group, or any other dichotomous classification. If the probabilities of the event in each of the groups are p (first group) and q (second group), then the odds ratio is:

$$\frac{p/(1-p)}{q/(1-q)} = \frac{p(1-q)}{q(1-p)}.$$

An odds ratio of 1 indicates that the condition or event under study is equally likely in both groups. An odds ratio greater than 1 indicates that the condition or event is more likely in the first group. And an odds ratio less than 1 indicates that the condition or event is less likely in the first group. The odds ratio must be greater than or equal to zero. As the odds of the first group approaches zero, the odds ratio approaches zero. As the odds of the second group approaches zero, the odds ratio approaches positive infinity.

For example, suppose that in a sample of 100 men, 90 have drunk wine in the previous week, while in a sample of 100 women only 20 have drunk wine in the same period. The odds of a man drinking wine are 90 to 10, or 9:1, while the odds of a woman drinking wine are only 20 to 80, or 1:4 = 0.25:1. The odds ratio is thus 9/0.25, or 36, showing that men are much more likely to drink wine than women. Using the above formula for the calculation yields the same result:

$$\frac{0.9/0.1}{0.2/0.8} = \frac{0.9 \times 0.8}{0.1 \times 0.2} = \frac{0.72}{0.02} = 36.$$

The above example also shows how odds ratios are sometimes sensitive in stating relative positions: in this sample men are 90/20 = 4.5 times more likely to have drunk wine than women, but have 36 times the odds. The logarithm of the odds ratio, the difference of the logits of the probabilities, tempers this effect, and also makes the measure symmetric with respect to the ordering of groups. For example, using natural logarithms, an odds ratio of 36/1 maps to 3.584, and an odds ratio of 1/36 maps to −3.584.

The increased use of logistic regression in medical and social science research means that the odds ratio is commonly used as a means of expressing the results in some forms of clinical trials, in survey research, and in epidemiology, such as in case-control studies. It is often abbreviated "OR" in reports. When data from multiple surveys is combined, it will often be expressed as "pooled OR".

<u>Conditional logistic regression</u> has been widely applied to model stratified data, such as case-crossover analysis and case-control analysis (Lin et al. 2005, Neas et al. 1999, Figuerias et al. 2005, and Redelmeier and Tibishirani 1997). Logistic regression is a form of regression used when the response is binary. Let $\mathbf{x}$ be a vector of k predictor variables (or covariates). Let Y be a binary response ($y = 0$ or $y = 1$). The conditional probability that $Y = 1$ is $P(Y = 1|x) = p(x)$. The logit of the logistic regression model is

$$f(\mathbf{x}) = \beta_0 + \beta_1 x_1 + ... + \beta_p x_p$$

so the logistic regression model is

$$p(\mathbf{x}) = \frac{e^{f(x)}}{1 + e^{f(x)}}$$

Let consider the system that has a binary response y and a two-level covariate x, $x = 0$ or $x = 1$. The logit transformation is defined in terms of $p(\mathbf{x})$ as

$$f(x) = \ln[p(x)/(1 - p(x))] = \beta_0 + \beta_1 x.$$

The conditional logistic regression works in similar fashion as regular logistic regression. It considers the stratification structure in the data specifying which individuals belong to which strata. Suppose there are K strata with n_k subjects in the kth stratum, where $k = 1, 2, 3,..., K$ There are n_{1k} case subjects, n_{0k} control subjects, and $n_k = n_{1k} + n_{0k}$ (Hosmer and Lemeshow 2000). The logistic regression model can be shown as

$$p_k(\mathbf{x}) = \frac{e^{\beta_{0k} + \boldsymbol{\beta}'\mathbf{x}}}{1 + e^{\beta_{0k} + \boldsymbol{\beta}'\mathbf{x}}}$$

where is a nuisance parameter with the contribution of all terms constant within the kth stratum, $\boldsymbol{\beta}' = (\beta_1, \beta_2,..., \beta_k)$ are the vector of coefficients of covariates, $\mathbf{x}$.

To analyze case-crossover design using conditional logistic regression, the PROC PHREG from SAS® statistical software package was used. Conditional logistic regression can be performed by the PHREG procedure by using the discrete logistic model and forming a stratum for each matched set. The dummy survival times are needed to be created so that all the cases in a matched set have the same event time value, and the corresponding controls are censored at later times.

From the logistic regression model defined earlier. The odds of $y = 1$ when the covariates have values x_1 is defined as $p(1)/(1-p(1))$ and the odds of $y = 0$ when the covariates have values x_0 is defined as $p(0)/(1- p(0))$. The odds ratio (OR) is defined as the odds for x_1 to the odds for x_0, odds ratios (OR) can be shown to be

$$
\begin{aligned}
\text{OR} \quad &= \quad \frac{p(1) / [1 - p(1)]}{p(0) / [1 - p(0)]} \\[2ex]
&= \quad \frac{\left(\dfrac{e^{\beta_0 + \beta_1}}{1 + e^{\beta_0 + \beta_1}} \right) \Big/ \left(\dfrac{1}{1 + e^{\beta_0 + \beta_1}} \right)}{\left(\dfrac{e^{\beta_0}}{1 + e^{\beta_0}} \right) \Big/ \left(\dfrac{1}{1 + e^{\beta_0}} \right)} \\[2ex]
&= \quad \frac{e^{\beta_0 + \beta_1}}{e^{\beta_0}} \;=\; e^{(\beta_0 + \beta_1) - \beta_0} \;=\; e^{\beta_1}
\end{aligned}
$$

The odds ratio is an associate measure of how much more likely (an odds ratio > 1), unlikely (an odds ratio < 1), or equally likely (an odds ratio = 1) it is for the response to present under x_1 than under conditions x_0.

GLOSSARY

ADEQ	Arizona Department of Environmental Quality
ADHS	Arizona Department of Health Services
ADT	Average Daily Traffic (vehicles per day)
AQS	Air Quality System, EPA's archive of ambient air pollution data
AZHQ	Arizona Health Query
CEFD	Center for Environmental Fluid Dynamics at ASU
CHIR	Center for Health Information and Research at ASU
CMAQ	Community Multi-scale Air Quality modeling system
COPD	Chronic Obstructive Pulmonary Disease
EPA	US Environmental Protection Agency
Eta	The global weather model of the National Weather Service
GIS	Geographic Information System
HC	Hospital Counts
HIPAA	Health Insurance Portability and Accountability Act
IDW	Inverse Distance Weighting (a numerical interpolation technique)
IQR	Interquartile Range
LST	Local Standard Time
MAE	Mean Absolute Error
MM5	Mesoscale Meteorological Model, version 5
MCDAQ	Maricopa County Department of Air Quality
$\mu g/m^3$	Micrograms per cubic meter, the units of concentration for PM
MLP	Multi-Layer Perceptron
NCAR	National Center for Atmospheric Research
NCEP	National Center for Environmental Prediction

NN	Neural Network
PM	Airborne Particulate Matter
PM_{10}	Particulate Matter 10 microns and smaller, aka "inhalable"
$PM_{2.5}$	Particulate Matter 2.5 microns and smaller, aka "fine particulates"
$PM_{2.5}$-$_{10}$	Particulate Matter 2.5 to 10 micros, aka "coarse particulates"
$[PM_{10}]$	Airborne concentration of PM_{10}
RMSE	Root Mean Square Error
SCERP	The Southwest Consortium for Environmental Research and Policy
SMOKE	Sparse Matrix Operator Kernal Emissions, software to build model-ready air pollutant emission fields